Electronic Resonances by the Method of Complex Scaling and Complex Absorbing Potentials within the Framework of Coupled Cluster Theory

Sajeev. Y

December 2005

Electronic Resonances by the Method of Complex Scaling and Complex Absorbing Potentials within the Framework of Coupled Cluster Theory

Thesis submitted to the
University of Pune
for the degree of

Doctor of Philosophy
in
Chemistry

by
Sajeev. Y

Physical Chemistry Division
National Chemical Laboratory
Pune - 411008, India.

December 2005

CERTIFICATE

This is to certify that the work presented in this thesis entitled, "**Electronic Resonances by the Method of Complex Scaling and Complex Absorbing Potentials within the Framework of Coupled Cluster Theory**" by **Sajeev. Y**, for the degree of Doctor of Philosophy, was carried out by the candidate under my supervision in the Physical Chemistry Division, National Chemical Laboratory, Pune, India. Any material that has been obtained from other sources has been duly acknowledged in the thesis.

Date: Dr. Sourav Pal

Place: Pune. (Research Guide)

Acknowledgements

It is a pleasure for me to thank my supervisor, Dr. Sourav Pal, for giving me the opportunity to work on an interesting problem. He enthusiastically supported my work and encouraged me. In addition to working under his guidance, I truly like him as a great teacher and more as a person.

Many of the practical implementations of the work have been done by collaboration with Prof. Manoj Mishra, IIT-Mumbai, Dr. Nayana Vaval, NCL-Pune, and Dr. Robin Santra, Argonne National Labs-USA. All of them were a constant source of ideas and provided deep insights into the work.

I thank the Director, National Chemical Laboratory-Pune, for permitting me to take up my research fellowship at the Physical Chemistry Division. I acknowledge the financial support from CSIR

I would like to thank all the past and present members of the theoretical chemistry group of Dr. Sourav Pal for providing me a pleasant and productive environment to work in. I wish to thank my batch mates, Akhilesh, Sophy, Prashant, Sharan and Subashini, for the pleasant atmosphere they created.

I wish to thank my roommates and Mallu friends for making my life easy and pleasant during my stay in Pune.

I acknowledge the great support and love from my parents, sister, brother-in-law and all my friends and well-wishers in my beautiful village (in the *God's own Country*). Finally, I thank my wife, Daly, for being a great colleague and a great wife.

Date:

Place: Pune. Sajeev. Y

Table of Contents

List of Tables

List of Figures

Acronyms

CAP	Complex Absorbing Potential
CAP-FSMRCC	Complex Absorbing Potential-based Fock Space Multireference Coupled Cluster
CC	Coupled Cluster
CCRACNA	Complex Coordinate Real Axis Clamped Nuclei
CCSD	Coupled Cluster Singles and Doubles Approximation
CGTO	Contracted Gaussian Type Orbital
CI	Configuration Interaction
CIP	Correlated Independent Particle
CAP-CIP	Complex Absorbing Potential-based Correlated Independent Particle
EA	Electron Affinity
EOMCC	Equations of Motion Coupled Cluster
FSMRCC	Fock Space Multireference Coupled Cluster
HF	Hartree-Fock
ICD	Intermolecular Coulombic Decay
IP	Ionization Potential
MRCI	Multireference Configuration Interaction
MRCC	Multireference Coupled Cluster
SCF	Self-Consistent Field
SEC	Subsystem Embedding Condition
TCAP	Transformative Complex Absorbing Potential

Abstract

Electronic resonance states are well-known manifestations of quantum effects in the electronic continuum.[1] The physics of resonance phenomena in the continuum can be characterized by *discrete* eigenstates of the Hamiltonian satisfying purely outgoing boundary conditions. These eigenstates, which are called Siegert states, Gamow vectors, or simply resonance states, have complex energy eigenvalues $E = E_r - i\Gamma/2$, where E_r gives the position of the resonance and Γ gives the width of the resonance.[1,2] The complex energy E is referred to as Siegert energy.

Much of the difficulty encountered in previous theoretical treatments of resonances, based either on the use of the scattering matrix or on the approximate expansion of the scattering wave function in a set of square-integrable basis function, [2] follows from two fundamental facts. First, when focusing, within conventional Hermitian quantum mechanics, on the continuous spectrum of the (N+1)-electron Hamiltonian H (the target is assumed to have N electrons), there exists an inherent difficulty in identifying which discrete positive eigenvalue of an approximate, finite-rank representation of H corresponds most closely to the metastable state of interest. Second, as the Siegert wave function diverges asymptotically and does not belong to the Hermitian domain of the Hamiltonian, the computational difficulties in treating such a state are potentially more severe than those encountered in the treatment of bound states. The role of correlation and relaxation in the formation and decay of metastable states has been reported.[3] Thus, the calculation of energy and lifetime of metastable states requires the simultaneous treatment of both correlation and continuum effects. Hence, the quantum-mechanical many-body problem of this type of metastable state is very difficult to tackle.

The method of analytical continuation of the Hamiltonian in the complex plane eliminates many of these difficulties.[2,4,5] The advantage of this general approach to investigating resonances is that the complex Siegert energy can be calculated directly within a Hilbert space of L^2 functions. The analytical continuation of the Hamiltonian is possible either by the complex scaling method [2,4,5] or by utilizing a complex absorbing potential (CAP). [6] Significant strides have been made

in the theoretical development and practical implementation of the complex scaling method and complex absorbing potential methods, which permit direct and simultaneous determination of both the resonance position and width from the eigenvalue of an analytically continued Hamiltonian. These methods have already been successfully applied to a variety of phenomena, mainly in atomic systems.[2,6,7,8] These methods offer great promise for the determination of accurate Siegert energies in a computationally viable form by a relatively straightforward modification of existing electronic structure codes for bound states.[6,7,8]

The general objective of the work is to formulate a complex scaling method and complex absorbing potential within the framework of coupled cluster theory to the direct and correlated calculations of resonance energy and width. Conceptual as well as practical aspects of this method will be studied. Specific objective and of the proposed work are:

1. Formulation of the Fock space multi-reference coupled cluster (FSMRCC) [9] based on an underlying bi-variational Hartree-Fock.[10]
2. Formulation of an analytical continuation method in which the complex absorbing potential combined with Fock space multireference coupled cluster method for the correlated calculations of resonance energy and width.
3. Formulation of an effective one-electron correlated potential that describes the interaction of an electron with a many-electron target for the description of resonances. The correlated effective one-particle potential is derived within the frame work of FSMRCC theory and complex absorbing potential
4. Use the formalisms developed above for the direct and correlational calculations of resonance energy and width. We will demonstrate the feasibility of the proposed methods by applying it to the resonances of the low energy region of the electron-atom/molecule collisions. The influence of correlation, dependence of scaling parameter and the strength of complex absorbing potential on the position and width of the resonance will also be discussed.

Methodology

The essential idea in the complex scaling method to the resonance problem is to make a transformation on Hamiltonian which results in a non-Hermitian operator, one of the square integrable eigenfunction of which corresponds to the resonant state. The dilation transformation of the electronic coordinates $r \rightarrow r\eta$, where η is a complex number is used to make the resonance function square integrable. A complex SCF technique, also called bi-variational SCF, has been attempted to calculate many electron atomic or molecular resonances. The accuracy of the SCF approximations in the case of an electron scattering resonance depends on the extent to which the electron correlation is important in the description of particular states. This can be achieved by an effective Hamiltonian, which corrects for the inadequacies of bi-variationaly obtained Hartree-Fock operator. Our proposed analytic continuation scheme for Fock space multi-reference coupled cluster theory which will make use of the complex one particle basis functions from a bi-variational SCF.

Though conceptually simple, difficulties may arise in treating molecular systems using complex scaling method. The graphical solution to optimize the complex scaling angle will be time consuming and computationally expensive as it needs the calculation of basis functions from the bi-variational SCF procedure for several rotation angles and the repetitive transformation from atomic to the molecular orbital basis. Introduction of an absorbing boundary condition in the exterior region of the molecular scattered target using a complex absorbing potential may be an alternative and numerically simpler route to solve resonance of the molecules. The CAP procedure is minimally invasive in the sense that neither the internal structure of the physical Hamiltonian is affected nor is there any need to use other basis sets than usual real Gaussians and thus many existing electronic structure calculations for bound state can adapt to the resonance. In the treatment of CAP to electronic resonance states, electron absorption is accompanied by replacing the molecular Hamiltonian H by

$$H(\eta)=H-i\eta W, \qquad (1)$$

where η is a real, non-negative number referred to as CAP strength parameter. W is a local, positive semidefnite one-particle operator. In the limit $\eta \rightarrow 0$, $H(\eta)$ defines an analytical continuation of H.[6]

The complex scaling and CAP will be introduced to the multi-determinantal Fock space coupled cluster method. This can describe the dynamic and non-dynamic electron correlation efficiently in the ionized or electron attached states. The basic purpose of our proposed work is to use a highly correlated Fock space multi-reference coupled cluster method using complex scaling method and complex absorbing potential method to compute ionization potential/electron affinity, and thus to provide a method to obtain more accurate energy and width of the resonance. The MRCC method is based on a pre-chosen model space and the main ionizations/electron-attached states can be conveniently described using a model space of important (N-1)/(N+1) electron determinants and an appropriate exponential wave operator to describe the dynamic electron correlation. Diagonalization of an effective Hamiltonian over the model space provides the multiple roots of the state. However, the effective Hamiltonian is a complex non-Hermitian matrix, in general. Using the restricted Hartree-Fock of N-electron system as vacuum, the (N-1)/(N+1) electron determinants constitute one-hole/one-particle Fock space. The Bloch effective Hamiltonian has been used quite successfully in the FSMRCC method to describe ionization potential, electron affinity and excitation energies. Quite clearly, a complex scaled FSMRCC and the FSMRCC combined with the CAP method can be potentially powerful candidates to compute resonance energies and the width of the resonances.

The organizations of the dissertation work will be as follows

We begin this thesis by reviewing the quantum theory of resonance. The first chapter explains some of the basic formulations and theoretical developments in the area of resonances and provides an overview of analytical continuation method as an introduction to the present work. Our main purpose here is to develop the an analytical continuation method in the coupled cluster theoretical frame work, which we shall use for calculating well known resonance phenomena in atomic and

molecular physics. Electron correlation and relaxation effects play a substantial role in the formation and decay of resonance states. The next 4 chapters give a detailed account of the analytical continuation scheme applied in the coupled cluster theoretical framework.

We begin to develop the analytical continuation method for the coupled cluster theory in the second chapter. The analytical continuation schemes we shall use for this purpose are based upon the well known complex scaling method, which is described in the 1st chapter. For an atom having more than a few electrons the atomic Hamiltonian is very complex and it is only possible to find its eigenfunctions within the framework of some approximate scheme. A natural approximation is to assume each electron moves in an average potential due to the nucleus and other electrons. This assumption leads to independent-particle model, which essentially reduces the many-electron problem to the problem of solving number of single particle equations. In this chapter we discuss the analytical continuation scheme for the restricted Hartree Fock method using the well know complex scaling technique, which can be regarded as the starting point of our analytical continuation scheme for coupled cluster equations. The FSMRCC method based on the complex SCF can describe the dynamic and non-dynamic electron correlation efficiently in the ionized or electron-attached metastable states. This formalism is then applied to the shape and auger resonance in atomic physics. The validity of this complex scaling method depends largely upon the dilation analyticity of the potential.

In Chapter 3, we formulate a complex absorbing potential combined with Fock space multireference coupled cluster method for the correlated calculations of resonance energy and width. This can describe the dynamic and non-dynamic electron correlation efficiently in the ionized or electron attached states. The CAP-FSMRCC method provides direct access to the energy difference $(E_s^{N+1} - E_0^N)$, where E_0^N is the ground-state energy of the neutral N-electron target at the same geometry. Both static and dynamic electron correlation in the N- and (N+1)-electron systems are treated in a consistent manner in this approach. Since the complex absorbing potential serves to render the wave function of the projectile square-integrable, while it must leave the target unaffected, the CAP must be introduced, in principle, only into the

description of the (N+1)-electron state. The N-electron ground state may be described by the Hamiltonian without CAP. This implies that adequate modifications to the FSMRCC method of energy differences need to be made.

In chapter 4, the technique CAP-FSMRCC is applied for the correlated calculation of the energy and width of a shape resonance in an electron-molecule collision. Accurate resonance parameters are obtained by solving a small non-Hermitian eigenvalue problem.

In chapter 5, we have formulated and applied an analytical continuation method for the recently formulated correlated independent particle potential [11] for solving the resonances in the low-energy electron-molecule collision problem. The complex absorbing potential defines the analytical continuation for the potential. An approximated form of the correlated complex independent particle potential makes it possible to treat the electron correlation and relaxation effects of the N+1 system and the CAP potential differently. The method is tested by application to molecular shape resonances.

References

1. P. A. M. Dirac, *Proc. Roy. Soc. London Ser.* A114, 243 (1927); A. F. J. Siegert, *Phys. Rev*. **56**, 750 (1939); H. S. Taylor*, Adv. Chem. Phys.* **18**, 91 (1970)
2. W. P. Reinhardt, *Ann. Rev. Phys. Chem*. **33**, 323 (1982); Y. K. Ho, *Phys. Repts*. **99**, 2 (1983)
3. N. Moiseyev and F. Weinhold, *Phys. Rev. A.* **20**, 27 (1979)
4. E. Balslev and J. M. Combes, *Commun. Math. Phys*. **22**, 280 (1971); J. Aguilar and J. M. Combes, *ibid.* **22**, 269 (1971);B Simon, *ibid* . **27**, 1 (1972); B. Simon, *Ann. Math*. **97**, 247 (1973)
5. N. Moiseyev, *Phys. Rep*. 302, 211 (1998). P. O. Löwdin, *Adv. Quantum. Chem***.** **20**, 87 (1989)
6. U. V. Riss and H.-D. Meyer, *J. Phys. B* **26**, 4503 (1993); R. Santra and L. S. Cederbaum, *J. Chem. Phys*. **115**,6853 (2001)
7. N. Rom, N. Lipkin, and N. Moiseyev, *Chem. Phys*. **151**, 199 (1991); N. Moiseyev, *J. Phys. B* **31**, 1431 (1998); U.V. Riss and H.-D. Meyer, *J. Phys. B* **31**, 2279 (1998).
8. T. Sommerfeld, U. V. Riss, H.-D. Meyer, L. S. Cederbaum, B. Engels, and H. U. Suter, *J. Phys. B* **31**, 4107 (1998).
9. D. Mukherjee and S. Pal, *Adv. Quantum. Chem*. **20**, 291 (1989); S. Pal, M. Rittby, R. J. Brtlett, D. Sinha and D. Mukherjee, *J. Chem. Phys*. **88**, 4357 (1988); U. Kaldor and M.A. Haque, *Chem. Phys. Lett*. **128**, 45 (1986); U. Kaldor and M. A. Haque, *J. Comp. Chem*. **8**, 448 (1987); D. Mukherjee, *Pramana*. 12, 1 (1979); A. Haque and D. Mukherjee, *J. Chem. Phys.,* **80**, 5088 (1984)
10. M. Mishra, Y. Öhrrn, and P. Froelich, *Phys. Lett* A. 84, 4 (1981); P. Froelich and P. O. Löwdin , *J. Math. Phys*. **24**, 89 (1983)
11. A. Beste and R. J. Bartlett, *J. Chem. Phys*. **120**, 839 (2004)

Chapter 1
General Introduction and Scope of the Thesis

Electronic resonance states correspond to metastable bound states coupled to continuum states which decay by electron emission. Resonance phenomena constitute some of the most interesting features of scattering experiments.[1] Resonances which occur in electron-atom/-molecule scattering and other areas of atomic and molecular physics, are associated with quasi-bound state with a lifetime long enough to be well characterized.[2] The accurate calculation of the energies and lifetimes of resonance state is very important for describing several physical processes, such as Auger decay, [3] intermolecular Coulombic decay [ICD] [4] and metastable anions. [5] Considerable progresses has been made in the development of practical methods to calculate the energy and lifetime of resonance in the framework of analytical continuation of Hamiltonian techniques.[2]

One of the main objectives of this thesis is to formulate the analytic continuation method in the coupled cluster theoretical framework. One of the principal means towards this end will be the use of complex scaling and complex absorbing potential based method as the analytical continuation tool in the coupled cluster theory. The first chapter is devoted to a brief review of the conceptual as well as the computational methods to solve the resonance. We shall begin this chapter with a quick survey of resonances in the scattering experiments. We shall then review

some of the theoretical methods to solve the resonance phenomena, with particular reference to complex scaling method and complex absorbing potential based methods.

1.1. Resonances in Scattering

The quantum formulation of resonance in scattering may be found in many text books and review articles [1,6-14] and is not developed in detail here. In discussing the resonance theory it is convenient to recognize various possible divisions of the subject. There are resonances coming in the elastic collision channels and inelastic collision channels. This thesis focuses itself mainly to the former. The formalism of resonances in elastic channel is naturally much simpler than that of the resonances in the inelastic channels. At the same time the former includes almost all of the basic concepts needed for the latter.

Consider the elastic scattering of an incident particle in the z direction by a central field potential. For large negative values of time, the incident particle is free [$V(r)$ is practically zero] and its state is represented by a plane wave packet [e^{ikz}]. When the wave packet reaches the region which is under the influence of potential $V(r)$, its structure is modified and its evolution is complicated. For large positive value of *t*, it has left this region and once more takes on a simple form: it is now split into a transmitted wave packet which continues to propagate in the positive *z* direction [hence having the form e^{ikz}] and a scattered wave. The eigenstates satisfying these conditions is called stationary scattering states $\gamma_k^{diff}(r)$ and are obtained by the superposition of a plane wave and a scatted wave. The asymptotic behavior of the stationary scattering state is of the form:

$$\gamma_k^{diff}(r) \underset{r\to\infty}{\sim} e^{ikz} + f_k(\theta,\varphi)\frac{e^{ikr}}{r}. \qquad 1.1.1$$

The factor *1/r* ensures that the total flux of energy passing through a sphere of radius *r* is independent of *r* for large *r*: in quantum mechanics, it is the probability flux passing through this sphere that does not depend on *r*. In this expression, only the function $f_k(\theta,\varphi)$, which is called scattering amplitude depends on the potential.

Schrödinger equation satisfying the time evolution of the wave packet representing the state of the incident particle can be expanded in terms of the eigenstates of the total Hamiltonian H .

$$\Psi(r,t) = \int_0^\infty g(k)\gamma_k^{diff}(r)e^{(-iE_k t/\hbar)}dk \qquad 1.1.2$$

where $E = \hbar^2 k^2 / 2\mu$ and $g(k)$ has a pronounced peak at $k = k_0$ and practically vanishes elsewhere. Briefly, the scattering is determined by the asymptotic form of the wave function,

$$\Psi(r,t) \underset{r\to\infty}{\sim} \int_0^\infty g(k)e^{ikz}e^{(-iE_k t/\hbar)}dk + \int_0^\infty g(k)f_k(\theta,\varphi)\frac{e^{ikr}}{r}e^{(-iE_k t/\hbar)}dk\,, \qquad 1.1.3$$

which is a sum of a plane wave packet and a scattered wave packet.

In the special case of central field potential $V(r)$, the orbital angular momentum is a constant of motion. Therefore, there exist stationary states with well-defined angular momentum, i.e., eigenstates common to H, L^2, and L_z. We shall call the wavefunctions associated with these sates as partial waves $\tilde{\varphi}_{k,l,m}(r)$. Their angular dependence is given by spherical harmonics $Y_l^m(\theta,\phi)$: the potential $V(r)$ influence only their radial dependence.

The asymptotic form of the wave function [Eq.1.1.3] determines the differential scattering cross section, but can not be found without solving the wavefunction throughout all space. This may be carried out by the method of partial waves. We can express the stationary scattering states as a linear combination of partial waves having the same energy but different angular momentum

$$\gamma_k^{diff}(r) = \sum_{l=0}^{\infty} C_l \tilde{\varphi}_{k,l,m}(r) \qquad 1.1.4$$

$$\tilde{\varphi}_{k,l,m}(r) = \frac{1}{r}u_{k,l}(r)Y_l^m(\theta,\phi)\,, \qquad 1.1.5$$

where the $u_{k,l}$ is the solution of the radial equation

$$\left[-\frac{\hbar^2}{2\mu}\frac{d^2}{dr^2}+\frac{l(l+1)\hbar^2}{2\mu r^2}+V(r)\right]u_{k,l}(r)=\frac{\hbar^2k^2}{2\mu}u_{k,l}(r) \qquad 1.1.6$$

with the total effective potential $V_{eff}(r)$ as

$$V_{eff}(r)=V(r)+\frac{l(l+l)\hbar^2}{2\mu r^2}. \qquad 1.1.7$$

We expect that, for large *r*, the partial waves will be very close to the common eigenfunctions of H_0, L^2, and L_Z. The corresponding wavefunctions $\tilde{\varphi}^{(0)}{}_{k,l,m}(r)$ are free spherical wavefunctions: their angular dependence is that of spherical harmonic. The asymptotic expression for the partial wave and free spherical wave is the superposition of the incoming wave e^{-ikr}/r and an outgoing wave e^{ikr}/r with well determined phase difference $l\pi$. But the potential *V(r)* introduces a supplementary phase shift δ_l in the partial waves.

$$\tilde{\varphi}^{(0)}_{k,l,m}(r)\underset{r\to\infty}{\sim}-\sqrt{\frac{2k^2}{\pi}}Y_l^m(\theta,\varphi)\frac{e^{-ikr}e^{il\pi/2}-e^{ikr}e^{-il\pi/2}}{2ikr} \qquad 1.1.8$$

$$\tilde{\varphi}_{k,l,m}(r)\underset{r\to\infty}{\sim}-Y_l^m(\theta,\varphi)\frac{e^{-ikr}e^{il\pi/2}-e^{ikr}e^{-il\pi/2}e^{2i\delta_l}}{2ikr} \qquad 1.1.9$$

The factor $e^{2i\delta_l}$ [which varies with *l* and *k*] thus finally summarizes the total effect of potential on a particle of angular momentum *l*. Each partial wave *l* contributes to the total cross section a term

$$\sigma_l=\frac{4\pi}{k^2}(2l+1)\sin^2\delta_l. \qquad 1.1.10$$

Generally the phase shift δ_l is slowly varying function of energy. A resonance occurs for some partial wave *l* when δ_l changes rapidly over a small energy change. The phase shift can be split into

$$\delta_l(E)=\delta_{bg}+\delta_{res}, \qquad 1.1.11$$

where δ_{bg} is the background phase shift and δ_{res} is the resonance phase shift.

At resonance the total cross-section will also change abruptly. For a given l the ratio $S_l(k)$ of the outgoing wave amplitude to the incoming wave amplitude at energy $E = \hbar^2 k^2 / 2\mu$ *is*

$$S_l(k) = e^{2i\delta_l(k)} \qquad 1.1.12$$

up to a constant factor. Here the dependence of the phase shift on the energy has been emphasized by writing $\delta_l = \delta_l(k)$. The wave number k is a real variable. However, by the process of analytic continuation, $\delta_l(k)$ can be regarded as a function of a complex variable k. Suppose there exists an imaginary value of k, that is

$$k = -i\kappa \qquad 1.1.13$$

where κ is a positive definite such that

$$S_l(\kappa) = e^{2i\delta l(\kappa)} = 0 \qquad 1.1.14$$

This implies that the energy is negative, and $\delta_l(k) = i\infty$. i.e., the asymptotic behavior of the wave function will go as

$$\tilde{\varphi}_{k,l,m}(r) \underset{r\to\infty}{\sim} -Y_l^m(\theta,\varphi)\frac{e^{-ikr}e^{il\pi/2}}{2ikr} \qquad 1.1.15$$

and there is no outgoing wave amplitude, only an exponentially dying form. This is exactly the condition of a bound state. Thus zeros of S_l corresponds to bound states. Conversely, when $k = -i\kappa$, S_l will grow without bound, and it follows that the poles [singularities in the complex plane] corresponds to scattering resonance. Close to resonance [using Eq.1.1.11]

$$S_l(k) = e^{2i\delta bg}\ \frac{e^{i\delta res}}{e^{-i\delta res}} = e^{2i\delta bg}\ \frac{1+i\tan\delta res}{1-i\tan\delta res}. \qquad 1.1.16$$

The simplest way of causing S_l to grow without a bound near E_0 is to make it have a simple pole at $E = E_0 - i(\Gamma/2)$.

$$S_l(k) = e^{2i\delta_{bg}} \frac{(E_0 - E) + i(\Gamma/2)}{(E_0 - E) - i(\Gamma/2)} \qquad 1.1.17$$

When the background phase shift is neglected, the partial cross section can be written as

$$\sigma_l = \frac{4\pi}{k^2}(2l+1)\frac{(\Gamma/2)^2}{(E_0 - E)^2 + (\Gamma/2)^2}. \qquad 1.1.18$$

Equation 1.1.18 is called the Breit-Wigner formula for an isolated scattering resonance. It describes a bell-shaped curve with a half-width at half-maximum of $\Gamma/2$. This suggests that the occurrence of a resonance at $E_0 (= E_r)$ in the partial cross section. From the practical point of view, one needs to know only the energy and width of a resonance to calculate, from the Breit-Wigner expression, its contribution to cross section. The scattering cross section is a rapidly varying function of incident energy in the resonant region and can be characterized by Breit-Wigner equation containing two parameters: the resonance energy $E_0 (= E_r)$ and width Γ. The resonance energy can be interpreted as the energy of the metastable state, whereas the width is related to its lifetime through the uncertainty relationship $\tau = \hbar/\Gamma$. In analogy to a bound state, the time dependence of the resonant state is given by

$$\Psi_R(r,t) = e^{-i(E - \Gamma/2)t/\hbar}\Psi_R(r) \qquad 1.1.19$$

The presence of $-i\Gamma/2$ in the energy term forces exponential decay and the probability,

$$|\Psi_R(r,t)|^2 = |\Psi_R(r)|^2 \, e^{-\Gamma t/\hbar}, \qquad 1.1.20$$

decays to zero as time passes at constant *r*. Therefore, the particle disappears from any given point in the coordinate space. When the lifetime of particle-target system in the region of interaction is larger than the collision time, *a/v* [*a* is the linear dimension of the target molecule and *v* is the incident electron velocity], we call the phenomenon a resonance phenomenon. A resonance state is defined as a long-lived state of a system which has sufficient energy to break-up into two or more subsystems. Qualitatively, resonant scattering involves the formation of a metastable, quasi-discrete state, which, because of its nonstationary character, decays after a short time into one of the open channels.

The negative ion resonances in electron-molecule collision appear as sharp changes in scattering cross section at low incident electron energies [typically 1-10 eV]. At some incident energies, the electron wavefunction has large amplitude within the target. This happens only when the incident energy falls in one of the discrete bands, where the incident electron finds a comfortable quasistationary orbit in the field of target molecule. The quasi stationary nature of the compound state is usually guaranteed by either one of the two following mechanisms. The first possibility and the most common situation that causes the appearance of resonance is an effective potential [Eq.1.1.7] made up of attractive potential [attractive polarization force at small distances] combined with a repulsive potential [repulsive centrifugal force at long distances] produces a barrier in the potential. For energies below the maximum in the barrier, there would be bound states inside the attractive part of the potential if tunneling could be ignored. However, the quantum mechanical tunneling permits particle 'trapped' inside the attractive part of the potential to escape to infinity, and the tunneling rate depends on the height and thickness of the barrier. Conversely, particles incident on the potential at energy close to the virtual states are able to penetrate inside the attractive barrier. This behavior explains why resonance generally becomes narrower as l increases. Larger l values causes bigger centrifugal barriers, thus suppressing tunneling.[8] Once the electron has entered the region inside the barrier, it will take some time before the electron leaks out to the outer region again by a tunnel effect. This type of resonance is called *shape resonance* or *potential resonance* since the resonance state is produced by an appropriate shape of the effective interaction potential between the electron and the molecule.

The second possibility arises when the inelastic channels are introduced. By exciting the target molecule, the electron loses its energy. Suppose that the incident electron energy is not large that after the excitation the electron energy becomes negative, and furthermore, its value coincides with one of the bound-state energies allowed in the field produced by the excited target molecule. Then it will take some time before the electron gets its energy back from the target and escape to outside. Thus one has a new type of resonance process which is called *core-excited type I* resonance or the resonance of *Feshbach resonance*. There exists also shape resonances associated with the effective potential in the inelastic channel. They are called *core-excited type II* resonance or *core excited shape resonances*.

All these resonance states can be considered as quasistationary states of negative ion M^- formed by the electron and the target molecule M. The configuration of a Feshbach resonance is that of an excited state of M, usually referred to a parent state, with an additional electron in an excited orbital. Alternatively the resonance configuration may be viewed as that of a state [often ground state] of M^+, referred to as grandparent state, with the addition of two electrons in excited orbitals. Feshbach resonances are generally long lived compared to typical vibrational period [10^{-14} s], as their decay involves the rearrangement of the orbitals of both excited electrons. Thus the temporary negative ions make many vibrations before decaying. Since the lifetimes of the Feshbach resonances tend to be long, resonance width are correspondingly small [typically less than 20 meV], and so the resonances appear as narrow structures in the cross sections of elastic and inelastic processes.

The structural and spectroscopic properties of electronic resonance states are similar to those of bound states and their study reveals deep physical insight into the complex many-body effects governing molecular physics and this is the reason why this states are of particular importance to physical chemists. Structurally, resonances provide information on metastable negative ions, negative electron affinities, orbital energies of unbound orbitals, and doubly excited electronic states.

1.2. Theoretical Methods to Solve Resonance

Before proceeding, a few additional comments are in order. The material which appears in this section is treated more extensively in several monographs that are devoted entirely to the quantum theory of resonance [2,6,7,9-12] and the reader is referred to these references for further details. We have tried, however, to include all the material we need for the treatment of electronic resonances. We also discuss a number of simplified schemes which have been reported in literature. Some important works in the area of resonance calculations have been sited extensively in chapters 2-5.

In recent decades, a number of methods have been proposed to calculate the energies and width of resonances. From the computational view point, there are roughly three methods by which a resonance is calculated. These methods are

(1) *From the scattering point of view*; In this method, resonances are related to the structures in the cross sections. Therefore the detail of the resonances can be analyzed by using the Breit-Wigner profile [13] [Eq 1.1.18] once the scattering wave functions in the vicinity of the resonances are obtained. The Kohn and Schwinger variational principles allow one to calculate resonance information by a basis set method.[14] These two methods are not fully L^2 methods because of the appearance of so called bound-free matrix elements in both the cases. The free [i.e., non-L^2] wavefunction is either explicitly in the basis set [Kohn] or originates from Green function [Schwinger]. Scattering calculations, beyond the one particle [i.e., static-exchange] level, are difficult. Moreover, using scattering approach, the resonance parameters must be extracted from a cross section or phase shift, and it is thus difficult to interpret the results in terms of chemical concepts.

(2) *From the point of view that a resonance is a quasibound state in the scattering continuum*; The basic motivation for this approach is the observation that the resonance state resembles to a negative molecular-ion in the region near the target molecule. These methods are based on a formalism that established resonance phenomena into a part of the formal scattering theory. The potential employed was in most cases static with or without exchange; polarization, when included, was obtained parametrically[15] or scaling the results to fit the experimental values.[16] An important development in the calculation of resonance is the application of L^2 or basis set method. In this L^2 method the resonance state can be obtained by diagonalization of a Hamiltonian after it has been projected onto a L^2-basis set. This L^2 state is then turned into resonance by coupling it to continuum using Feshbach projection techniques.[17]. This is a powerful method. However, it requires the knowledge of the projected Green function.[11] A number of other L^2 methods were also used in practically all electron-molecule collision processes.[18] Parallel to these developments, many of the theoreticians have been applying hybrid theories which extensively uses the both the scattering calculations and the L^2 methods. These theories were successful in incorporating non-adiabatic effects, polarization of the target due to the incoming electron and many other many-body effects. Two methods seem to have special promise. These are T-matrix expansion method [19] and a variant of R-matrix theory.[20] The R matrix calculation of *Schneider* et al. uses a potential, which is

obtained from "stabilization self-consistent field" calculation of the compound state. The vibrational-excitation cross section calculation done by Hazi et al [21] uses a complex-potential or boomerang model with the electronic resonance parameters determined *ab initio*. However, in this case, the fixed nuclei resonance parameters were extracted from complex SCF calculations of the target and the anionic potential energy curves. The most serious attempt in a boomerang model to calculate cross sections near $^2\Pi_g$ resonance in e-N_2 scattering is the work of Dube and Herzenberg.[22] They have applied the R-matrix theory for the vibrational excitation cross section calculations e-N_2 scattering. Birtwistle and A. Herzenberg have done cross section calculation using the potential energy curves by fitting the experimental data within the boomerang model.[23] Krauss and Mies applied molecular orbital calculations for the description of the resonance states.[24]

Another important development in the basis set method to calculate resonance is the stabilization method.[25,26] In the stabilization method the Hamiltonian is diagonalized in a basis of discrete, exponentially decaying functions, and the resonance eigenvalues are recognized by remaining essentially unchanged as the basis size varies. The intuitive justification of the stabilization method is that resonance states, in contrast to the scattering states, are relatively insensitive to the position of the effective wall set by the finite basis, since the rapid changes in the phase shifts ensures that there is a value of E close to the resonance position for which the wavefunction vanishes at the effective box edge. The concept of stabilization method subsequently leads to the development of artificial absorbing potential to define the resonances, which will be discussed in the next section.

(3) *From the point of view that resonance is related to the complex eigenvalue of the Hamiltonian*; This approach, which is a direct calculation of resonance eigenvalue of the Hamiltonian, has not received enthusiasm among atomic theorists before the method of complex scaling became known. Since the resonance wavefunction [The so called Siegert wave function [27,28]] diverges at the complex resonance eigenvalue, this direct resonance approach seemed to have great computational difficulty. This method was unfortunately interpreted as `tried and rejected' method.[7] Historically the direct access to resonance states began with the treatment of the radioactive decay of nuclei by Gamow [27] and later by Siegert.[28] Instead of extracting the resonance

parameters from the cross section, the metastable state is described by an eigenfunction belong to a complex eigenenergy. The Gamow-Siegert wavefunction is a solution of Schrödinger equation with purely outgoing boundary condition. The outgoing boundary condition enforces the eigenenergy to become complex, $\mathrm{E}_{\mathrm{res}}=\mathrm{E}_{\mathrm{r}}-i\Gamma/2$.

The Simplest mathematical description of such states is that they resemble bound stationary states in that they are localized in space [at t=0], and their time evolution is given by Eq.1.1.19. Due to the exponential divergence, the number of particle is conserved only when the reaction coordinate, r and the time, t, approach the limit of infinity. A characteristic for these states is their exponential growth in the asymptotic region. Thus they are not square integrable and do not belong to the Hermitian domain of the Hamiltonian.[29] The Gamow-Siegert wave functions possess large amplitude in the inner molecular region resembling a bound state. The wavefunction in this region is affected by physical interactions, while the asymptotic exponentially growing part describes the decay. In fact, resonance states can be understood as a discrete state coupled to continuum. They represent a particularly challenging problem to quantum chemist because one has to treat a continuum problem and the electron correlation simultaneously. In particular, the latter effect plays a crucial role in most temporary anions.

When one solves the Schrödinger equation $H\Psi = E\Psi$ for a self-adjoint Hamiltonian subject to standard boundary condition, one obtains a spectrum $\{\boldsymbol{E}\}$ of real eigenvalues E which are discrete or continuous. In 1927, Dirac showed that, if one changes the boundary conditions and considers a system consisting of a scatterer and incoming and outgoing waves, then the scatterer may have certain resonance states with finite life times and exponential decay in time. [30] The changing of boundary conditions to include the incoming waves, which by way of a scatterer are turned into outgoing waves, results a non-Hermitian Hamiltonian and may have complex eigenvalue $\boldsymbol{E}$ corresponding to the resonance state with a finite lifetime. Within an L^2 space, the spectrum of the Hamiltonian is necessarily real. However H can be modified [analytically continued] in several ways such that direct access is gained to Siegert energies E_{res}. Each Siegert energy is an eigenvalue of the resulting

non-Hermitian Hamiltonian, and the associated eigenfunctions are square integrable, i.e., they can be represented in Hilbert space. Analytic continuation can achieved either by complex scaling of the electronic coordinates [2,12,31-33] or by utilizing a complex absorbing potential [CAP] based methods.[34,35] However, even without detailing any of the discussion, it is straight forward to state that one of the major purposes of introduction of complex scaling and CAP nonrelativistic quantum theory is to produce exactly those [non-Hermitian] operators which have the complex energies. The advantage of this general approach to investigating resonances is that the complex Siegert energy can be calculated directly within a Hilbert space of L^2 functions. Therefore, many of the methods of bound-state calculations can be readily adapted to the resonance problem in this form.

1.3. Complex Scaling

The theory of resonance was greatly simplified when it was discovered that they could be evaluated by the method of complex scaling. The fundamental work of Balslev, Combes and Simon has provided a mathematical foundation for the description of atomic and molecular resonances by the method of complex scaling.[32] This method is associated with a similarity transformation [most of the theorems in quantum mechanics to non-Hermitian operators can be made by carrying out similarity transformations.], in which the many-particle Hamiltonian loses its self-adjoint character. The resonance state can be described by square integrable functions associated with the eigenfunctions of a transformed Hamiltonian $\hat{U}\hat{H}\hat{U}^{-1}$, obtained from the original Hamiltonian H by an unbounded similarity transformation.[36]

That is,

$$(\hat{U}\hat{H}\hat{U}^{-1})(\hat{U}\Psi_R) = (E_{res} - i\Gamma/2)(\hat{U}\Psi_R) \qquad 1.3.1$$

such that

$$\hat{U}\Psi_R \to 0 \quad \text{as } r \to \infty \qquad 1.3.2$$

and $\hat{U}\Psi_R$ in Hilbert space although Ψ_R are not. The method of complex scaling provides such an unbounded similarity transformation. The complex scaled

Hamiltonian is no longer self-adjoint and the original spectrum $\{\boldsymbol{E}\}$ has been changed: some energy eigenvalues are persistent, others may be lost, and new eigenvalues may occur also in the complex plane. The theory of change of spectra of a many-particle Hamiltonian associated with the unbounded similarity transformation- due to the change of boundary condition-is reviewed by Löwdin.[36] The complex-scaling operator is given by

$$\hat{U} = e^{i\theta r\partial/\partial r} \qquad 1.3.3$$

such that $\hat{U}f(r) = f(re^{i\theta})$ for any analytical function $f(r)$

By scaling the reaction coordinate, the resonance wave function becomes square integrable and, consequently, the number of particles in the coordinate space is conserved. Therefore, complex scaling has the advantage of associating the resonance phenomenon with the discrete part of the spectrum of the complex scaled Hamiltonian. Moreover, the resonance state is associated with a single square integrable function, rather than with a collection of continuum eigenstates of the unscaled Hermitian Hamiltonian. Complex scaling may be viewed as a procedure which compresses the information about the evolution of a resonance state at infinity into a small well defined part of the space.

Boundary conditions determines whether an operator has eigenvalues, and whether the corresponding eigenfunctions are L^2 [bound states] or non-L^2 [scattering states]. The boundary condition of square integrability is preserved during the complex scaling for a θ value of $|\theta| \geq \Pi/2$. Conversely, no new square integrable eigenfunctions with real eigenvalues suddenly appear as $r \to re^{i\theta}$. That is H and $H(\theta)$ has same real bound state eigenvalues. On the other hand, are scattering wave functions, the continuum solutions of H, which are non-normalizable and remain finite as $r \to \infty$, is not preserved as such. Unless the potentials are too long ranged, radial scattering solution looks like the linear combinations of $(e^{+ikr})/r$ and $(e^{-ikr})/r$ as $r \to \infty$. To preserve this [bounded] asymptotic form as $r \to re^{i\theta}$ we must simultaneously take $k \to ke^{-i\theta}$. If we don't, one of the exponentials will grow exponentially at ∞, violating the boundary condition of everywhere finite wave

functions. If $k \to ke^{-i\theta}$, then $E = k^2/2 \to e^{-i2\theta}k^2/2$, for the allowed scattering eigen energies. That is the continuum is rotated into the lower half complex energy plane. It is the fact that the continuous spectrum of $H(\theta)$ is different from that of H which is the key to the utility of $r \to re^{i\theta}$ transformation. With this very qualitative motivation, we now simply state the result of the spectral theory of dilation analytic N body coulomb system:

1) Bound state eigenvalues of $H(\theta)$ are independent of θ, and identical to those of H for $\theta \le \pi/2$.

2) Scattering threshold corresponding to the possibility of fragmentation of different systems in different states of excitations are also independent of $\theta, \theta \le \pi/2$

3) The continuous spectra of the original Hamiltonian H are rotated around their respective starting points around an angle 2θ into the lower half plane. During this process, certain new discrete complex eigenvalues may revealed in the lower half complex energy plane, in the sector $0 > \arg(z - E_0^{thres}) \ge -2\theta$, where z is the complex energy, and E_0^{thres} is the lowest energy scattering threshold. These new discrete state corresponds to resonance states in the sense of Dirac. The corresponding eigenfunctions $\Psi(\theta)$ are L^2, as befits their association with discrete eigenvalues. Note that the $\Psi(\theta)$ obtained by taking $\lim_{\theta\to 0}\Psi(\theta)$ will not be L^2, unless its eigenvalues were real to begin with, and it represents a bound state. The discrete complex eigenvalues of $H(\theta)$ are independent of θ as long as they remain isolated from the parts of the continuum. As the continua rotate as a function of θ, discrete complex eigenvalues may be exposed.

1.4. Complex Scaled Hamiltonians, Dilation Analyticity and Complex Absorbing Potentials

For the case of an N body coulomb problem,

$$H(\vec{r}) = -\frac{\nabla^2}{2} + V^{coul}(\vec{r}), \qquad 1.4.1$$

the complex scaled Hamiltonian is given by

$$H(\vec{r}e^{i\theta}) = -e^{-2i\theta}\frac{\nabla^2}{2} + e^{-i\theta}V^{coul}(\vec{r}) \qquad 1.4.2$$

It is thus easy, at least in principle, to relate the properties of the matrix elements of the transformed Hamiltonian for N-body systems with only pair wise coulomb interactions, to the properties of the kinetic and potential energy matrices of unscaled Hamiltonian. Not only does the coulomb potential scale in a simple manner; the coulomb interaction belongs to a special class of potentials called *dilation analytic*, a more restrictive condition than the simple analyticity in the interparticle coordinates. The precise definition, and determination of which potentials are not dilation analytic, is a nontrivial mathematical technicality. The N body coulomb potential is dilation analytic.

Encouraged by the success of complex scaling method in atomic calculations, several workers have extended this method to calculate the molecular resonances. According to the theorem of Balslev and Combes, the formalism is valid for the centre of mass Hamiltonian of a system of particles interacting through the dilation analytic potentials. The complex scaling theory so far discussed is valid for the full molecular problem also, treating all nuclei and electron as mobile particles. Therefore, to scale both the nuclear and atomic coordinate seem to be the natural consequences of the Balslev Combes theorem. However, such a procedure is impractical since the wave function would then depend both on nuclear and electronic coordinate. The first approximation to study molecular resonances is to use the Born-Oppenheimer Hamiltonian. The complex scaling method is consistent with the Born-Oppenheimer approximation and the application of complex scaling method to molecular potential would [applying the Born-Oppenheimer approximation after

dilation], however, result in the determination of electronic spectra for unphysical complex internuclear separations. [37,38] There is an incredibly strong resistance to thinking of complex internuclear distances. What is done instead is to clamp the nuclei on the real axis, and scale only the electronic coordinates. To scale only electronic coordinate may be computationally sound but not mathematically rigorous. The problem in this complex coordinate real axis clamped nuclei approximation [CCRACNA] arises from the fact that if the nuclear coordinates are left real, and an electronic coordinates $\vec{r}_i$ is scaled $\vec{r}_i \rightarrow \vec{r}_i e^{i\theta}$, the nuclear electron interaction

$$\sum_{\alpha} \left| \vec{r}_i e^{i\theta} - \vec{R}_\alpha \right|^{-1} \qquad 1.4.3$$

is non-analytic [39] as the argument of the absolute value can vanish for a continuous range of value such that

$$\left| \vec{r}_i e^{i\theta} \right| = \left| \vec{R}_\alpha \right|, \quad \hat{r}_i . \hat{R}_\alpha = \cos\theta , \qquad 1.4.4$$

giving rise to a continuous range line of square branch points. The existence of these continuous branch points makes the Hamiltonian non-analytic, thus making the Balslev-Combes theorem inapplicable to the Born-Oppenheimer Hamiltonian. McCurdy and Rescigno[40] and independently Moiseyev and Corcoran,[41] nevertheless established that the CCRACNA could be made to work. McCurdy and Rescigno used Gaussian basis functions where only the exponents are scaled by a complex factor. Also the exponents are back rotated by $e^{-i\theta}$. They then diagonalized this wave function using a real Hamiltonian and argued that the uses of the back rotated wave functions and a real Hamiltonian is equivalent to using real wave functions and a complex Hamiltonian. The procedure used by Moiseyev and Corcoran is also to use the Born-Oppenheimer approximation. When the method of coordinate rotation is applied to such a Hamiltonian, these authors rotate only the electronic coordinate but not the nuclear coordinates. To scale only the electronic coordinate has become some practical advantage since the matrix elements become similar to that given in Eq.1.4.2. Moiseyev and Corcoran applied this procedure to autoionizing states of H_2 and H_2^- by scaling only the electronic coordinates of the Born-Oppenheimer Hamiltonian.[41] The success of the CCRACNA prompted a quick response by Simon,[42] who suggested to use an exterior scaling method to avoid any interior non-

analyticities by keeping the coordinates on the real axis long enough. The exterior complex-scaling operator in this case is

$$U = \begin{cases} 1 \quad if \quad r < r_o \\ \mathrm{e}^{i\theta(r-r_0)\partial/\partial r} \quad if \quad r \geq r_o \end{cases} \qquad 1.4.5$$

and the Hamiltonian is given by

$$H(\theta) = \begin{cases} H(r) \quad if \quad r < r_0 \\ H\left((r-r_0)e^{i\theta}\right) \quad if \quad r \geq r_0. \end{cases} \qquad 1.4.6$$

Lipkin et al applied the Simon's exterior-scaling procedure to model systems within the framework of the finite-basis-set approximation.[43] Within the framework of basis-set approximation, the basis itself, rather than the Hamiltonian is scaled. Therefore in the case of exterior scaling, the orthonormal basis functions are given by

$$\tilde{\Phi}_i = \begin{cases} \Phi_i(r) \quad if \quad r < r_0 \\ e^{-i\theta/2}\Phi_i\left((r-r_0)e^{-i\theta} + r_0\right) \quad if \quad r \geq r_0. \end{cases} \qquad 1.4.7$$

In the spirit of Simon's proposition, to avoid the need of carrying out analytical continuation of the potential term in the Hamiltonian into the complex coordinate plane Rom and coworkers proposed a smooth exterior scaling path which is defined as [44]

$$f(r) = \frac{\partial F(r)}{\partial r} = 1 + (e^{i\theta} - 1)g(r) \qquad 1.4.8$$

where $F(x)$ is a path in the complex coordinate plane such that.

$$F(r) \to re^{i\theta} \quad as \quad r \to \infty \qquad 1.4.9$$

and $g(r)$ is varied from 0 to 1 value around the point $r = r_0$. If $V(r \geq r_0) = 0$, then one can use the unscaled potential $V(r)$. Note, however, that the path which defined in Eq 1.4.8 is very general and is not necessarily limited to the case where $V\left(f(r)\right) = V(r)$ or $V\left(f(r)\right) \sim V(r)$. Consequently, the smooth exterior scaled Hamiltonian derived by Moiseyev,[45]

$$H = \frac{-\nabla^2}{2} + V\left(F(r)\right) + V_{CAP} \qquad 1.4.10$$

where V_{CAP} is a universal energy-independent complex absorbing potential [CAP]. When the smooth exterior scaling is used, the CAP gets non-zero values in the region where the interaction potential vanishes. The complex smooth exterior scaling Hamiltonian is obtained by adding to the unscaled Hamiltonian matrix a matrix which represents the universal CAP.

In the case of a complex scaling method, using a truncated basis $\phi = \{\phi_\mu\}$ of order M, one obtains the matrix relation;

$$\bar{\boldsymbol{H}} = \bar{\boldsymbol{T}} + \bar{\boldsymbol{V}}. \qquad 1.4.11$$

However, $\bar{\boldsymbol{H}}$ has a large number of complex eigenvalues. The 'bar' notation in the matrix elements denotes the scaling, which can be either be a direct scaling approach, CCRACNA or exterior scaling techniques. In this complex 'eigenvalue galore', an important problem is to find out which complex eigenvalue may correspond to resonance states. A guiding principle is provided by the fact that, in the limiting case of an infinite complete basis, during the process of increasing the rotation angle θ, once a resonance eigen value $\boldsymbol{E}_{res}$ has been revealed, it becomes independent of complex scale factor $\eta = \boldsymbol{e}^{i\theta}$, so that

$$\frac{\partial \boldsymbol{E}_{res}}{\partial \eta} = \frac{\partial^2 \boldsymbol{E}_{res}}{\partial \eta^2} = . \quad . \quad . = 0. \qquad 1.4.12$$

In the applications using a finite basis set of order M, the resonance eigenvalue $\boldsymbol{E}_{res}$ ought hence to be fairly stationary, and-in practice- one finds then by using various types of 'stabilization graphs'. [46-48]. Some details about the stabilization technique will be discussed in Chapter 2 and a similar kind of stabilization approach can be applied for finding the resonance parameters for the CAP method and this will be discussed in Chapter 4.

If the scaling operator satisfies the mathematical condition $\left(\boldsymbol{U}^{\dagger}\right)^{-1} = \boldsymbol{U}^{*}$,then the transformed Hamiltonian becomes complex symmetric, which greatly simplifies

the theory and computer implementation. For a complex symmetry operator, if Ψ is an L^2 eigenfunction with the eigenvalue $\boldsymbol{E}$, then Ψ^* is an L^2 eigenfunction with the eigenvalue $\boldsymbol{E}^*$. This fact is of essential importance in formulating the bi-variational principle for the $\bar{\boldsymbol{H}}$ and $\bar{\boldsymbol{H}}^\dagger$.[49]. Without any lose of generality, one may further choose the basis set $\phi = \{\phi_\mu\}$ real, and for the associated matrix elements, one then obtains $\bar{\boldsymbol{H}}^\dagger = \bar{\boldsymbol{H}}^*$, i.e., $\bar{\boldsymbol{H}}$ is a symmetric matrix with complex elements, where $\bar{\boldsymbol{H}}_{kl} = \bar{\boldsymbol{H}}_{lk}$. This is of importance in simplifying the matrix calculations. In this case, the dilated Hamiltonian is a nonself-adjoint operator defined on a L^2 Hilbert space and the eigenvalue problem is treated by means of boundary conditions related to this space.

Significant strides have been made in the theoretical development and practical implementation of complex coordinate method, which permits direct simultaneous determination of position and width from the eigenvalue of a complex scaled Hamiltonian. The self-consistent-field method provides a natural starting point for the methods to solve the nonself-adjoint Hamiltonian using more exact calculations. The complex scaled SCF methods generate an adequate dilation adapted basis set. Such a computational technique has been pursued by two groups of workers. In the procedure proposed by McCurdy et al, a real Hamiltonian was used together with complex wave functions.[50,51] The resonant eigen values were obtained by a self consistent method similar the Hartree Fock Method. Another complex SCF method was proposed by Mishra et al.[52] These authors preferred to use a complex Hamiltonian with real basis functions. In such an approach they were able to carry the resonance eigenvalue calculations with small modifications of the existing code. The details about this method will be discussed in Chapter 2.

Until fairly recently, the main theoretical method for treating the analytical continuation method for the molecular Hamiltonian relied on complex scaling based methods. Finite box methods are also particularly appealing to calculate resonance widths and energies due to the quasi bound character of resonance states. Complex absorbing potentials are best for treating the electronic resonances in molecules.[34,35] The molecular Hamiltonian is perturbed by an appropriate complex potential, which enforces an absorbing boundary condition. This artificial potential absorbs the

emitted particle and consequently transforms the former continuum wavefunction into a square integrable one. CAPs were first used for this aim by Jolicard and Austin [53-56] and later by Riss and Meyer.[35,57-59] Jolicard and Austin suggested and demonstrated that the stability of the resonance eigenvalue could also be achieved by varying the strength or the location of the absorbing potential, whose job would be to absorb the perfectly outgoing Siegert state without creating any "reflection".[54] The basic concepts introduced by Jolicard and coworkers were refined and developed further by Riss and Meyer.[35] However, the most serious problems with these approaches are the conditions and approximations at which the spectrum of CAP augmented Hamiltonian resembles with the spectrum of complex scaled Hamiltonian. Unlike other methods such as complex scaling method which stays on solid mathematical ground given by Balslev, Combes and Simon,[32] the use of CAP was based on the intuition and numerical experience. It has been proved that the poles of scattering matrix are also the eigenvalues of the complex scaled Hamiltonian, but it has not been proved that they are the eigenvalues of the Hamiltonian which is perturbed by a CAP. Riss and Meyer addressed the question under what condition the resonances obtained by the CAP are the poles of the scattering matrix. Their strategy and derivation is as follows.

The eigen spectrum of a perturbed Hamiltonian

$$H(\eta) = H - i\eta W(r) \qquad 1.4.13$$

has a purely discrete spectrum, where

$$H = -\frac{1}{2}\frac{d^2}{dr^2} + V(r),\ \eta > 0 \qquad 1.4.14$$

and $W(r)$ is a piecewise continuous coulomb potential which satisfies the properties. The exact prerequisites that $W(r)$ must satisfy are derived in Ref. 35. For $\eta \to 0$, the eigenvalues of $H(\eta)$ converge towards the poles of the Green function on its physical sheet provided $\pi \geq 0 \geq \arg(E) \geq 0$. Applying a CAP is not equivalent to complex scaling: it becomes equivalent only in the limit $\eta \to 0^+$. Since this limit cannot be easily carried out unless there is a complete basis set, there is always [at finite η] nonanalytic perturbation. These large values of η causes artificial reflections. There

have been many correction schemes devised for removing the artificial reflections.[35,53] The correction process would not be necessary if reflections were avoided. Assume a $W_0(r)$ which is twice the differentiable and satisfies

$$W_0(r) = \begin{cases} = 0 & \text{for} \quad r \le r_c \\ > 0 & \text{for} \quad r > r_c \end{cases} \qquad 1.4.15$$

$W_0'(r) \ge 0$ and $W_0(r) \to \infty$ for $r \to \infty$.

The parameter r_c is the cut off parameter. For a reflection free CAP, the regular solution is identical to the exact Siegert resonance wavefunction up to r_c, and E_0 is the exact Siegert resonance energy. This perturbation is particularly undesirable on the target, so the CAP is set to zero in the vicinity of the target. There may, however, be a nonnegligible artificial perturbation of the projectile if η cannot be chosen small enough [if the basis set is too small]. Riss and Meyer proposed another method called "transformative CAP" [TCAP]. [57,58] In exchange part, it implies a modified kinetic energy instead of adding a local complex potential.

There is a connection here with the smooth exterior scaling [SES] with the "transformative CAP" [TCAP].[58-60] The TCAP and SES in fact become identical for cut-off potentials. For the TCAP method, Riss and Meyer started from the Hamiltonian perturbed by a CAP and ended up with a complex-scaled operator. Instead, For the SES method, Moiseyev started with the complex coordinate method and ended up with a non-scaled Hamiltonian perturbed by a perfectly absorbing [universal] "potential" which is energy and problem independent.[45] For a detail discussion of comparisons between the smooth exterior CAP, which is derived from a complex scaling method and the other forms artificial perturbations applied to trap the projectile, we refer to the review article by N. Moiseyev, and more references therein. The order of presentation just outlined is by no means the order in which the idea of CAP was originally developed. Historically, the subject developed in terms of

the artificial potential generated by several workers.[35,53-59] Only later was the CAP potential derived from the first principles of Quantum mechanics by N. Moiseyev [45] to provide a proper justification of the results already derived.

In addition to the calculations and methods mentioned above, the application of complex scaling and CAP methods in the framework of post Hartree -Fock method have been documented. The forthcoming chapters, while presenting the work of the thesis, review for some of the recent development in the implementation of complex scaling and CAP method in the framework of post Hartree -Fock theories.

1.5. Goal and Scope of the Thesis

In this thesis work, we shall concentrate mainly on formalism appropriate to the simplest of all the resonances, the negative ion resonances occurring in the elastic channels. The machinery for handling the more complicated resonances, e.g. the resonances in inelastic channels, will be discussed at the end of this section.

In the elastic collision experiments, the electron-atom or electron-molecule shape resonance can be thought of as metastable anionic state which decay by electron emission and the temporary anion formation in this case can be represented like

$$e + A \rightarrow \left(A^{-}\right)^{*} \rightarrow e + A . \qquad 1.5.1$$

The resonance energy of the metastable state relative to the target can be defined as

$$E_{res} = E_{\left(A^{-}\right)^{*}} - E_{A} \qquad 1.5.2$$

which is nothing but the electron affinity of the target in the complex plane. In a similar way the resonance energy of the metastable state associated with the Auger resonance

$$h\nu + A \rightarrow \left(A^{+}\right)^{*} + e$$

$$\left(A^{+}\right)^{*} \rightarrow e + A^{++} \qquad 1.5.3$$

is the ionization potential of the target system in the complex plane.[62]

$$E_{res} = E_{A} - E_{\left(A^{+}\right)^{*}} \qquad 1.5.4$$

Much of the difficulty encountered in previous theoretical treatments of electronic resonances based either on the use of the scattering matrix[63] or on the approximate expansion of the scattering wave function in a set of square-integrable basis function[26] follows from two fundamental facts. First, when focusing, within conventional Hermitian quantum mechanics, on the continuous spectrum of the Hamiltonian H of the metastable system, there exist an inherent difficulty in identifying which discrete positive eigenvalue of an approximate, finite-rank representation of H corresponds most closely to the metastable state of interest. Second, as the Siegert wave function diverges asymptotically and does not belong to the Hermitian domain of the Hamiltonian, the computational difficulties in treating such a state are potentially more severe than those encountered in the treatment of bound states. The role of correlation and relaxation in the formation and decay of metastable states has been reported.[64,65] Thus, the calculation of energy and lifetime of metastable states require the simultaneous treatment of both correlation and continuum effects. Hence, the quantum-mechanical many-body problem of this type of metastable state is very difficult to tackle. The method of analytical continuation of the Hamiltonian in the complex plane eliminates many of this difficulties.[2]

Typically, the calculation of resonances in atomic/molecular systems has been performed by numerical diagonalization of complex scaled Hamiltonian, $H(\theta)$ represented in a set of basis functions. This method has already been successfully applied to a variety of phenomena, mainly in atomic systems.[2,9,66] Despite their great success, the complex scaling method have several well known limitations, e.g. difficulty in scaling the molecular potential and the problems with the computation of resonance parameters using finite basis set. The method of using a CAP is closely related to complex scaling. The major advantage of the former is its simplicity. The CAP procedure is minimally invasive in the sense that neither the internal structure of the physical Hamiltonian is affected nor is there any need to use other basis sets than

usual real Gaussians.[67] Thus, this method offers great promise for the determination of accurate Siegert energies in a computationally viable form by a relatively straightforward modification of existing electronic structure codes for bound states.[65,67,68]

The complex scaling and CAP approach have already been successfully applied to molecular shape resonances. [35,50-52,65,68-70] It can be used at the static-exchange level,[35,52,71] but it is particularly powerful and interesting when the inclusion of electron correlation effects is considered.[64,65,67-70,72] The method of complex scaling and the CAP have been demonstrated both at the multireference configuration interaction level [MRCI] [65] and in the context of electron propagator theories.[68,72-74] Recently, a non-Hermitian Rayleigh-Schrödinger perturbation theory for the single and the multireference have also been devised using the CAP method to calculate the resoances.[75] The difference in energy between the (N+1)-electron metastable state and the N-electron target ground state gives the kinetic energy of the projectile at which the resonance occurs. However, it is well known that the configuration interaction [CI] method is not a very desirable electronic-structure technique, mainly because of the size-inextensive manner in which the dynamic correlation is included.

The Coupled Cluster [CC] theory has firmly been established in electronic structure theory as a highly accurate and reliable method for molecular structure of ground state or excited states, molecular properties and molecular spectroscopy.[76-78]. Coupled cluster based methods, with exponential wave operator, treat dynamic correlation efficiently and in a size-extensive manner.[79] Further, the multireference coupled cluster [MRCC] approach treats the non-dynamic correlation, and thus this type of method is ideal for *ab initio* electronic structure calculations.[80,83] In addition, the evaluation of energy differences can be done in a direct manner in the Fock space multireference coupled cluster [FSMRCC] method.[80,81] The eigen roots corresponding to the resonance can be obtained by diagonalizing a complex effective Hamiltonian. Although the effective Hamiltonian is a non-Hermitian matrix, this is not a problem, since the size of the matrix is small. In this context, the introduction of a CAP or complex scaling into FSMRCC theory does not introduce any additional

complexity, while in the context of CI, the analytical continuation methods makes the large CI matrix non-Hermitian.

Coupled cluster theory has already been used in describing the electron correlation effects of the target molecule in the low energy e-molecule elastic scattering based on optical potential approaches.[84-87] In the optical potential based methods, the electron-molecule scattering process is conveniently formulated by introducing an optical potential instead of checking the evolution of many particle scattering states.[88,89] This allows for treating the scattering process in a one particle picture, while all the correlation, polarization, and relaxation effects are accounted for the optical potential.

$$\boldsymbol{V_{opt} = V_{SE} + \sum(\infty) + M^{I}(E) + M^{II}(E)} \qquad 1.55$$

The optical potential is conveniently divided into an energy dependent dynamical part $[\boldsymbol{M^{I}(E) + M^{II}(E)}]$ and an energy independent static part $[\boldsymbol{V_{SE} + \sum(\infty)}.]$. The dynamical part accounts for the response of the molecule due to scattering electron. The static part describes the static exchange interaction with the electron density of the correlated target. The lowering of the resonance energy in e-N_2 collision due to use of correlated target compared to the uncorrelated target have been studied using perturbative methods, configuration interaction and coupled cluster based methods by several authors.[84-86] The formulation of optical potential will be discussed further in connection with our formulation of complex correlated independent particle potential in Chapter 5.

The general objective of the thesis is to formulate a complex scaling method and complex absorbing potential within the framework of coupled cluster theory to the direct and correlated calculations of resonance energy and width. Conceptual as well as practical aspects of this method will be studied. Specific objective and technical details of the proposed work are:

1. Formulation of the Fock space multi-reference coupled cluster [FSMRCC] based on an underlying bi-variational Hartree-Fock.

2. Formulation of an analytical continuation method in which the complex absorbing potential combined with Fock space multireference coupled cluster method for the correlated calculations of resonance energy and width.

3. Formulation of an effective one-electron correlated potential that describes the interaction of an electron with a many-electron target for the description of resonances. The correlated effective one-particle potential is derived within the frame work of FSMRCC theory and complex absorbing potential.

4. Use the formalisms developed above for the direct and correlational calculations of resonance energy and width. We will demonstrate the feasibility of the proposed methods by applying it to the resonances of the low energy region of the electron-atom/molecule collisions. The influence of correlation, dependence of scaling parameter and the strength of complex absorbing potential on the position and width of the resonance will also be discussed.

The remaining challenge, however, is to extend the above formulated methodologies to larger molecules without compromising the accuracy and reliability. Correlated wavefunction techniques such as coupled cluster theory enable the quantum chemist to make highly accurate predictions of molecular spectra, but only for small relative systems, because such calculations are very demanding computationally. This is because reaching the desired level of accuracy requires the use of quite extensive one particle basis set and the computational cost of a correlated calculation for a given system grows at least as the number of basis functions to the fourth power. For the analytic continuation procedures in which the calculations are performed for each discrete finite eta values, the computational expenditures are even worse. In analytic continuation using the CAP procedure, however, the procedure could be simplified without a corresponding increase in the computational cost; if the CAP unperturbed correlated potential for the projectile target system is used for the analytical continuation.

We conclude this chapter by examining the possibility of applying the CAP-FSMRCC / CAP-CIP [formulated in chapter 4/5] theory to the most striking phenomena, namely, *intermolecular Coulombic decay* [4] and the *core excited shape*

resonances [3,17] as the areas of interest for the future developments. For elastic scattering it is possible to formulate an effective one-particle theory. In the last part of the thesis, we have made such an attempt to formulate a potential from the coupled cluster framework of theories for the resonances in the low energy electron-molecule collisions. For low-lying shape resonances in electron-molecule scattering, the dominating configurations are of the 1p-type. Similarly, the Auger decay can be represented by the 1h-type configurations. The optical potential derived from the single valence sectors of CAP-FSMRCC/CIP-CAP method will work for resonances that have large overlap with the (1,0) model space functions [these functions are 1p type in configurations] and (0,1) model space functions [these functions are 1h type in configurations]. However, for electronically decaying holes and Feshbach resonances, this is questionable. Whenever the projectile energy coincides with excitation energy of the target, a new channel opens up. This leads to a loss in the elastic channel. The excited state configurations [from the higher order Fock space sectors] are needed for describing the many-body physics. The inelastic channels open up can in principle be described by the potential derived from the higher sectors of Fock Space Multireference calculation. Solving the CAP-FSMRCC for the higher Fock-Space sectors or deriving an energy dependent optical potential from the higher Fock-Space sectors in correlated independent particle theory would be particularly important in solving the important problems like *inter molecular columbic decay* in the columbic clusters and other Feshbach resonances which involves inelastic channels in formation and decay of resonances.

Another important aspect which is worth mentioning at this point is that the energy dependence of the wave operator used. Each Fock space sector is necessarily energy-dependent. It can only provide as many eigenvalues as there are vectors in the model space. It has been known for decades that, if one uses the Feshbach-type projection operator approach, an effective Hamiltonian active in the chosen subspace can be constructed which gives [in principle] all eigenvalues, as long as there is overlap between the subspace and the eigenvectors in the full space. However, a solution of a higher order Fock Space sector is inherently carrying the information about the lower valence sectors as the procedure is based on the sub system embedding condition. This means that if the model space functions of a higher order Fock space sector overlap with the higher energy decaying channels of the projectile-

target system, then the solution of this Fock space sector intuitively contain all low energy decaying channels too and the solutions of CAP-FSMRCC or CAP-CIP will be universally [in principle] applicable to elastic scattering even at high projectile energies. This valence-universality and the subsystem embedding condition [81] together makes higher sector of CAP-FSMRCC or the CAP-CIP model an energy independent Feshbach type model provided each sector is energetically separable. However, for a decaying hole, the situation is very different. Even if the hole can be well described by a 1h-configuration, the decay is entirely due to 2h1p and so forth. In other words, there is an infinite number of eigenstates energetically nearby that are almost completely 2h1p or higher. That means, a model space function of the low order Fock space sector is intrude by the functions from the complementary space. The mixing of these configurations from the complementary space with the model space may then be so strong that this leads to convergence problems. Instead of limiting the model space to 1h configurations, one can then extend the model space to include the 2h1p configurations also and yet it is possible still to have the intruder problem, makes the model space is enlarged to a computationally unmanageable size. Thus, the FSMRCC method for the ICD problems and other Feshbach resonances in most cases would be computationally expensive and even may not be feasible.

References

1. J. R. Taylor, *Scattering Theory: The quantum theory on nonrelativistic collisions* (John Wiley & Sons, New York ,1972)
2. W. P. Reinhardt, *Ann. Rev. Phys. Chem*. **33**, 223 (1982)
3. *The Auger effect and other radiationless transition*, edited by E. H. Burhop, (Cambridge monographs on physics, Krieger, Melbourne, 1980)
4. L. S. Cederbaum, J. Zobeley and F. Tarantelli, *Phys. Rev. Lett*. **79**, 4778 (1997); J. Zobeley, L. S. Cederbaum and F. Tarantelli, *J. Chem. Phys*. **108**, 9737 (1998); R. Santra and L. S. Cederbaum, *Phys. Rep*. **368**, 1 (2002)
5. K. D. Jordan and P. D. Burrow, *Chem. Rev*. **87**,557 (1987)
6. P.G. Burke, *Adv. At. Mol. Phys*, **4**,173 (1968)
7. H. S. Taylor, *Adv. Chem. Phys* **18**, 91 (1970)
8. R. N. Zare*, Angular momentum*, (Wiley Interscience, New.York.,1988)
9. B. D. Buckley, P. G. Burke, and C. J. Noble, in *Electon molecule collisions*, edited by I. Shimamura and K.Takayanagi.(Plenum Press New York,1984) pp.495-556.
10. Y. K. Ho, *Phys. Rep*. **99,** 2 (1983).
11. V. I. Kukulin, V. M. Krasnopol'sky, and J. Horácek, *Theory of Resonances* (Kluwer, Dordrecht, 1989).
12. N. Moiseyev, *Phys. Rep*. **302**, 211 (1998).
13. R. I. Hall and F. H. Read in *Electron molecule collisions*, edited by I. Shimamura and K. Takayanagi, (Plenum Press. New.York,1984)
14. R. K. Nesbet, Phys. Rev.**179**,60 (1969);*Variational methods in electron atom scattering; Theory*,(Plenum Press, New.York.1980)
15. N. Chandra and A. Temkin, *Phys. Rev. A* **13** 188 (1976); **14**,507 (1976)
16. D. T. Birtwistle and A. Herzenberg, *J. Phys. B*. **4,** 53 (1971)
17. H. Feshbach, *Ann. Phys*. (N.Y) **5**, 357 (1958); **19**, 287 (1962), W. Domcke, *Phys. Rep*, **208**, 97 (1991)
18. C.W. McCurdy, T. N. Rescigno and V. McKoy, *J. Phys. B*. **9**, 691,(1976); M .A. Morrison, and N. F. Lane , *Phys. Rev. A*. **12**, 2361 (1975).
19. T. N. Rescigno, C. W. McCurdy, and V. McKoy, *Chem. Phys. Lett.*. **27**, 401 (1974)

20. B. L. Schneider, M. Le. Dourneuf and Vo Ky Lan, *Phys. Rev. Lett*. **43**, 1926 (1979).
21. A.U. Hazi, T.N. Rescigno and M. Kurilla, *Phys Rev A*, **23**, 1089 (1981)
22. L. Dube and A. Herzenberg, *Phys Rev A,* **20**, 194 (1979)
23. D. T. Birtwistle and A. Herzenberg, *J. Phys. B*, **4**, 53 (1971)
24. M. Krauss and F. H. Mies, *Phys Rev A*, **1**, 1592 (1970)
25. I. Elizer, H. S. Taylor, J. K. Williams, *J. Chem. Phys*. **47,** 2165 (1967).
26. A. U. Hazi, H. S. Taylor, *Phys. Rev. A* **1**, 1109 (1970).
27. G. Gamow, *Z. Phys*. **51**, 204 (1928)
28. A. F. J. Siegert, *Phys. Rev*. 56, 750 (1939)
29. A.I. Baz', Ya.B. Zel'dovich, and A.M. Perelomov, *Scattering, Reactions, and Decays in Nonrelativistic Quantum Mechanics* (Nauka, Moscow, 1971); N. Moiseyev and J. O. Hirschfelder, J. Chem. Phys., **88**, 1063 (1988).
30. P. A. M. Dirac, *Proc. Roy. Soc. London Ser.* A**114,** 243 (1927); see also *The principles of Quantum mechanics*, (Clarendon Press, Oxford, 1958).
31. B. R. Junker, *Adv. At. Mol. Phys*. **18**, 207 (1982); *Int. J. Quantum. Chem*. **14,** No. 4 (1978) is devoted entirely to complex scaling and more references therein
32. E. Balslev and J .M. Combes, *Commun. Math. Phys*. **22,** 280 (1971); J. Aguilar and J. M. Combes, *ibid.* **22,** 269 (1971);B Simon, *ibid* . **27**, 1 (1972); B. Simon, Ann. *Math*. **97,** 247(1973)
33. C.W. McCurdy, *Autoionization: Recent Developments and Applications,* edited by A. Temkin (New York: Plenum,1985) pp153-70
34. J. G. Muga, J. P. Palao, B. Navarro, I. L. Egusquiza, *Phys, Rep*, **395**, 357(2004)
35. U.V. Riss and H.-D Meyer, *J. Phys. B.* **26**, 4503 (1993)
36. P. O. Löwdin *Adv. Quantum. Chem*. **20**, 87 (1989)
37. B. R. Junker, *Phys. Rev. Lett*. **44**, 1487 (1980)
38. J. N. Bardsley, *Int J. Quantum. Chem*, **14**, 343 (1978).
39. B. Simon, *Int J. Quantum. Chem*, **14**, 529 (1978)
40. C. W. McCurdy and T.N. Rescigno, *Phys. Rev. Lett*. **41**, 1364 (1978)
41. N. Moiseyev and C. Corcoran, *Phys. Rev. A*. **20**, 814 (1979)
42. B. Simon, *Phys Lett. A*, 71, 211, (1979)
43. N. Lipkin, N. Moiseyev and E. Brandas, *Phys. Rev. A*. **40**, 549 (1989)
44. N. Rom, E. Engdahl, N. Moiseyev, *J. Chem. Phys*. **93,** 3413 (1990)
45. N. Moiseyev, *J. Phys. B*. **31**,1431 (1998)

46. E. Brandas and P. Froelich. *Phys Rev. A* **16**, 2207 (1977)
47. P.Froelich, M. Hehenberger, E. Brandas. *Int. J. Quantum. Chem, Sym*, No **11**, 295, (1977)
48. N. Moiseyev, P. R. Certain and F. Weinhold, *Mol. Phys*. **36**, 1613 (1978)
49. P. O. Löwdin *J. Math. Phys* **24**, 70 (1983)
50. C. W. McCurdy, T. N. Rescigno, E. R. Davidson and J. G. Lauderdale, *J. Chem. Phys*. 73**,** 3268 (1980)
51. T. N. Rescigno, A. E. Orel and C. W. McCurdy, *J. Chem. Phys*. **73,** 6347 (1980).
52. M. Mishra, Y. Öhrn, and P. Froelich, *Phys. Lett* A. **84**, 4 (1981)
53. G. Jolicard, J. Humbert, *Chem. Phys*. **118,** 397 (1987)
54. G. Jolicard, E.J. Austin, *Chem. Phys. Lett*. **121**, 106 (1985)
55. G. Jolicard, E.J. Austin, *Chem. Phys*. 103, 295 (1986)
56. G. Jolicard, C. Leforestier, E. J. Austin, *J. Chem. Phys*. **88,** 1026 (1988)
57. U.V. Riss, H.D. Meyer, *J. Phys. B* **28**, 1475 (1995)
58. U.V. Riss, H.D. Meyer, *J. Phys. B* **31**, 2279 (1998)
59. U.V. Riss, H.D. Meyer, *J. Chem. Phys*. **105,** 1409, (1996)
60. N. Rom, N. Moiseyev, *J. Chem. Phys*. 99, 7703 (1993)
61. H. A. Kurtz and K. D. Jordan, *J. Phys.* B **14**, 4361 (1981)
62. M. Mishra, O. Gescinski and Y. Ohrn. *J. Chem. Phys*. **79**, 5494 (1983)
63. D. G. Truhlar, in *Modern Theoretical Chemistry,* vol. **8**, edited by G. A. Segal (Plenum, New York, 1977).
64. N. Moiseyev and F. Weinhold, *Phys. Rev. A* **20**, 27 (1979); M. N. Medikeri, and M. K. Mishra, *Adv. Quantum Chem*. **27**, 223 (1996).
65. T. Sommerfeld, U. V. Riss, H.-D. Meyer, L. S. Cederbaum, B. Engels, and H. U. Suter, *J. Phys. B* **31**, 4107 (1998).
66. R. A. Donnelly and J. Simons, J. *Chem. Phys*. **73**, 2858 (1980)
67. R. Santra and L. S. Cederbaum, *J. Chem. Phys*. **115**, 6853 (2001).
68. R. A. Donnelly, *J. Chem. Phys*. **84**, 6200 (1986)
69. T. Sommerfeld and R. Santra, *Int. J. Quantum Chem*. **82**, 218 (2001).
70. T. Sommerfeld, U. V. Riss, H.-D. Meyer, and L. S. Cederbaum, *Phys. Rev. Lett*. **79**, 1237 (1997).
71. P. Froelich and P. O. Löwdin , *J. Math. Phys*. **24**, 89 (1983)
72. M. Mishra, H.A. kurtz, O. Goscinski and Y. Öhrn, *J. Chem. Phys*. **79**, 1896(1983)
73. R. Santra and L. S. Cederbaum, J. Chem. Phys. **117**, 5511 (2002).

74. S. Feuerbacher, T. Sommerfeld, R. Santra, and L. S. Cederbaum, *J. Chem. Phys*. **118**, 6188 (2003).

75. C. Buth, R. Santra and L.S. Cederbaum, *Phys. Rev. A*. **69**, 032505 (2004)

76. F. Coester, *Nucl. Phys*. **7**,421 (1958); F. Coester and H. Kummel, *Nucl. Phys*. **17**, 477 (1960)

77. J. Cizek, *J. Chem. Phys*. **45**,4256 (1966); *Adv. Chem. Phys*. **14**, 35 (1969)

78. J. Paldus, J. Cizek, I. Shavitt, *Phys. Rev. A.* **5**, 50 (1972), J. Paldus, *J. Chem. Phys*.**77**, 303 (1977)

79. R. Offermann, W. Ey, and H. Kümmel, *Nucl. Phys*. A **273**, 349 (1976); R. Offermann, *Nucl. Phys*. A **273**, 368 (1976); W. Ey, *Nucl. Phys. A* **296**, 189 (1978).

80. D. Mukherjee and S. Pal, *Adv. Quantum. Chem*. **20**, 291 (1989)

81. U. Kaldor and M. A. Haque, *Chem. Phys. Lett*. **128**, 45 (1986); U. Kaldor and M. A. Haque, *J. Comp. Chem*. **8**, 448 (1987); D. Mukherjee, *Pramana* **12**, 1 (1979); M. A. Haque and D. Mukherjee, *J. Chem. Phys*. **80**, 5058 (1984).

82. I. Lindgren and D. Mukherjee*, Phys. Rep*. **151**, 93 (1987).

83. J. Paldus, L. Pylypow and B. Jezioroski, in *Many-body methods in Quantum Chemistry, Lecture notes in Chemistry,* edited by U. Kaldor (Springer-Verlag, 1989)Vol.**52**, p151, J. Paldus, P. Piecuch, B. Jezioroski, and L. Pylypow, in *Recent Advances in Many-Body Theories*, edited by T. L. Ainsworthy, C. E. Campbell, B. E. Clements, and E. Krotschek (Plenum, New York, 1992), Vol.**3**, p287; L. Meissner, K. Jankowski and J. Wasilewski, *Int. J. Quant. Chem*. **34**, 535 (1888)

84. H.-D. Meyer, S. Pal, and U. V. Riss, *Phys Rev A.* **46**, 186 (1992)

85. K. B. Ghose, S. Pal and H.-D. Meyer, *J. Chem. Phys*. **99**, 945 (1993)

86. S. Pal. K. B. Ghose and H.-D. Meyer, *Int. J. Quant. Chem*. **55**, 291 (1995)

87. N. Vaval and S. Pal, *Chem. Phys. Lett*. **345**, 319 (2001)

88. S. J. Bell and E. J. Squires, *Phys. Rev. Lett*. **3**, 96 (1956)

89. H.-D. Meyer, *Phys. Rev. A*. **40**, 5650 (1989)

Chapter 2

Fock Space Multireference Coupled Cluster Calculations Based on an Underlying Bi-Variational Self-Consistent Field

Abstract: The Fock space multi-reference coupled cluster based on an underlying bi-variational SCF is applied to the problem of computing complex energy associated with Auger and shape resonances in e-atom scattering. It is concluded that FSMRCC based on a bi-variational SCF provides a useful and practical approach to calculation of resonance parameters. Numerical results are presented for the ^{2}P shape resonance of Mg and Auger $1s^{-1}$ hole of Be.

2.1. Introduction

As explained in chapter 1, The resonances are characterized by the complex energy eigenvalues $Z=E-i\Gamma/2$, where E gives the position of the resonance and Γ gives the width of the resonance.[1] The corresponding eigenfunctions diverge asymptotically and do not belong to the Hermitian domain of the Hamiltonian. The dilation of atomic Hamiltonian has emerged as a practical and potentially accurate method for the calculation of resonance parameters in electron-atom scattering. [2,3,4] These methods are based on the mathematical developments of Aguilar, Balslev, Combes, and Simon. [5] The essential idea in these methods to the resonance problem is to make a transformation on Hamiltonian which results in a non-Hermitian operator,

one of the square integrable eigenfunctions of which corresponds to the resonant state. The associated complex eigenvalue then gives the position and width of the resonance or auto-ionizing state.

The dilation transformation of the electronic coordinate $r \rightarrow r\eta$, where η is a complex number, is used to make the resonance function square integrable. In atomic physics, in which particles are interacting with coulomb forces, the transformation $r \rightarrow r\eta$ is quite straightforward. For arg(η) larger then some critical values, the complex eigenvalues correspond to the resonance Z=E-iΓ/2 of H(η), are invariant to changes. i.e.

$$\frac{d^n Z}{d\eta^n} = 0; \quad n = 1,2,.. \qquad 2.1.1$$

The advantage of this method over complex continuum calculations is that the resonance eigenfunctions are square integrable and thus many existing electronic structure calculation for the bound state can be adapted to the resonance. Though conceptually simple, difficulties may arise in treating molecular systems using complex scaling method. [6] Introduction of an absorbing boundary condition in the exterior region of the molecular scattered target using a complex absorbing potential (CAP) [7] may be an alternative and numerically simpler route to solve resonance of the molecules. CAP potentials have been applied to molecules in the context of configuration interaction and electron propagator techniques. [8]

A complex SCF [9] technique, also called bi-variational SCF [10,11] has been attempted to calculate many electron atomic or molecular resonances. In these calculations the resonance energies and width are calculated as a difference between the ground state total energies of the (N±1) and the neutral target. The total energy of the ion is stabilized with respect to scale parameter η while the total energy of the neutral target is assumed to be stable for η=1.0. The resonant energy eigenvalues were obtained by a SCF method in a manner very similar to standard SCF technique. Mishra *et al.* [12] showed that a crude approximation of the resonance eigenvalues can be deduced using Koopmans` theorem once the complex energies for all orbitals are obtained. The ionization potential / electron affinity studies using Koopmans`

theorem provide with the simultaneous calculation of both energy (real part) and width (twice the imaginary part) of electron detachment Auger resonance (E_0^N-E_s^{N-1}) and electron attachment shape resonance (E_s^{N+1}-E_0^N), where s labels a stationary state and E_0^N is the ground state total energy of the neutral N-electron target. In this case, any stabilization is attributed to the total energies of the corresponding N±1 system. The resonance eigenvalues obtained by the Koopmans` theorem can always be modified by correlation studies.

The role of correlation and relaxation in the formation and decay of metastable states has been reported. [13] The accuracy of the SCF approximations in the case of an electron scattering resonance depends on the extent to which the electron correlation is important in the description of particular states. This can be achieved by an effective Hamiltonian, which corrects for the inadequacies of bi-variationaly obtained Hartree-Fock operator. Thus complex SCF calculations on resonance will provide the best starting point for more accurate calculations.

The Fock space multireference coupled cluster (FSMRCC) [14-16] method has been quite successful in the calculation of electron affinity and ionization potential. In this chapter, we formulate a FSMRCC method based on the complex SCF for the first time to the direct and correlated calculations of resonance energy and width. This can describe the dynamic and non-dynamic electron correlation efficiently in the ionized or electron attached states. The MRCC method is based on a pre-chosen model space and the main ionizations can be conveniently described using a model space of important (N-1) electron determinants and an appropriate exponential wave operator to describe the dynamic electron correlation. Diagonalization of an effective Hamiltonian[17] over the model space provides the multiple roots of the state. Using the restricted Hartree-Fock of N-electron system as vacuum, the (N-1) electron determinants constitute one-hole Fock space. Similarly with one-particle model space, electron affinity can be determined. The Bloch effective Hamiltonian[18] has been used quite successfully in the FSMRCC method to describe ionization potential, electron affinity and excitation energies. Quite clearly, a complex scaled FSMRCC can be a potentially powerful candidate to compute resonance energies and the width of the resonances.

In this chapter we present resonant parameters and optimal scaling values obtained by FSMRCC method. The $1s^{-1}$ hole in Be leads to a KLL Auger resonance and has been studied both experimentally and theoretically. [12,19,20] The ^2P shape resonance in e-Mg scattering serves as a problem for checking the theoretical scheme for the treatment of shape resonance and has been studied extensively. [9,21,22] We have utilized a (10s/6p) CGTO [10] and a (14s/11p) CGTO [23a] bases for Be and a (4s/9p) CGTO [23b] bases for Mg since other theoretical results are available in these basis.

The section 2.2 contains a brief outline of the bi-variational SCF method which serves as a starting point of our MRCC method to compute the resonance. In section 2.3 we will develop the FSMRCC technique to compute resonance energy and a trajectory method to singling out the resonance orbital. In section 2.4 we will present our results for the calculation of $1s^{-1}$ Auger hole in Be and ^2P shape resonance in Mg. Further improvement in the characterization of the resonance using MRCC methods are presented in the concluding section.

2.2. Bi-Variational SCF

In the complex self-consistent field method (bi-variational SCF) proposed by Mishra et al. [10], a complex Hamiltonian was used together with real basis functions. The difference between usual Hartree-Fock theory and bi-variational SCF is that in the latter, the energies of various orbitals are now complex. For the complex values of the dilation parameter η, the dilated atomic Hamiltonian

$$\boldsymbol{H}(\eta) = \sum_i (\frac{1}{2}\eta^2\nabla_i^2 - \eta\frac{\boldsymbol{Z}}{\boldsymbol{r}_i}) + \sum_{i<j}\eta\frac{1}{\boldsymbol{r}_{ij}}; \qquad \eta = \alpha \boldsymbol{e}^{-i\theta} \qquad 2.2.1$$

is non-Hermitian, and therefore variational theorem does not apply. However, a bi-variational theorem for non-Hermitian operators can be applied and the bi-variational SCF equations for the complex scaled Hamiltonians are derived by extremizing the generalized functional.

$$\varepsilon(\Phi_0, \Psi_0) = \langle \Phi_0 | H(\eta) | \Psi_0 \rangle / \langle \Phi_0 | \Psi_0 \rangle \qquad 2.2.2$$

The trial functions Φ_0 and Ψ_0 are built from linearly independent one-particle functions or spinorbitals:

$$\Phi_0 = (N!)^{-1/2} \det\{\phi_i(x_i)\}, \quad 2.2.3$$

$$\Psi_0 = (N!)^{-1/2} \det\{\psi_j(x_j)\}, \quad 2.2.4$$

where the indices i and j go from 1 to N.

The sets $\{\phi_I\}_1^M$ (,and $\{\varphi_I\}_1^M$ (M≥N) of spin orbitals are biorthonormal,

$$\left\langle \phi_i \middle| \psi_j \right\rangle = \delta_{ij} \quad 2.2.5$$

Extremization of the functional in Eq. 2.2.2 results in the following SCF equations:

$$F^{\dagger}\phi_i = \varepsilon^*_i \phi_i \quad 2.2.6$$

$$F\psi_i = \varepsilon_i \psi_i \quad 2.2.7$$

where

$$F_1(\eta,\psi,\phi) = -\frac{1}{2}\eta^2\nabla_1^2 - \eta Z/r_1 + \eta\int_{x_2'=x_2} \frac{1-p_{12}}{r_{12}}\rho(x_2,x_2')dx_2 \quad 2.2.8$$

$$\rho = \sum_i^{occ} \psi_i \phi_i^* \quad 2.2.9$$

The complex symmetry nature of the dilated Hamiltonian $H^+(\eta)=H^*(\eta)$ suggests the dual choice of basis Φ and Ψ having the property $\Phi=\Psi^*$ and the consequent association $\{\varphi_i\}=\{\phi^*_i\}$ to make the approximate many-electron wave function satisfy same relation as the exact one. The advantages of this assumption $\{\varphi_i\}=\{\phi^*_i\}$ and the details of the implementation of the bi-variational SCF procedure are given in Ref. 10.

2.3. Fock Space MRCC Method to Calculate Resonance

We choose the restricted Hartree-Fock determinant for N electron as the vacuum. With respect to this vacuum, holes and particles are defined. Depending on the energies of interest, these are further divided into active and inactive set such that each determinant ϕ_I of the model space has at least one active particle For an (N+1)/(N-1) electron state, the model space consists of determinants consisting of one active particle/hole. These are called one-particle or one-hole model space. The active particles or holes can be so defined as to make the model space complete.

$$\Psi_{\mu}^{0(1,0)} = \sum_{i \in ap} c_{\mu i} \Phi_i \qquad 2.3.1$$

where, (1,0) denotes one active particle and zero active holes present in the model space determinants $\{\phi_I\}$. $C_{\mu i}$ are the model space coefficients. The exact wavefunction can be written in the Fock space method using Lindgren`s normal ordered ansatz [16] as,

$$\Psi_{\mu}^{(1,0)} = \Omega \Psi_{\mu}^{(0)(1,0)} \qquad 2.3.2$$

$$\Omega = \{e^{\tilde{T}^{(1,0)}}\} \qquad 2.3.3$$

where, Ω is a valence-universal wave operator, and the curly bracket denotes operator within it to be normally ordered. The valence-universality of the wave operator ensures connectivity and size-extensivity of the Fock space Bloch equations. To ensure this, $\tilde{T}^{(1,0)}$ is defined to contain the amplitudes for lower valence sectors too. Hence the T`s used are capable of describing the problem consisting of lower valence electrons.

$$\tilde{\boldsymbol{T}}^{(1,0)} = \boldsymbol{T}^{(0,0)} + \boldsymbol{T}^{(1,0)} \qquad 2.3.4$$

where $T^{(0,0)}$ is only a hole-particle creation operator and $T^{(1,0)}$ operator destroy exactly one valence particle in the model space. Each of these T's can be written as sum of different n-body operators. If the one-body scaling term is introduced in the Hartree-Fock level, the Fock space MRCC theory has a complex vacuum and consequently

the complex molecular orbitals dictate that the T-operator for all the sectors will be complex.

$$\boldsymbol{T}^{(0,0)} = \sum_{\boldsymbol{n}} \boldsymbol{T}_{\boldsymbol{n}}^{(0,0)} \qquad 2.3.5$$

$$\boldsymbol{T}^{(1,0)} = \sum_{n} \boldsymbol{T}_{n}^{(1,0)} \qquad 2.3.6$$

To calculate the electron affinity, we substitute the wave function into Schrödinger equation for the multiple roots of the (N+1) electron states. The roots are obtained as eigenvalues of the effective Hamiltonian [17] defined over the model space. The model space and the wave operator Ω are obtained by the Bloch equation [18] projected to the (1,0) model space as well as its lower sector, in this case (0,0) sector.

$$\boldsymbol{H}^{(1,0)}_{\boldsymbol{eff}}\boldsymbol{C} = \boldsymbol{CE} \qquad 2.3.7$$

$$\boldsymbol{Q}^{(\boldsymbol{m},\boldsymbol{n})}\boldsymbol{H}\Omega\boldsymbol{P}^{(\boldsymbol{m},\boldsymbol{n})} = \boldsymbol{Q}^{(\boldsymbol{m},\boldsymbol{n})}\Omega\boldsymbol{H}_{\boldsymbol{eff}}\boldsymbol{P}^{(\boldsymbol{m},\boldsymbol{n})} \qquad 2.3.8$$
$$\forall \boldsymbol{m} = 0,1 \qquad \forall \boldsymbol{n} = 0,1$$

$$\boldsymbol{P}^{(\boldsymbol{m},\boldsymbol{n})}\boldsymbol{H}\Omega\boldsymbol{P}^{(\boldsymbol{m},\boldsymbol{n})} = \boldsymbol{P}^{(\boldsymbol{m},\boldsymbol{n})}\Omega\boldsymbol{H}_{\boldsymbol{eff}}\boldsymbol{P}^{(\boldsymbol{m},\boldsymbol{n})} \qquad 2.3.9$$
$$\forall \boldsymbol{m} = 0,1 \qquad \forall \boldsymbol{n} = 0,1$$

The Eigenvalues of the H_{eff}'s, E_μ's, are the exact energies of the system. Equations for cluster amplitudes are solved using subsystem embedding condition i.e., first equations for lowest sector are solved. With the T's of the lower sectors as constants, equations for higher Fock space sectors are solved progressively upwards. Normal ordering and subsystem embedding condition together decouple the equations for each Fock space sector. The solution of the Bloch equation defines the effective Hamiltonian over the model space. It has dimension same as model space dimension and eigenvalues correspond to the exact energies of the system i.e. EA of the system. The vacuum expectation value of the effective Hamiltonian is the energy of the closed shell N-electron state or zero-valence problem. Diagrammatically, this can be dropped easily and the eigenvalues of the resultant effective Hamiltonian of one valance Fock space sector provides us with direct difference energies. However, the

effective Hamiltonian is a complex non-Hermitian matrix, in general. In a similar manner, we can solve the MRCC equations for (0,1) sector of the model space and can carry out the IP calculations. In this chapter, we have used a singles and doubles approximation for the cluster amplitudes of both zero and one valence sector. This FSMRCCSD approximation has been noted to be quite accurate for the purpose of IP/ EA calculation. However, one may note that in the FSMRCC method of computing direct difference energies, the energy of the ground state is computed with the scaled Hamiltonian. This is a result of the direct evaluation of the difference energies. The dependence of the electron affinity/ionization potential as well as the ground state energy with the scaling parameter is worth investigating. We may note that the dependence on the scaling parameter is a feature with all methods, which obtain these difference energies in a direct manner. The dependence of the scaling parameter is, however, manifestation of the finite basis set as we will be discussed in the next section.

2.4. The Trajectory Method for Resonance Energies and Width by the EA /IP Search.

Aguilar, Balslev, Combes and Simon [5] have studied the transformations of the spectrum of the Hamiltonian for an N+1 particle system under complex scaling. The spectrum is transformed in such a way that the resonance states become isolated in the complex energy plane. Based on these spectrum transformation results, the EA= $E_n^{N+1}(\eta) - E_0^N$ obtained from MRCC calculations may be classified as follows.

(1) Bound state eigenvalues and scattering thresholds are invariant of η and if n denotes a bound state $E_nN^{+1}(\eta)$ is real and persistent. Therefore $E_n^{N+1}(\eta) - E_0^N$ is a persistent real energy.

(2) As continua rotate as a function of η, complex eigenvalues may be exposed. These eigenvalues are independent of η as long as they are isolated from continuum. These complex energies correspond to resonances. If n denotes a resonant (metastable state) of the ion, $E_n^{N+1}(\eta)= E_r^{N+1} -i\Gamma/2$ and the corresponding energy

difference $E_n^{N+1}(\eta) - E_0^N = (E_r^{N+1}(\eta) - E_0^N) - i\Gamma/2$ gives the position(real part) and half width(imaginary part) of the resonances.

A similar analysis may be carried out for the ionization potential to calculate the position and width of Auger resonance. With this brief discussion of the calculation of energy differences as a common background, its utility in direct and simultaneous treatment of resonances of N±1 electron systems becomes manifest.

While the EA/IP corresponding to the resonance is persistent once uncovered and should be invariant to further changes in the complex scaling parameter, applications employing the manageable basis sets do not fulfill the condition.

$$\frac{d^k y}{d\eta^k} = 0 \qquad \forall k = 1,2,3... \qquad 2.4.1$$

This condition for total stability is instead seen to manifest itself as quasistability in short range of η . The stability of resonance is then examined through the following relation:

$$\partial Z/\partial \eta = 0 \qquad 2.4.2$$

and for $\eta = \alpha e^{-i\theta}$ one has the reciprocity relations:

$$(\partial Z/\partial \theta)_{\alpha opt} = -i\eta\,(\partial Z/\partial \eta) = 0 \qquad 2.4.3$$

and

$$(\partial Z/\partial \alpha)_{\theta opt} = i\eta/\alpha\,(\partial Z/\partial \eta) = 0 \qquad 2.4.4$$

Eq. 2.4.3 can be solved by plotting θ trajectory, which is a graphical method in which resonance energy Z is plotted as a function of θ, holding α fixed. In a similar way Eq. 2.4.4 can also be solved. The stationary point along the trajectories which satisfies the complex form of virial theorem corresponds to slowing down (closing of distance between consecutive points) or cusps of these trajectories. The tedious and expensive graphical solutions of equations 2.4.3 and 2.4.4 is the principal bane of complex coordinate calculations.

2.5. Results and Discussion

2.5.1. The $1s^{-1}$ Auger Hole in Be

The $1s^{-1}$ Auger hole in Be is studied by checking the ionization potential calculations using FSMRCC method for various scaling parameters. A comparative study of θ trajectories between the uncorrelated SCF and FSMRCC for the α =0.85 is shown in Fig. 2.1 using 10s/6p basis set. The noticeable difference between the two trajectories shows the need for the inclusion of correlation and relaxation in the study of Auger resonances. It is seen that by including the correlation, the energy is lowered. This can be due to the additional screening of nucleus by other electrons. The positive imaginary part coming in the bi-variational SCF level away from the optimum values of the scaling parameter may be due to the instability of complex SCF and use of finite basis set. The θ trajectories for α=0.80, 0.85, 0.90 and 0.95 are shown in Fig. 2.2 The slowing down accompanied by a small cusp is seen in the trajectories for α=0.90 and 0.95. To determine the optimal value of alpha we next examine the alpha trajectories (Fig. 2.3) for θ=0.08, 0.09, and 0.10rad. These trajectories displays a coalescence of the points near the α=0.90 and this value of alpha is taken as the optimal value. After the optimal point, the trajectories show monotonous increase of distance between the consecutive points. The values for the energy and width obtained by various theoretical and experimental methods are shown in Table 2.1. Our results also show a good agreement with these results. We have done similar calculations using the 14s/11p basis set. The alpha trajectories for these calculations are shown in Fig. 2.4. The optimum value of the scaling parameters (α_{opt}=0.75 to 0.78, θ_{opt}=0.26rad) for this basis set is different from that of 10s/6p basis used. The results we got using this higher basis set is more close to experimental result and higher order dilated -propagator theory results. The trajectories plotted by using higher basis sets are more stable than that of lower basis set and showing less dependence of scaling parameters near the resonant point.

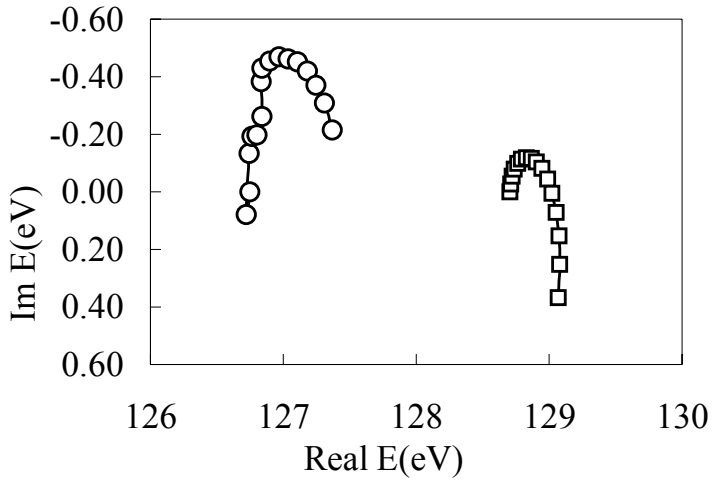

Figure 2.1 The θ trajectory (10s/6p basis) for the Auger $1s^{-1}$ hole in Be. α =0.85 and θ increments are in the steps of 0.02rad. The θ values begin with 0.0rad for the Im E =0.0 eV. SCF (—□—); FSMRCC (—O—)

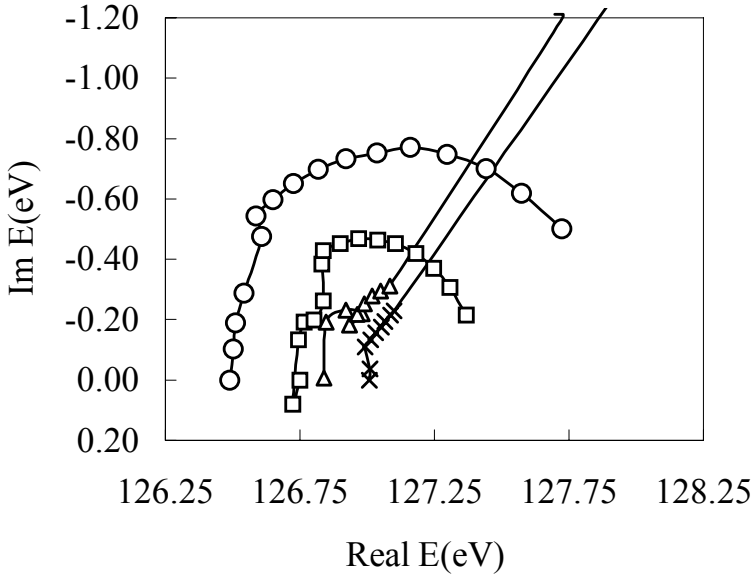

Figure 2.2 The θ trajectory(10s/6p basis) for the Auger $1s^{-1}$ in Be. θ increments are in the steps of 0.02rad. The θ values begin with 0.0rad for the Im E=0.0 eV. α =0.80(—O—); α =0.85(—□—); α =0.90(—Δ—); α =0.95(—×—)

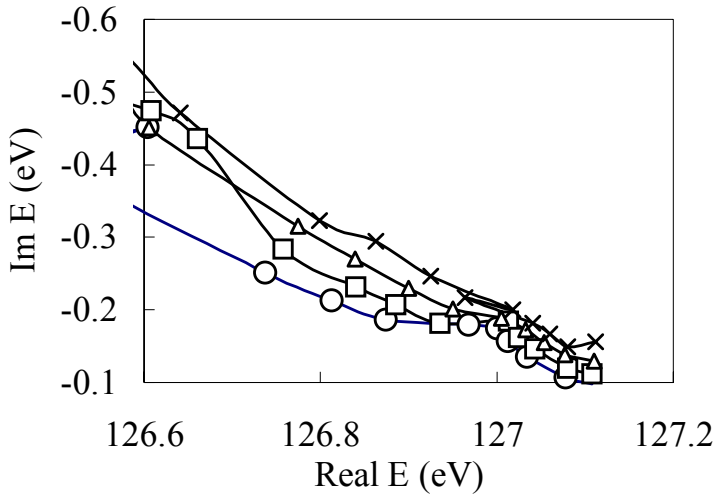

Figure 2.3 The α trajectory(10s/6pbasis) for the Auger $1s^{-1}$ hole in Be. α increments are in the steps of 0.2. The trajectories starts from the right for the α value=1.00; θ =0.07rad (—○—); θ=0.08rad (—□—); θ =0.09rad (—Δ—); θ =0.10rad (—×—)

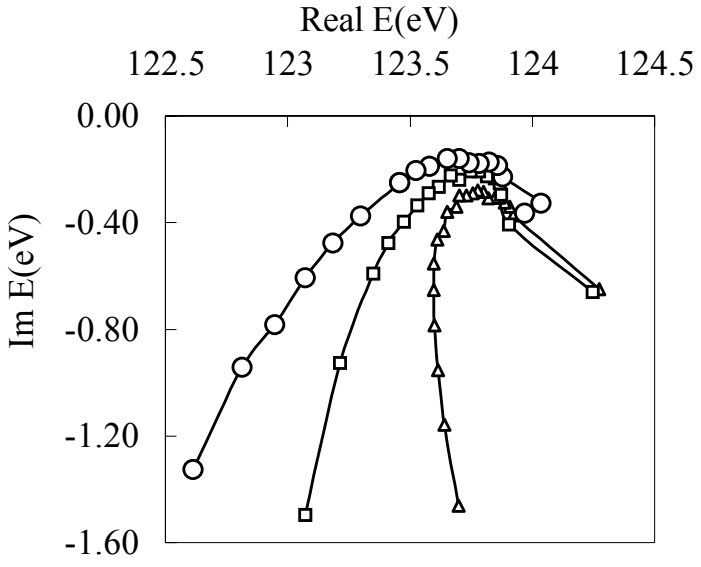

Figure 2.4 The α trajectories (14s/11p basis) for the Auger $1s^{-1}$ hole in Be. α increments are in the steps of 0.02. The trajectories start from the bottom part for the initial value of α=0.62 . θ =0.24rad (—○—); θ =0.26rad (—□—); θ =0.29rad (—Δ—)

Table 2.1 Energy and width of Be^{+} $(1s^{-1})$ ^{2}S Auger resonance

Method	Energy(eV)	Width(eV)
Experiment [25]	123.63	---
Many body Perturbation Theory [19]	----	0.09
Second Order Dilated electron Propagator [26]	124.98	0.05
Quasiparticle Diagonal 2ph-TDA Dilated Electron propagator [27]	127.90	0.54
Zeroth Order Dilated electron Propagator [27]	128.80	0.24
Second order electron propagator with Siegert boundary condition [20]	125.47	0.02
Third order decoupling of dilated electron Propagator (14s/11p basis) [23a]	124.63	0.76
Fock space MRCC based on bi-variational SCF(this work)		
10s/6p basis	126.97	0.38
14s/11p basis	123.82	0.45

2.5.2. ^{2} P shape Resonance in Mg

The shape resonances belong to the continua attached to the first threshold of the target and are easiest to analyze. The alkaline earth element Mg has P-type orbital as the lowest unoccupied orbital. These p orbitals are ideally suited for providing centrifugal angular momentum barrier of adequate width and depth to temporarily trap the impinging electron. We have performed a series of calculations with different values of scaling parameter alpha and theta on this system, which employs a 4s/9p basis of real valued Gaussian functions.

The results obtained from experiment and various theoretical methods and for e-Mg Scattering are collected in Table 2.2. Our result for energies and width are in good agreement with experimental and other theoretical methods. In a MRCC calculation using the complex Hamiltonian H({ηr}),there is a stationary behavior of the complex electron affinity with respect to variation of the theta and alpha to be expected ,at some value of θ and α, $\partial E/\partial\theta$ and $\partial E/\partial\alpha$ vanishes respectively. However, in calculations utilizing a limited basis sets only quasi-stability in a narrow region of alpha and theta values are observed. The resonances are identified by plotting the complex electron affinity as a function of theta (theta trajectory) for alpha values near the optimal values and the quasi-stable region in the trajectory is associated with resonance energy (real part) and half width (imaginary part). The same way alpha trajectories are also constructed for theta values near the optimal values.

The lowering of both the energy and width near the stationary point in the theta trajectories shown in Fig. 2.5 and Fig 2.6 seems to indicate that relaxation of the target helps the impinging electron to see more nuclear attraction (lower energy),whereby it spends more time in the vicinity of he target(has smaller width). This is reflected in our MRCC calculations by the cusp near the stationary points in the trajectories.

MRCC calculations also shows some of the notable features of stabilization method [24] that at the point of optimal stabilization of the resonant root there is an avoided crossing with another nearly degenerate root which descends from above and replaces the stabilization root when further changes in the stabilization parameter is affected. The two theta trajectories in Fig. 2.7 corresponds to two different scattering roots approaches to each other from the opposite direction in the complex energy plane and there is almost an avoided crossing near the resonance. These trajectories are corresponding to different orbitals and display an identical resonance behavior near the crossing point. The wave packet nature of the incoming electron beam can explain the multiple resonant roots. The key idea of the stabilization theory is that the resonances are localized inside the potential barrier. The wave packet is made up of many waves falling within the width of the packet center. As such, orbital bases of

the kind employed here with nearly degenerate orbital energies in close proximity to the resonance energy will give rise to different roots describing the different roots of the packet whose width is determined by the width of the widest root.

The optimum value of α (α_{opt} =0.72 to 0.75) is same as that of the dilated electron propagator calculation [21] which is also based on an underlying bi-variational SCF. But our method needs a larger rotation to uncover resonance (θ^{MRCC}_{opt}=.26rad to .30rad, $\theta^{propagator}_{opt}$=.12rad). This may be due to the high theta dependency of the ground state energy of the n electron target, $E_n(\theta_{opt})$.

Table 2.2 Energy and Width of ^{2}P shape resonance in e-Mg Scattering

Method	Energy(eV)	Width(eV)
Experiment [28]	0.15	0.13
Static Exchange Phase shift [29]	0.46	1.37
Static Exchange plus Polarizability Phase Shift [29]	0.16	0.24
Static Exchange cross Section [30]	0.91	2.30
Static Exchange plus Polarizability cross Section [30]	0.19	0.30
S-Matrix pole(x alpha) [31]	0.08	0.17
Second Order biorthogonal Dilated electron propagator [32]	0.15	0.13
Complex SCF [33]	0.51	0.54
CI [33]	0.20	0.23
Fock Space MRCC calculation based on Bi-variational SCF [this work]	0.13	0.18

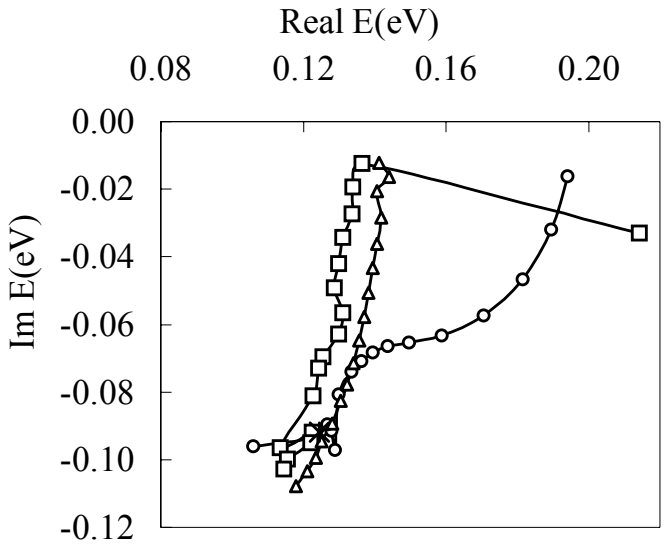

Figure 2.5 The θ trajectories for the ^{2}P shape resonance in Mg^{--}. Initial value of θ=0.02 rad and its starts from the top. θ increments are in the steps of 0.02 rad. The average value near the converged points is marked as α=0.72(—Δ —); α=0.73(—□—); α=0.75(—○—)

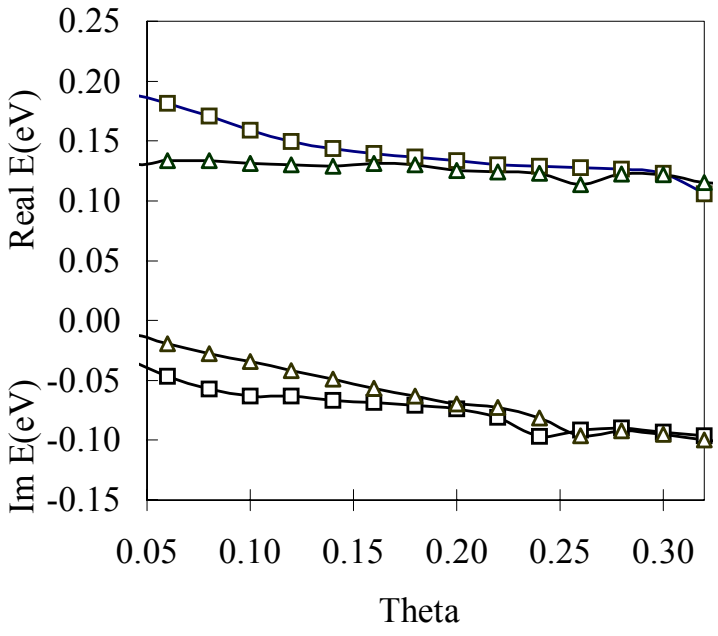

Figure 2.6 Variation of Real(E) and Im(E) with respect to θ; α=0.72(—Δ —); α=0.73(—□—)

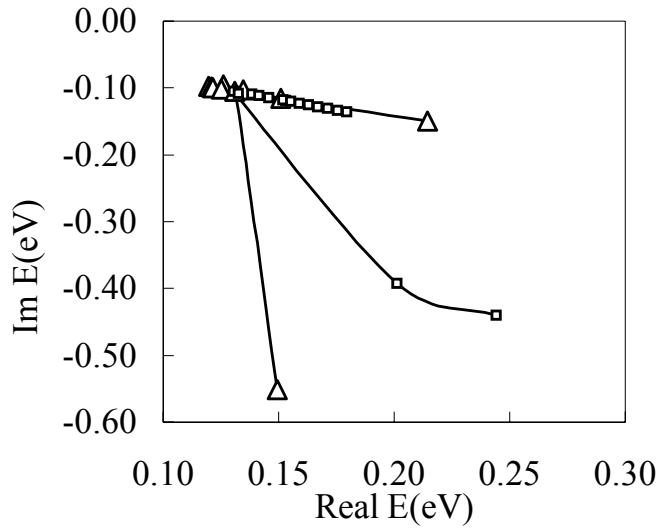

Figure 2.7 The θ trajectories for multiple resonant roots. Root I (—□— : α initial=0.7, α increment=0.01) starts from bottom right and root II (—Δ — : α initial=0.65, α increment=0.01)starts from top right.

2.6. Concluding Remarks

The electron correlation and relaxation effects are playing a substantial role in the formation and decay of resonance. The description of the resonance energy levels at the bi-variational SCF level is included only to discriminate the correlation and relaxation effects characterize the resonance.

The basic purpose of our work is to use a highly correlated Fock space MRCC method using complex scaling to compute ionization potential/electron affinity, and thus to provide a method to obtain more accurate energy and width of the resonance. Our results show the correlation and relaxation effects in the calculation of resonance.

References

1. W.P. Reinhardt, *Ann. Rev. Phys. Chem*. **33,** 323 (1982)
2. B.R. Junker, *Adv. At. Mol. Phys*. **18**, 207 (1982)
3. Y.K. Ho, *Phys. Repts*. **99,** 2 (1983)
4. *Int. J. Quantum. Chem*. **14,** No. 4 (1978) is devoted entirely to complex scaling and more references therein.
5. E. Balslev and J .M . Combes, *Commun. Math. Phys*. **22,** 280 (1971); J. Aguilar and J. M. Combes, *ibid.* **22,** 269 (1971);B Simon, *ibid.*.**27**, 1 (1972); B. Simon, Ann. *Math*. **97,** 247(1973)
6. C.W. McCurdy, *Autoionization: Recent Developments and Applications,* edited by A. Temkin (New York: Plenum,1985) pp153-70
7. U.V. Riss and H.-D Meyer, *J. Phys. B* **26**, 4503 (1993); R. Santra and L. S. Cederbaum, *J.Chem. Phys*. **115**,6853 (2001)
8. R. Santra and L. S. Cederbaum, *J. Chem. Phys*. **117**, 5511 (2002); S. Feuerbacher, T. Sommerfeld, R. Santra and L.S. Cederbaum, *J. Chem. Phys*. **118**, 6188 (2003); T. Sommereld, U.V. Riss, H.-D. Meyer, L.S. Cederbaum, B. Engels and H.U. Suter, *J. Phys. B*, **31**, 4107 (1998)
9. C. W. McCurdy, T. N. Rescigno, E. R. Davidson, and J.G. Lauderdale, *J. Chem. Phys*. **75**, 1835 (1981)
10. M. Mishra, Y. Öhrrn, and P. Froelich, *Phys. Lett.* A. **84**, 4 (1981)
11. P. Froelich and P. O. Lowdin, *J. Math. Phys*. **24**, 89 (1983)
12. M. Mishra, O. Goscinski and Y.Öhrrn, *J. Chem. Phys*. **79**, 5494 (1983)
13. N. Moiseyev and F Weinhold, *Phys. Rev. A*. **20**, 27 (1979)
14. R. Offerman, W. Ey, and H. Kummel, *Nucl. Phys. A*. **273**, 349 (1976); R. Offerman, *Nucl. Phys*. *A*.**273**, 368 (1976); W.Ey, *Nucl. Phys. A*. **296**, 189 (1978)
15. D. Mukherjee and S. Pal, *Adv. Quantum. Chem*. **20**, 291(1989); S. Pal, M. Rittby, R. J. Bartlett, D. Sinha and D. Mukherjee, *J. Chem. Phys*. **88**, 4357 (1988); U. Kaldor and M.A. Haque, *Chem. Phys. Lett*. **128**, 45 (1986); U. Kaldor and M.A. Haque, *J. Comp. Chem*. **8**, 448 (1987); D. Mukherjee, *Pramana*. **12**, 1 (1979); A. Haque and D. Mukherjee, *J. Chem. Phys.,* **80**, 5088 (1984)
16. I. Lindgren*, Inter. J. Quantum. Chem*. **S12**, 33 (1978); J. *Phys. B*. **24**, 1143 (1991); Phys*. Script*. **32**, 291 (1985); I. Lindgren and D. Mukherjee, *Phys. Repts*. **151**, 93 (1987); W. Kutzelnigg*, J. Chem. Phys*. **77**, 2081 (1982); W. Kutzelnigg and H. Koch, *J. Chem. Phys*. **79**, 4315 (1983)

17. P. Durand and J. P. Malrieu, *Adv. Chem. Phys*. **67**, 321 (1987); J. P. Marlrieu, P. L. Durand and J. P. Daudey*, J. Phys. A*. **18**, 809 (1985)
18. C. Bloch, *Nucl. Phys.* **6**, 329 (1958)
19. H. P. Kelly, *Phys. Rev. A*. **11**, 556 (1975)
20. a) M. Palmquist, P. L. Altick, J. Richter, P. Winkler and R Yaris, *Phys. Rev. A*. **23**,1787(1981); b) P. Bisgard, R. Bruch, P.Dahl, and M. Rodbro, *Phys. Scr*. **17**,1931 (1978)
21. M. Mishra, H. A. kurtz, O. Goscinski and Y. Öhrn, *J. Chem. Phys*. **79**, 1896 (1983)
22. C. W. McCurdy, J. G. Lauderdale, and R. C. Mowrey , *J. Chem. Phys*. **75**, 1835 (1981)
23. a) A. Venkitnathan, S. Mahalakshmi and M.K. Mishra, *J. Chem. Phys* **114**, 35 (2001); b) R. A. Donnelly, *J. Chem. Phys*. **75**, 5414 (1982)
24. H. S. Taylor, *Adv. Chem. Phys*. **18**, 91 (1970)
25. P. Bisgard, R. Bruch, P. Dahl, B. Fatrup and M. Rodbro*, Phys. Scr*. **17**, 49 (1978); M. Robro, R. Bruch and P.Bisgard, *J. Phys. B*. **12**, 2413 (1979)
26. M. Mishra, O. Goscinski and Y. Öhrn, *J. Chem. Phys*. **79**, 5505 (1983)
27. M. N. Medikeri, M. Mishra, *Adv. Quantum. Chem*. **27,** 223 (1996)
28. P. D. Burrow, J. A. Michejda and J. Comer, *J. Phys.* B **9**, 3255 (1976)
29. H. A. Kurtz and Y. Öhrn*, Phys. Rev.* A. **19** , 43 (1979)
30. H. A. Kurtz and K.D. Jordan, *J. Phys. B*.**14**, 4361 (1981)
31. P. Krylstedt, N. Elander, E. J. Brandas, *J. Phys. B*. **21**, 3969 (1988)
32. M. N. Medikeri, J. Nair, M. Mishra, *J.Chem. Phys.,***99**, 1869 (1993)
A. U. Hazi, *J. Phys. B*. **11,** L259 (1978)

Chapter 3

A General Formalism of Fock Space Multireference Coupled Cluster Method for Investigating Electronic Resonances in Molecules

Abstract: Electron correlation and relaxation effects play a substantial role in the formation and decay of resonance states. In this chapter we formulate a complex absorbing potential combined with Fock space multireference coupled cluster method for the correlated calculations of resonance energy and width. This can describe the dynamic and non-dynamic electron correlation efficiently in the ionized or electron attached states.

3.1. Introduction

The analytical continuation of the Hamiltonian in the complex plane giving the direct access to the resonance parameters has attracted considerable attention. [1-4] The advantage of this method to investigate resonance is that the resonance parameters can be obtained by using L^2 wavefunction. This method in which the asymptotic wavefunctions are not necessarily included appears to have great computational advantage. The analytical continuation of the Hamiltonian is possible either by a complex scaling method [2-5]or by a complex absorbing potential [CAP] method.[6-8] However, difficulties arise in molecular systems and, moreover, the implementation of this method in *ab initio* codes that go beyond the one-particle level

is very difficult. [2] In a previous chapter, the combination of complex scaling with Fock space multireference coupled cluster theory was proposed, which makes use of the complex one-particle basis functions from a bi-variational self-consistent field method. [9] This has been applied to the $1s^{-1}$ Auger resonance of Be and the ^2P shape resonance in e^--Mg scattering. However, the graphical solution to optimize the complex-scaling angle θ is time-consuming and computationally expensive, as it requires the calculation of basis functions from the bi-variational self-consistent field method procedure for several scaling angles and the repetitive transformation from the atomic to the molecular orbital basis.

The idea underlying complex absorbing potentials to calculate the resonance parameters is to introduce an absorbing boundary condition in the exterior region of the molecular scattered target. In this way the wavefunction of the scattered electron becomes square-integrable. The CAP procedure is minimally invasive in the sense that neither the internal structure of the physical Hamiltonian is affected nor is there any need to use other basis sets than usual real Gaussians and thus many existing electronic structure calculations for bound states of molecule can adapt to the resonance. [10]

CAP potentials have been applied to the molecular resonances in the context of configuration interaction [CI] and electron propagator theories. [4,10,11] Recently CAP technique at the multireference configuration interaction level, has been applied to the resonance states in metastabe ions. [4,12] In these calculations the resonance energies and width are calculated as a difference between the ground state total energies of the [N±1] and the neutral target. The ionization potential/electron affinity studies provide the simultaneous calculation of both energy [real part] and width [twice the imaginary part] of electron detachment Auger resonance [E_0^N-E_s^{N-1}] and electron attachment shape resonance [E_s^{N+1}-E_0^N], where s labels a stationary state and E_0^N is the ground state total energy of the neutral N-electron target. However, it is well known that the CI method is not a very desirable electronic structure technique mainly because of size-inextensive manner in which the dynamic correlation is included. Coupled cluster [CC] based methods, with exponential wave-operator, includes this dynamic correlation efficiently and in a size-extensive manner. [13] Further, the multireference coupled cluster [MRCC] [14-16] treats the non-dynamic correlation inherent in the

ionized states and thus this class of method represents method of choice in the electronic structure calculation. In addition, the evaluation of energy differences can be done in a direct manner in the MRCC method

In shape resonances, where the trapping of the projectile electron occurs in the potential well created by low lying electronic states, target electrons are not affected dynamically, except through a minor polarization. The vertical energy difference approximation, i.e., by assuming the same geometry for (N+1) and N electron system, adopted in the above mentioned methods, determines the resonance energy, is valid for this kind of short-lived resonances, where the time delay is too small for the nuclei to relax. For longer-lived resonances, where nuclei relax before the extra electron reemitted, one has to treat the relaxation of the nuclei in the presence of electronic autoionization. When the attachment occurs in a dissociating negative-ion state, the molecule may dissociate into fragments, stabilizing the electron attachment in the process. Since there is always a chance that electron will escape [autodetach] before it is stabilized, the magnitude and variation of the lifetime of the molecule state with respect to internuclear separation are crucial in determining which process dominates.[17] Adiabatic energy differences, i.e., by assuming different geometry for neutral target and metastable states, is particular useful in this case to correlate the lifetime of the metastable state with internuclear separation.

The objective of this chapter is to formulate a method in which CAP can be combined with Fock space multireference coupled cluster [FSMRCC] method for the first time to the highly correlated calculation of resonance energy and width by calculating vertical and adiabatic energy differences. For the problem of resonance, the CAP is introduced only into the description of the N+1 electron state and the N electron ground state is described by the Hamiltonian without CAP. This use of perturbation term in correlating N+1 system only implies that adequate modifications to the FSMRCC method of energy differences need to be made. Even for the vertical energy differences, no longer the energy differences can be calculated in a direct manner. The FSMRCC method is based on a pre-chosen model space and the main ionizations and affinities can be conveniently described using a model space of important (N-1)/(N+1) electron determinants which span one-hole/one-particle Fock space with respect to a ground state restricted Hartree-Fock vacuum. Incidentally, it

has been shown that the one-valence Fock space multireference coupled cluster theory is equivalent to the equation of motion based coupled cluster theories [EOMCC]. [18] A valence-universal exponential wave-operator describes the dynamic electron correlation [14] in the FSMRCC method. Diagonalization of an effective Hamiltonian [16] over the model space provides the multiple roots of the state. The Bloch effective Hamiltonian [19] has been used quite successfully in the FSMRCC method to describe the ionization potential, electron affinity and excitation energies. Although the effective Hamiltonian is usually a non-Hermitian matrix, this is not a problem, since the size of the matrix is small. In this context, the introduction of CAP potential does not introduce any additional complexity, while in the context of CI, CAP makes the large CI-matrix non-Hermitian. Section 3.2 details the inclusion of CAP at the coupled cluster singles and doubles [CCSD] level and subsequently the introduction of CAP at the one-valence level of Fock space in the singles and doubles approximation is presented in Section 3.4. Calculations of resonances energy for both short-lived and long-lived cases are discussed.

3.2. A CCSD Formulation of H(η)

3.2.1. Form of CAP

In the treatment of CAP to electronic resonance states, electron absorption is accompanied by replacing the molecular Hamiltonian H by

$$H(\eta) = H - i\eta W \qquad 3.2.1$$

where η is a real, non-negative number referred to as CAP strength parameter. W is a local, positive semidefinite one-particle operator. In the limit $\eta \to 0^+$, H(η) defines an analytical continuation of H. Given a complete basis set, for every resonance state there exists an eigenvalue E(η) of H(η) with the property, limit $\eta \to 0^+$ $E(\eta)=E_r-i\Gamma/2$. In order to keep the target as unperturbed, we eliminate the effect of CAP on the Hartree-Fock ground state,

$$\hat{W} \to \hat{P}\hat{W}\hat{P} \qquad 3.2.2$$

where

$$\hat{P} = \sum_i |\phi_i\rangle\langle\phi_i| \qquad 3.2.3$$

The redefinition is easily accomplished by setting

$$\langle\phi_p|\hat{W}|\phi_q\rangle = 0 \qquad 3.2.4$$

if either $|\phi_p\rangle$ or $|\phi_q\rangle$ is an occupied orbital. The advantages of the above form of CAP and the details of the implementation in the post Hartree-Fock methods are given in reference. [10]

3.2.2 Formalism of CAP in CCSD Method

The second-quantized form of H(η)

$$H(\eta) = \sum_{p.q}\langle p|\hat{h}|q\rangle a_p^\dagger a_q + \frac{1}{4}\sum_{p.q,r,s}\langle pq||rs\rangle a_p^\dagger a_q^\dagger a_s a_r - i\eta\sum_{p.q}\langle p|\hat{W}|q\rangle a_p^\dagger a_q. \qquad 3.2.5$$

The normal ordering of the operator strings in the above equation will give

$$H(\eta) = \sum_{p.q}\langle p|\hat{F}|q\rangle\{a_p^\dagger a_q\} + \frac{1}{4}\sum_{p.q,r,s}\langle pq||rs\rangle\{a_p^\dagger a_q^\dagger a_s a_r\} - i\eta\sum_{p.q}\langle p|\hat{W}|q\rangle\{a_p^\dagger a_q\} + \sum_i\langle i|\hat{h}|i\rangle + \frac{1}{2}\sum_{i,j}\langle ij||ij\rangle - i\eta\sum_{i,j}\langle i|\hat{W}|j\rangle. \qquad 3.2.6$$

where { } defines the normal ordering of the operator with respect to vacuum state. The indexing convention we will use for this section is that *p*, *q*, *r* and *s* denote the orbitals which may be either occupied or unoccupied in the reference state extend over all spin orbitals; *i*, *j*, *k* and *l* refer to spin-orbitals occupied in the Hartree-Fock ground state [or some other suitably chosen state]; and *a*, *b*, *c* and *d* refer to spin-orbitals unoccupied in the reference. The first and second term on the RHS of the Eq. 3.2.6 is the normal ordered form of CAP unperturbed Hamiltonian and the fourth and fifth term together gives the Fermi vacuum expectation values of the electronic

Hamiltonian H. The last term corresponds to Fermi vacuum expectation value of CAP and by definition it is zero.

The operator H(η) can written as

$$H(\eta) = F_N + V_N - i\eta W_N + \langle \phi_0 | H | \phi_0 \rangle \qquad 3.2.7$$

$$H(\eta) = H_N - i\eta W_N + \langle \phi_0 | H | \phi_0 \rangle \qquad 3.2.8$$

$$H(\eta) = H_N(\eta) + \langle \phi_0 | H | \phi_0 \rangle \qquad 3.2.9$$

where the subscript N indicates normal ordering of all the component operator strings. Because of the complete elimination of the influence of CAP on SCF ground state,

$$\langle \phi_0 | H(\eta) | \phi_0 \rangle = \langle \phi_0 | H | \phi_0 \rangle, \qquad 3.2.10$$

$H_N(\eta)$ can be written as ,

$$H_N(\eta) = H(\eta) - \langle \phi_0 | H(\eta) | \phi_0 \rangle \qquad 3.2.11$$

i.e., the operator H(η) minus its SCF energy. In this context, the operator $H_N(\eta)$ can be viewed as a correlation operator.

The exact many particle eigenfunction $|\Psi(\eta)\rangle$ of the operator H(η) can be written as an exponential cluster operator acting on an independent particle function $|\phi_0\rangle$

$$|\Psi(\eta)\rangle = e^{T(\eta)} |\phi_0\rangle \qquad 3.2.12$$

The cluster operator T(η) consists of various n-hole n-particle excitations.

$$T(\eta) = \sum_n T_n(\eta) \qquad 3.2.13$$

Generally an n-orbital cluster operator may be defined as

$$T_n(\eta) = \left(\frac{1}{n!}\right)^2 \sum_{\substack{i,j.... \\ a,b....}} t_{ij}^{ab}(\eta) a_a^\dagger a_b^\dagger ..... a_j a_i \qquad 3.2.14$$

The eigenvalue equation of the operator H(η) can be written as

$$H(\eta) e^{T(\eta)} \left|\phi_0\right\rangle = E^{CCSD}(\eta) e^{T(\eta)} \left|\phi_0\right\rangle \qquad 3.2.15$$

The reference energy can be removed from the above equation by normal ordering the of the operator strings in the H(η), i.e.,

$$H_N(\eta) e^{T(\eta)} \left|\phi_0\right\rangle = \delta E_{corre}^{CCSD}(\eta) e^{T(\eta)} \left|\phi_0\right\rangle \qquad 3.2.16$$

where $\delta E_{corre}^{CCSD}(\eta)$ is the correlation energy which is the difference between the CAP perturbed ground state energy at the CCSD level and unperturbed Hartree-Fock ground state energy. Left multiplying the above equation by $e^{-T(\eta)}$ and subsequent left projection of this equation onto the reference and the excited determinants, one obtains the energy and amplitude equations.

$$\left\langle \phi_0 \right| e^{-T(\eta)} H_N(\eta) e^{T(\eta)} \left|\phi_0\right\rangle = \delta E_{corre}^{CCSD}(\eta) \qquad 3.2.17$$

$$\left\langle \phi_u^\beta \right| e^{-T(\eta)} H_N(\eta) e^{T(\eta)} \left|\phi_0\right\rangle = 0 \qquad 3.2.18$$

$$\langle \phi_{uv}^{\beta\gamma} | e^{-T(\eta)} H_N(\eta) e^{T(\eta)} | \phi_0 \rangle = 0 \qquad 3.2.19$$

$$\langle \phi_{uv...}^{\beta\gamma...} | e^{-T(\eta)} H_N(\eta) e^{T(\eta)} | \phi_0 \rangle = 0 \qquad 3.2.20$$

Since H(η) is at most a two-particle operator, the Hausdorff formula gives finite number of terms when replaced in the above equations.

$$e^{-T} H(\eta) e^{T} = H(\eta) + \left[H(\eta)T\right] + \frac{1}{2}\left[\left[H(\eta)T\right]T\right] + ... \qquad 3.2.21$$

where T =T(η) and we will continue this convention through out this chapter. The relevance of the formulation of CAP at the CCSD level for the calculation of resonance energy will be discussed in the Section 3.3.

3.2.3. CCSD Energy and Amplitude Equations

Using the connected cluster theorem of Cizek, [20] the CCSD [where $T=T_1+T_2$] energy and amplitude equation can be written as

$$\left\langle \phi_0 \left| H_N(\eta)[1+T_1+T_2+\frac{1}{2}T_1^2]_c \right| \phi_0 \right\rangle = \partial E_{corre}^{CCSD}(\eta) \qquad 3.2.22$$

$$\left\langle \phi_u^\beta \left| H_N(\eta)[1+T_1+T_2+\frac{1}{2}T_1^2+T_1T_2+\frac{1}{3!}T_1^3]_c \right| \phi_0 \right\rangle = 0 \qquad 3.2.23$$

$$\left\langle \phi_{uv}^{\gamma\beta} \left| H_N(\eta)[1+T_1+T_2+\frac{1}{2}T_1^2+T_1T_2+\frac{1}{3!}T_1^3 \right.\right.$$
$$\left.\left. +\frac{1}{2}T_2^2+\frac{1}{2}T_1^2T_2+\frac{1}{4!}T_1^4]_c \right| \phi_0 \right\rangle = 0 \qquad 3.2.24$$

where *c* indicates that unlinked terms must be dropped.

3.2.4. Diagrammatic Analysis and Derivation of CCSD Equations

Diagrammatic representation of basic parameters, rules for deriving and evaluating diagrams, and the diagrams contributing to CCSD energy and amplitude equations of the Hamiltonian without the CAP are well known and can be found in several publications and texts. [21] The convention we will abide for deriving CCSD diagrams and equations is that *u* and *v* will denote external holes; *i* and *j* internal holes; β and γ external particles; and *a* and *b* internal particles. The extra component diagrams necessary for CAP model and their contribution to energy and amplitude of CCSD equations are shown in Fig. 3.1. These arise from the complex operator W, which is particle-particle one-body operator. The diagram *a* in Fig. 3.1 corresponds to the matrix element of W:

$$w_a^b = \left\langle a \left| \hat{W} \right| b \right\rangle \qquad 3.2.25$$

No non-vanishing *w* containing diagrams arise when the Schrödinger equation projected onto reference state and the CCSD correlation energy is obtained as

$$\Delta E(\eta) = 2\sum_{i,a} F_a^i t_i^a + \sum_{\substack{i,j \\ a,b}} (2v_{ab}^{ij} - v_{ba}^{ij})\tau_{ij}^{ab} \qquad 3.2.26$$

where F is the Fock operator and

$$\tau_{ij}^{ab} = t_{ij}^{ab} + t_i^a t_j^b . \qquad 3.2.27$$

Diagram *b* in Fig. 3.1 represents the possible non-vanishing *w* diagrams arising from the projection of Schrödinger equation onto the singly excited determinants. These diagrams contribute to the t_1 amplitude and the final expression for the t_1 amplitude are presented in Table 3.1 . The t_2 equation obtained when projecting onto doubly excited space is simply found from Table 3.1 by replacing the external indices $[\cdots]_{uv}^{\beta\gamma}$ by $2[\cdots]_{uv}^{\beta\gamma}$ -$[\cdots]_{uv}^{\gamma\beta}$ and the W diagrams contributing to this amplitude is given in diagram *c* in Fig. 3.1. In Table 3.1, we assume summation over all repeated indices. A permutation operator of the form

$$P_{uv}^{\beta\gamma}[...]_{uv}^{\beta\gamma} = [...]_{uv}^{\beta\gamma} + [...]_{uv}^{\gamma\beta} \qquad 3.2.28$$

is used in the Table 3.1. The cluster amplitudes are complex numbers and dependent on η. The equations in Table 3.1 correspond to a unitary group approach spin integration scheme.[22]

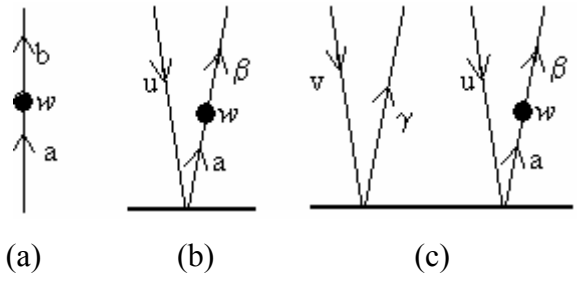

(a) (b) (c)

Figure 3.1 The diagrammatic representation of CAP and their contribution to CCSD energy and amplitude equations.

Table 3.1

CCSD equations for t_1 amplitudes

$$f_u^\beta - 2f_a^i t_i^\beta t_u^a + h_a^\beta t_u^a - h_u^i t_i^\beta + h_a^i (2t_{iu}^{\alpha\beta} - t_{ui}^{\alpha\beta} + t_u^a t_i^\beta)$$
$$+(2v_{au}^{i\beta} - v_{ua}^{i\beta})t_i^a + (2v_{ab}^{i\beta} - v_{ba}^{i\beta})\tau_{iu}^{ab} - (2v_{au}^{ij} - v_{au}^{ji})\tau_{ij}^{a\beta} = 0$$

$$h_u^i = f_u^i + (2v_{ab}^{ij} - v_{ba}^{ij})\tau_{uj}^{ab}$$

$$h_a^\beta = f_a^\beta - i\eta w_a^\beta - (2v_{ab}^{ij} - v_{ab}^{ji})\tau_{ij}^{\beta b}$$

$$h_a^i = f_a^i + (2v_{ab}^{ij} - v_{ba}^{ij})t_j^b$$

CCSD equations for t_2 amplitudes

$$v_{uv}^{\beta\gamma} + a_{uv}^{ij}\tau_{ij}^{\beta\gamma} + b_{ab}^{\beta\gamma}\tau_{uv}^{ab} - P_{uv}^{\beta\gamma}\{g_a^\beta t_{uv}^{a\gamma} - g_u^i t_{iv}^{\beta\gamma} + (v_{ua}^{\beta\gamma} - v_{ua}^{i\gamma}t_i^\beta)t_v^a$$
$$-(v_{uv}^{\beta i} + v_{ua}^{\beta i}t_v^a)t_i^\gamma + \frac{1}{2}(2j_{ua}^{\beta i} - k_{ua}^{i\beta})(2t_{iv}^{a\gamma} - t_{iv}^{\gamma a}) - \frac{1}{2}k_{ua}^{i\beta}t_{iv}^{\gamma a} - k_{ua}^{i\gamma}t_{iv}^{\beta a}\} = 0$$

$$g_u^i = h_u^i + f_a^i t_u^a + (2v_{ua}^{ij} - v_{ua}^{ji})t_j^a$$

$$g_a^\beta = h_a^\beta + f_a^i t_i^\beta + (2v_{ab}^{\beta i} - v_{ba}^{\beta i})t_i^b$$

$$a_{uv}^{ij} = v_{uv}^{ij} + v_{ua}^{ij}t_v^a + v_{av}^{ij}t_u^a + v_{ab}^{ij}\tau_{uv}^{ab}$$

$$b_{ab}^{\beta\gamma} = v_{ab}^{\beta\gamma} - v_{ab}^{\beta i}t_i^\gamma - v_{ab}^{i\gamma}t_i^\beta$$

$$j_{ua}^{\beta i} = v_{ua}^{\beta i} - v_{ua}^{ji}t_j^\beta + v_{ba}^{\beta i}t_u^b - v_{ab}^{ij}T_{uj}^{b\beta} + \frac{1}{2}(2v_{ab}^{ij} - v_{ba}^{ij})t_{uj}^{\beta b}$$

$$k_{ua}^{i\beta} = v_{ua}^{i\beta} - v_{ua}^{ij}t_j^\beta + v_{ba}^{i\beta}t_u^b - v_{ba}^{ij}T_{uj}^{b\beta}$$

$$T_{uj}^{b\beta} = \frac{1}{2}t_{uj}^{b\beta} + t_u^b t_j^\beta$$

3.3. Formalism of CAP in the FSMRCC Method

We discuss in the section CAP-FSMRCC formulation suitable for the study of electron molecule resonance. However, for the N+1 electron system, the Hamiltonian contains the CAP; while the N electron molecule uses the unperturbed Hamiltonian .We first describe the Fock space MRCC for the N+1 electron with CAP Hamiltonian. As in the normal FSMRCC, the restricted Hartree-Fock determinant $|\phi_0\rangle$ for N electron molecule corresponding to the unperturbed Hamiltonian is chosen as the vacuum. With respect to this vacuum, holes and particles are defined. Depending on the energies of interest, these are further divided into active and inactive set such that each determinant ϕ_i of the model space has m active particles and n active holes, e.g., an (N+1)/(N-1) electron state, the model space consists of determinants consisting of one active particle/hole. These are called one-particle or one-hole model space. For each sector (m,n) of Fock space, our zeroth-order wave function consists of a linear combination of model-space functions:

$$\Psi_{\mu}^{0(m,n)} = \sum_{i \in ap} C_{\mu i} \phi_i^{(m,n)} \qquad 3.3.1$$

$C_{\mu i}$ are the model space coefficients and m, n denotes the particle-hole rank of the Fock space sector. The exact [1,0] sector eigenfunctions of H(η) can be written in the Fock space method using Lindgren`s normal ordered ansatz [15] as,

$$\Psi_{\mu}^{(1,0)}(\eta) = \Omega(\eta)\Psi_{\mu}^{0(1,0)} \qquad 3.3.2$$

$$\Omega(\eta) = \{e^{\tilde{T}^{(1,0)}(\eta)}\} \qquad 3.3.3$$

where Ω(η) is the wave-operator, and the curly bracket denotes operator within it to be normally ordered. The perturbation due to CAP is incorporated while correlating the target. Hence the wave-operator and the cluster operators will be complex, while the vacuum corresponds to the RHF of the N-electron Hamiltonian without the CAP. The wave-operator in FSMRCC theory is known to be valence-universal and this ensures connectivity and size-extensivity of the Fock space equations. In general, the wave-operator for the Fock space sector of m active particles and n active holes correlates all lower active particle-active hole Fock space sectors. The cluster

operator $\tilde{T}^{(m,n)}(\eta)$ corresponding to the wave-operator for [m, n) sector is defined to consist of cluster operator for the lower Fock space sectors. Hence the T`s used are capable of describing the problem consisting of lower valence electrons.

$$\tilde{T}^{(m,n)}(\eta) = \sum_{a=0}^{m}\sum_{b=0}^{n} T^{(a,b)}(\eta) \qquad 3.3.4$$

In particular, the

$$\tilde{T}^{(1,0)}(\eta) = T^{(0,0)}(\eta) + T^{(1,0)}(\eta) \qquad 3.3.5$$

where $T^{(0,0)}(\eta)$ is the cluster operator for the single reference coupled cluster case containing only hole-particle excitation operators. In this case, however, due to CAP, $T^{(0,0)}(\eta)$ amplitudes will be complex. The $T^{(1,0)}(\eta)$ destroys exactly one active particle and is also complex.

The normal ordering of the wave-operator prevents the different T operator to contract among themselves and leads to a decoupling of the Bloch equations [19] or different sectors. Equations for cluster amplitudes for different sectors can be solved using subsystem embedding condition [SEC] [15], i.e., first equations for lowest sector are solved. With the T's of the lower sectors as constants, equations for higher Fock space sectors are solved progressively upwards. The Bloch equations for general (m, n) sector can be written as

$$\begin{aligned} &P^{(k,l)}H(\eta)\Omega(\eta)P^{(k,l)} = P^{(k,l)}\Omega(\eta)H_{eff}(\eta)P^{(k,l)} \\ &k = 0,1,...m \\ &l = 0,1,...n \end{aligned} \qquad 3.3.6$$

$$\begin{aligned} &Q^{(k,l)}H(\eta)\Omega(\eta)P^{(k,l)} = Q^{(k,l)}\Omega(\eta)H_{eff}(\eta)P^{(k,l)} \\ &k = 0,1,...m \\ &l = 0,1,...n \end{aligned} \qquad 3.3.7$$

where

$$H_{eff}(\eta) = P^{(m,n)}\Omega(\eta)^{-1}H(\eta)\Omega(\eta)P^{(m,n)} \qquad 3.3.8$$

is an effective Hamiltonian [16] whose eigenvalues determine the roots of the Fock space sector (m,n).

$$H_{eff}(\eta)C(\eta) = C(\eta)E(\eta) \qquad 3.3.9$$

Since the effective Hamiltonian is complex, one can see that model space coefficients along with the roots are complex. Thus although the model space determinants obtained from the real zeroth order Hamiltonian in the N-electron Hamiltonian are real, the model space, Ψ_{μ}^{0}, referred in Eq. 3.3.1 by virtue of the coefficients, assumes a complex character.

Introducing normal ordering for the Hamiltonian in equations 3.3.6 and 3.3.7 we get

$$\begin{aligned}[H(\eta)_N + \langle\phi_0 \mid H \mid \phi_0\rangle]\Omega(\eta)P^{(m,n)} = \Omega(\eta)P^{(m,n)}\Omega^{-1}(\eta)[H(\eta)_N \\ + \langle\phi_0 \mid H \mid \phi_0\rangle]\Omega(\eta)P^{(m,n)}\end{aligned} \qquad 3.3.10$$

$$H(\eta)_N \Omega(\eta)P^{(m,n)} = \Omega(\eta)H(\eta)_{N,eff}P^{(m,n)} \qquad 3.3.11$$

One can further show that this equation holds for connected operators only, i.e.,

$$[H(\eta)_N \Omega(\eta)]_{connected}P^{(m,n)} = [\Omega(\eta)H(\eta)_{N,eff}]_{connected}P^{(m,n)} \qquad 3.3.12$$

The Bloch equation from Eq. 3.3.11 can be written as

$$[\bar{H}(\eta)_N \bar{\Omega}(\eta)]_{connected}P^{(m,n)} = [\bar{\Omega}(\eta)\bar{H}(\eta)_{N,eff}]_{connected}P^{(m,n)} \qquad 3.3.13$$

by redefining the wave-operator

$$\bar{\Omega}(\eta) = e^{-T^{(0,0)}(\eta)}\Omega(\eta) \qquad 3.3.14$$

where the new operator, $\bar{H}(\eta)_N$,

$$\bar{H}(\eta)_N = [H(\eta)_N e^{T(\eta)}]_{connected,open}. \qquad 3.3.15$$

The vacuum expectation value of the effective Hamiltonian is the energy of the closed shell N-electron state [$E^{CCSD}(\eta)$] or zero-valence problem. Diagrammatically, this can be dropped easily and the eigenvalues of the resultant effective Hamiltonian,

$$\bar{H}_N(\eta)_{eff} = H(\eta)_{eff} - E^{CCSD}(\eta), \qquad 3.3.16$$

of one-valence Fock space sector (1,0) provides us with direct difference energies of CAP perturbed N +1 electron and N electron system, where CAP has been introduced into both the Hamiltonians

$$\Delta E_{direct}(\eta) = E^{N+1}(\eta) - E^{N}(\eta), \qquad 3.3.17$$

The direct difference energy $\Delta E_{direct}(\eta)$, obtained in this method is nothing but the vertical difference energy $\Delta E_{vertical}(\eta)$ [i.e., by assuming same geometry for N and N+1 electron system]. In a similar manner, we can solve MRCC equations for the (0,1) sector of the model space and can carry out the ionization potential calculations which gives the electron detachment Auger resonance.

Finding the CAP perturbed energy states of N+1 electron system are important, because only for the N+1 electron state we have a continuum electron present and the CAP serves to render the wavefunction of the scattered electron square-integrable. A calculation of the ground state energy of the unperturbed N electron system comes into play as soon as we want to express the resonance energy relative to the unperturbed N electron target. However, the vertical difference energy $\Delta E_{vertical}(\eta)$ obtained from Eq. 3.3.17 is not the resonance energy as it uses the perturbed ground state energy of the N electron target. If the CAP perturbation on the N electron target$[\delta E^{CCSD}_{corre}(\eta) - \delta E^{CCSD}_{corre}(\eta = 0)]$, where δE^{CCSD}_{corre} is the CCSD *correlation energy* corresponding to the ground state of N electron target as given in Eq. 3.2.16 is very small, then the vertical energy difference obtained from Eq. 3.3.17 is a good approximation to the resonance state energy of short-lived states, where the relaxation time for the nuclei is higher than that of electron passage time in electron-

molecule collisions. CAP perturbation on the target system can be removed from the vertical difference energy $\Delta E_{vertical}(\eta)$ in a consistent manner.

$$\Delta E_{vertical}(\eta) = [\Delta E_{direct}(\eta) + \delta E^{CCSD}_{corre}(\eta) - \delta E^{CCSD}_{corre}(\eta = 0)]_{\text{Evaluated for same geometry}} \quad 3.3.18$$

Elimination of this perturbation is justified in view of the fact that perturbation of the target should kept as small as possible, and it is only the diffusive unoccupied orbitals that contribute to the description of scattering electron outside the target. [10] The vertical difference energy $\Delta E_{vertical}(\eta)$ using Eq. 3.3.18, calculates the energy differences between CAP perturbed energy states of N+1 electron system and unperturbed N electron ground state energy for the same fixed geometry for N and N+1 electron systems and is the resonance energy of short lived states.

This vertical energy difference approximation is no longer valid for long-lived resonances, where the nuclei relax before the electron reemits. The adiabatic difference energy $\Delta E_{adiabatic}(\eta)$ [i.e., by assuming different geometry for N and N+1 electron system], suitable for a long-lived resonance state, can be calculated by doing direct difference energy calculation [from Eq. 3.3.17] for a geometry corresponding to an N+1 electron system and a separate CCSD calculation for a geometry corresponding to an N electron system.

$$\Delta E_{adiabatic}(\eta) = \left[E^{N+1}(\eta) \right]_{geometry=N+1} - \left[E^{CCSD}_{Nelectron}(\eta = 0) \right]_{geometry=target}$$

$$= \left[\Delta E_{direct}(\eta) + E^{CCSD}_{Nelectron}(\eta) \right]_{geometry=N+1} - \left[E^{CCSD}_{Nelectron}(\eta = 0) \right]_{geometry=target} \quad 3.3.19$$

The calculations of $\delta E^{CCSD}_{corre}(\eta)$ and $E^{CCSD}_{Nelectron}(\eta)$ are not any more computationally demanding, as the calculations make use of the redefinition of the wave-operator given in Eq. 3.3.14, which is an integral part of FSMRCCSD formulation.

The resonances can be identified by plotting η trajectories, which is a graphical method in which the energy difference $[\Delta E(\eta)]$ correspond to various energy states of interest are plotted as a function of η. The stationary point along the

trajectories which minimizes the $|\eta d(\Delta E(\eta))/d\eta|$ corresponds to the resonance. The resonance parameters correspond to short-lived states can be easily obtained by the graphical solution of the vertical energy difference $\Delta E_{vertical}(\eta)$ calculated from Eq. 3.3.18. Through a similar graphical solution, the adiabatic energy difference $\Delta E_{adiabatic}(\eta)$ [Eq. 3.3.19], which is a useful quantity in correlating life time of the long-lived resonance state with internucelar separation, corresponds to resonance can be identified.

The working equations of the $T^{(0,0)}(\eta)$ are presented diagrammatically in the earlier papers. [23] CAP-FSMRCC equations for (1,0) sector are fundamentally equivalent to those of the FSMRCC equations without the complex absorbing potentials. The contribution of CAP terms in the one-valence problem comes through the modification of $\bar{H}$ terms. The one-body particle-particle part of non-Hermitian $\bar{H}$ includes one extra term W(η), in addition to the modifcation of other terms through the appearance of complex $T^{(0,0)}(\eta)$ solved by CAP-CCSD equations presented in the Section 3.2

3.4. Concluding Remarks

The basic purpose of our work is to formulate a highly correlated FSMRCC method using a complex absorbing potential to compute complex vertical/adiabatic energy differences, and thus to provide a method to obtain more accurate energy and width of resonance. The electron correlation and relaxation effects play an important role in the formation and decay of both long- lived and short-lived metastable states. Clearly a state-of-the-art CAP/FSMRCC method should be capable of describing the above resonant states. The formulation demonstrated here and its future extensions will open up the possibility of a highly correlated ab initio treatment of electronic resonance states. Efforts along the above mentioned lines are underway in our group.

References

1. W. Domcke, *Phys. Repts*. **208**, 97 (1991)
2. W. P. Reinhardt, *Ann. Rev. Phys. Chem*. **33**, 223 (1982)
3. T. Sommerfeld, U.V. Riss, H-D. Meyer, L. S. Cederbaum, B. Engels, and H. U. Suter, *J. Phys. B.* **31**, 4107 (1998)
4. N. Moiseyev,, Phys. *Repts*. **302**, 211 (1998)
5. R. Junker, Adv. *At. Mol. Phys*., **18**, 207 (1982); Y.K. Ho, Phys. *Repts*. **99**, 1 (1983); *Int. J. Quantum. Chem*, Vol **14**, No. 4 (1978), is devoted entirely to complex scaling and more references therein
6. U. V. Riss and H –D. Meyer, *J. Phys. B.* **26**, 4503 (1993); *J. Phys. B.* **31**, 2279 (1998); N. Moiseyev, *J. Phys. B.* **31**, 1431(1998)
7. N. Moiseyev, *J. Phys. B.* **31**, 1431(1998)
8. G. Jolicard, and E. J. Austin, , *Chem. Phys.,* **103**, 295 (1986)
9. M.K. Mishra, Y. Öhrn, and P. Froelich, Phys. Lett. A **84**, 4 (1981).
10. R. Santra, and L. S. Cederbaum, J. *Chem. Phys*. **115**, 6853 (2001)
11. R. Santra, and L. S. Cederbaum, J. *Chem. Phys.* **117**, 5511 (2002); S. Feuerbacher, T. Sommerfeld, R. Santra, and L. S. Cederbaum, *J. Chem. Phys*., **118**, 6188 (2003).
12. T. Sommerfeld, U. V. Riss, H.-D. Meyer, and L. S. Cederbaum, *Phys. Rev. Lett.* **79**, 1237 (1997); T. Sommerfeld, F. Tarantelli, H.-D. Meyer, and L. S. Cederbaum, *J. Chem. Phys.,* **112**, 6635 (2000); T. Sommerfeld, *J. Phys. Chem. A.* **104**, 8806 (2000)
13. R. Offerman, W. Ey, and H. Kummel, *Nucl. Phys. A*. **273**, 349 (1976); R. Offerman, *Nucl. Phys*. *A*., **273**, 368 (1976); W. Ey, *Nucl. Phys. A*. **296**, 189 (1978).
14. D. Mukherjee, and S. Pal, Adv. *Quantum. Chem*., **20**, 291 (1989); U. Kaldor and M. A. Haque, *Chem. Phys. Lett*., **128**, 45 (1986) ; U. Kaldor, and M. A. Haque, *J. Comp. Chem*. **8**, 448 (1987); D. Mukherjee, *Pramana*. **12**,1 (1979); M. A. Haque, and D. Mukherjee, *J. Chem. Phys.* **80**, 5058 (1984).
15. I. Lindgren, *Inter. J. Quantum. Chem*. S**12**, 33 (1978); *J. Phys. B*. **24**, 1143(1991); *Phys. Script*. **32**, 291(1985); I. Lindgren, and D. Mukherjee, *Phys. Repts*. **151**, 93(1987); W. Kutzelnigg*, J. Chem. Phys*. **77**, 3081 (1982)*;* W. Kutzelnigg and S. Koch, *J. Chem. Phys*. **79**, 4315 (1983)

16. P. Durand, and J. P. Malrieu, *Adv. Chem. Phys*. **67**, 321 (1987); J. P. Marlrieu, P. L. Durand and J. P. Daudey*, J. Phys. A*. **18**, 809 (1985)
17. N. F. Lane, *Rev. Mod. Phys.* **52**, 29 (1980)
18. J. F. Stanton, and R.J. Bartlett, *J. Chem. Phys*. **98,** 7029 (1983); M. Nooijen, and R. J. Bartlett, *J. Chem. Phys*. **102,** 3629 (1995); J.F. Stanton, and J. Gauss,, *J. Chem. Phys*. **111,** 8785 (1999).
19. C. Bloch, *Nucl. Phys.* **6**, 329 (1958)
20. J. Cizek, *Adv. Chem. Phys.,* **14**, 35 (1969).
21. M. R. Hoffmann and H. F. Schaefer, *Adv. Quantum. Chem*., **18**, 207 (1986)
22. G. E. Scuseria, C. L. Janssen and H. F. Schaefer, *J. Chem. Phys*. **89**, 7382 (1988).
23. S. Pal, M. Rittby, R.J. Bartlett, D. Sinha and D. Mukherjee *J. Chem. Phys.* **88***,* 4357 (1988); C. M. L. Rittby and R. J. Bartlett, *Chem. Phys. Lett*. **80**, 469 (1991)

Chapter 4

Analytically Continued Fock Space Multireference Coupled Cluster Theory: Application to the $^2\Pi_g$ Shape Resonance in e-N_2 Scattering

Abstract: The technique of Fock space multireference coupled cluster [FSMRCC] is applied for the first time to the correlated calculation of the energy and width of a shape resonance in an electron-molecule collision. The procedure is based upon combining a complex absorbing potential [CAP] with FSMRCC theory. Accurate resonance parameters are obtained by solving a small non-Hermitian eigenvalue problem. The potential energy curve of the $^2\Pi_g$ state of N_2^- is calculated using the FSMRCC and multireference configuration interaction [MRCI] level of theories. Comparison with the single-determinant Hartree-Fock theory indicates that correlation effects are important in determining the behavior of the resonance state.

4.1. Introduction

Shape resonances are dominant features in the scattering cross sections of low-energy electrons colliding with molecules.[1] These are associated with metastable anionic states formed by the temporary trapping of an electron by an effective potential barrier through which the electron may eventually tunnel out and escape. The physics of resonance phenomena in the continuum can be characterized by *discrete* eigenstates of the Hamiltonian satisfying purely outgoing boundary

conditions. The method of analytical continuation of the Hamiltonian in the complex plane to calculate these resonance energy states are possible either by the complex scaling method [2,3,4] or by utilizing a complex absorbing potential [CAP][5,6]. Significant strides have been made in the theoretical development and practical implementation of the complex scaling method, which permits direct and simultaneous determination of both the resonance position and width from the eigenvalue of an analytically continued Hamiltonian $H(\theta)$. However, difficulties arise in molecular systems and, moreover, the implementation of this method in *ab initio* codes that go beyond the one-particle level is very difficult.[3,7] In Chapter 2, the combination of complex scaling with Fock space multireference coupled cluster theory was proposed, which makes use of the complex one-particle basis functions from a bi-variational self-consistent field method.[8] This has been applied to the $1s^{-1}$ Auger resonance of Be and the ^2P shape resonance in e^--Mg scattering. However, the graphical solution to optimize the complex-scaling angle θ is time-consuming and computationally expensive, as it requires the calculation of basis functions from the bi-variational self-consistent field method procedure for several scaling angles and the repetitive transformation from the atomic to the molecular orbital basis.

The method of using a CAP is closely related to complex scaling.[9-11] The major advantage of the former is its simplicity. The idea underlying complex absorbing potentials is to introduce an absorbing boundary condition in the exterior region of the molecular scattering target. In this way, the wave function of the scattered electron becomes square-integrable. The CAP procedure is minimally invasive in the sense that neither the internal structure of the physical Hamiltonian is affected nor is there any need to use other basis sets than usual real Gaussians.[12] Thus, this method offers great promise for the determination of accurate Siegert energies in a computationally viable form by a relatively straightforward modification of existing electronic structure codes for bound states.[12-14]

In this chapter we test the applicability and accuracy of the CAP-FSMRCC method for the calculation of the $^2\Pi_g$ shape resonance in e-N_2 scattering. The $^2\Pi_g$ shape resonance in e-N_2 scattering is well characterized, and the extensive literature on this resonance [5,13,15-23] utilizing many different theoretical techniques makes it an

excellent testing ground of the efficacy of new theoretical techniques for the treatment of molecular resonances.

In shape resonances, where the trapping of the projectile electron occurs in the potential well created by an angular momentum barrier and the attractive interior of the molecule, target electrons are affected both statically and dynamically. The latter effect is manifested primarily in the polarization of the target. Let s label a resonance state of the (N+1)-electron system, and let E_s^{N+1} denote the corresponding Siegert energy. The CAP-FSMRCC method provides direct access to the energy difference $(E_s^{N+1} - E_0^N)$, where E_0^N is the ground-state energy of the neutral N-electron target at the same geometry. Both static and dynamic electron correlation in the N- and (N+1)-electron systems are treated in a consistent manner in this approach. A more detailed description of the theory can be found in the previous chapter.

The calculations presented are limited to single and double excitation operators [CAP-FSMRCCSD]. Sections 3.2 and 3.3 contain a resume of the theoretical method employed. In Sec. 4.2 we will consider some practical aspects of the method. Section 4.3 contains a discussion of our results. The results are compared with experimental results as well as those obtained using other theoretical approaches. In this section we also discuss the importance of correlation effects in determining resonance parameters in the vicinity of the internuclear distance at which the resonance state becomes a bound state.

4.2. Practical Considerations

The resonances can be identified by plotting η trajectories, which is a graphical method in which the energy differences $[\Delta E_{vertical}(\eta)]$ obtained from equation 3.3.18 corresponding to various energy states of interest are plotted in the complex plane as a function of η. CAP-FSMRCC equations for the (1,0) sector are structurally similar to those of the FSMRCC equations without complex absorbing potential. The contribution of CAP terms in the one-valence problem comes through the modification of $\bar{H}$ terms. The one-body particle-particle part of the non-

Hermitian $\bar{H}$ operator includes one extra term $W(\eta)$, in addition to the modification of other terms through the appearance of complex $T^{(0,0)}(\eta)$. The latter is determined by solving the CAP-SRCC equations presented in Sec. 3.2. A key aspect in the implementation of CAP-FSMRCC is the rearrangement of cluster equations for the higher Fock space sectors using the excitation amplitudes from the lower Fock space sectors. A rearrangement of this type comes in the construction of $\bar{H}$ matrix elements. In principle, the CAP has to be applied in the single-reference SRCC method [(0,0) sector of Fock space] to generate $T^{(0,0)}(\eta)$ amplitudes, which are later used for the generation of the $T^{(1,0)}(\eta)$ amplitudes of the (1,0) Fock space sector. Performing, for each η value, a SRCC calculation and the subsequent construction of $\bar{H}(\eta)_N$ matrix elements [$\bar{V}(\eta)_N$, $\bar{F}(\eta)_N$, and $\bar{W}(\eta)_N$] for CAP-FSMRCC calculations is time-consuming and computationally demanding. In practice, the ground-state SRCC calculation is typically at least an order of magnitude more expensive than the FSMRCC step. Since the CAP is defined only for the particle-particle interactions in the CAP-SRCC formulation, few CAP diagrams appear at the SRCC level and, as a result, the effect of the CAP in the correlation energy of the N-electron system is negligibly small. Here we approximated $T^{(0,0)}(\eta)$ by $T^{(0,0)}(\eta=0)$ for the generation of the $\bar{H}(\eta)_N$ matrix. The artificial nature of the absorbing potential and its application only to the virtual orbitals justify our approximation. Such an approximation has a number of advantages. Principally, it drastically reduces the incremental cost of η-trajectory generation as only one SRCC calculation [for $\eta=0$] is needed. Construction of $\bar{V}(\eta)_N$ and $\bar{F}(\eta)_N$ matrix elements has to be carried out only once for the whole η trajectories for any box size. The $\bar{W}(\eta)_N$ matrix is constructed for each η value using the $T^{(0,0)}(\eta=0)$ amplitudes:

$$\bar{W}(\eta)_N = -i\eta W\, \mathrm{e}^{T^{(0,0)}(\eta=0)}. \qquad 4.2.1$$

Since this approximation to the $T^{(0,0)}(\eta)$ amplitude removes the CAP perturbation completely from the SRCC level, $[\delta E_{corre}^{SRCC}(\eta) - \delta E_{corre}^{SRCC}(\eta=0)]$ becomes zero and the complex electron affinity calculation using Eq. 3.3.17 requires no further correction. The initial search for the stationary point along the trajectories is performed utilizing

this strategy. Although this approximation makes the theory inexact, it is now a relatively easy task to find the exact resonance parameters, since we can always employ an exact CAP-FSMRCC calculation focusing on the vicinity of the previously determined stabilization point. A further optimization of the CAP box is not necessary. In the numerical calculations we will limit ourselves to the coupled cluster singles and doubles level [CCSD] of approximation, which means that we will restrict our operators in the wave operator to be of one- and two-body type.

In practice, one can not solve for the eigenenergy spectrum exactly, and one is forced to use truncated basis sets. The truncated basis sets will lead to substantial η dependency in the eigenenergies. If η is too small, the absorbing potential does not have any overlap with the finite basis set and the projectile becomes artificially bound within the walls imposed by the basis set. Therefore, it is only possible to minimize the CAP perturbation for finite η values. If the basis set contains a sufficient number of diffuse functions, one observes along the η trajectory of a resonance state a region of stabilization, characterized by the appearance of a cusp. The Siegert energy of the resonance is examined through the minimization of the magnitude of the logarithmic velocity $v_i(\eta) = \eta dE_i / d\eta$. The existence of a pronounced minimum,

$$\left| v_i(\eta_{opt}) \right| = \min , \qquad 4.2.2$$

gives the optimal η value, and the best approximation to the Siegert energy is $E_i(\eta_{opt})$.[5] This resonance energy is insensitive to a particular basis set unless too small basis sets are used. The complex electron affinity at the optimal point is associated with position of the resonance [real part] and decay width [the imaginary part].

In our calculations we chose a box-shaped CAP of the form[19]

$$W(\mathbf{x};\mathbf{c}) = \sum_{i=1}^{3} W_i(x_i;c_i) , \qquad 4.2.3$$

where

$$W_i(x_i;c_i)=\begin{cases}0, & |x_i|\le c_i\\ (|x_i|-c_i)^2, & |x_i|>c_i\end{cases}, \qquad 4.2.4$$

which can be easily represented in a Gaussian basis set.[18] It has been applied in the peripheral region of the target to absorb the scattered electron while keeping the target unperturbed. The CAP box parameters c_i (i=1, 2, 3) can be optimized accordingly in the calculations.

4.3. Results and Discussions

4.3.1. The $^2\Pi_g$ shape resonance in N_2^-

In the following, we present the first application of the CAP-FSMRCC method to the problem of resonances in electron-molecule scattering. Atomic units are used throughout unless otherwise stated. We have tested the formalism using the $^2\Pi_g$ shape resonance in N_2^- as an example. This resonance has been studied extensively by other theoretical methods. We have utilized a TZ(7p2d) basis [13] for each nitrogen atom, since results are available with respect to this basis set. We do not discuss the basis-set effect on the position and width of the resonance, as a number of such studies can be found in the literature.[5,13,15] The N_2 molecule is placed along the z axis symmetrical to the origin with a bond length of 2.07 a.u. The CAP box is set up by $c_x = c_y = \delta c$, $c_z = 1.035 + \delta c$, where c_x, c_y, c_z are the distances from the center of the coordinate system along the x, y, and z axis, respectively, and δc is a nonnegative variable. We selected the twenty energetically lowest virtual orbitals to span our active particle space. Consequently, the effective Hamiltonian is represented by a 20×20 matrix, and we will obtain twenty electron affinities. The nonlinear coupled cluster equations are solved using an iterative Jacobi-type algorithm. An alternative algorithm that is conceivable for this purpose is based on the conjugate gradient concept. However, the wide range of magnitude of the complex eigenvalues and the lack of diagonal dominance of the $H(\eta)_{N,eff}$ matrix cause convergence problems in conjugate gradient-based algorithms.

The $^2\Pi_g$ shape resonance is identified by plotting the complex electron affinity spectra using the CAP-FSMRCC method for various box sizes and CAP strengths. We typically run initial η trajectories [for fixed CAP-box size] at an increment of 1×10^{-4}. Such a small η increment is essential in order that one not miss the stabilization point in the resonance trajectory. The η trajectories for some of the eigenstates of the CAP-FSMRCC calculation for a box size of $\delta c = 2.5$ a.u. are shown in Fig. 4.1. The eigenvalues that move quickly into the complex plane as η is increased demonstrate strong interaction with the complex absorbing potential. The associated eigenfunctions are, in contrast to the wave function of a resonance in the presence of a CAP, not localized in the vicinity of the target. Thus, the behavior of their η trajectories identifies them as continuum states [discretized by the absorbing potential and the finite basis set]. In Fig. 4.1, the second eigenvalue from the right shows a pronounced stabilization in the complex plane. This is the root associated with the resonance. The resonance parameters are determined by analyzing the stabilization behavior of the η trajectory of this eigenvalue. The η trajectories predicted, for example, by CAP-MRCI [Ref. 13] are qualitatively similar to those obtained in the CAP-FSMRCC calculations presented here.

The Siegert energy for elastic e-N_2 scattering has been studied in three sets of CAP-FSMRCC calculations. First, to calculate the optimum box size for which the absorbing potential is best adapted to the basis set and the size of the target system, CAP-FSMRCC calculations were performed for various CAP-box sizes. The η trajectories of the resonance eigenvalue for these calculations are displayed graphically in Fig. 4.2, and the resulting resonance parameters are collected in Table 4.1. The optimum value of η is increasing as the box size increases. The quality of the description of the resonance, as expressed by the magnitude of the logarithmic velocity $v_i(\eta_{opt})$ at the stabilization point of the trajectory, however, is not a monotonic function of η. The optimum value of box size is found to be $\delta c = 2.5$. For smaller box sizes, the artificial perturbation caused by the CAP is too large; for larger box sizes, the finite spatial extension of the underlying basis set becomes apparent. Therefore, all further investigations of the complex resonance eigenvalue were performed using $\delta c = 2.5$.

Table 4.1 The variation of the resonance parameters with respect to CAP-box sizes.

δc	$\eta_{opt} \times 10^4$	$\left\|v_i(\eta_{opt})\right\| \times 10^4$	Energy (eV)	Width (eV)
2.00	42	1.43	2.475	0.357
2.25	44	1.83	2.475	0.364
2.50	50	1.17	2.475	0.372
2.75	54	1.62	2.475	0.381
3.00	58	2.11	2.467	0.388
3.50	68	3.19	2.477	0.416
4.00	78	5.49	2.479	0.444

The total number of cluster amplitudes entering the cluster operators in the description of electron excitation is a measure to describe the extent to which electron correlation is taken into account. We investigated the changes in the resonance position and width with respect to the number of cluster amplitudes in the (1,0) sector of Fock space. The division of particles into active and inactive particle depends on the range of energy difference in which we are interested. A reasonable gap between the active and inactive groups helps to establish numerical stability of the FSMRCC equations, and the total number of cluster amplitudes for each sector is selected in such a way that it takes into account all cluster excitations within the model space and then to the complementary space. The η trajectories of the resonance eigenvalue in these calculations are shown in Fig. 4.3. The width and position of the resonance is increasing with respect to the number of excitations. As the number of excitations increases, the velocity of the trajectory near the stationary point is decreasing. The optimum value of η is not changing with respect to the number of excitations. This is very useful for practical purposes, as it implies that the determination of η_{opt} can be carried out with only a moderate number of cluster amplitudes. The resulting resonance parameters obtained with different number of excitations are compared in Table 4.2. Berman *et al.*[18] have fitted to the experimental scattering cross section a

parameterized model describing the nonlocal nature of the vibrational excitation in e-N_2 collisions. In this way, they determined, in the fixed-nuclei limit at equilibrium geometry, a resonance energy of 2.32 eV and a width of 0.41 eV. The calculated decay width in Table 4.2. is seen to approach the value extracted from experiment. The calculated position of the resonance appears to converge to a value that is a little too high, but that may simply be an indication that the SD level of CAP-FSMRCC is limited to an accuracy of a hundred milli-electron volts or so. On the other hand, since the "experimental" parameters are model-dependent, there is no reason to expect perfect agreement.

In addition to the correlation effects, it is a fairly simple matter, and not computationally expensive, to obtain a feel about the optimization of the resonance parameters with respect to the number of cluster amplitudes. For the (1,0) sector of Fock space, the changes in values of roots obtained by diagonalizing $H(\eta)_{N,eff}$ for different active spaces used in the FSMRCC calculations are found to be negligible. Very high excitation classes from model space to complementary space are unimportant in describing the $^2\Pi_g$ resonance. Examining Table 4.2, the results suggest that a reasonable estimate of error bars in the energy and width of the resonance due to a change in the number of cluster amplitudes of order 10^5 lies in the order of $\pm 10^{-2}$ eV and $\pm 10^{-3}$ eV, respectively. These facts and the small magnitude of the velocity of the trajectories for the different number of cluster amplitudes given in Table 4.2 indicate that for the one-particle basis chosen the resonance parameters we obtain for the largest number of cluster amplitudes are converged to within the quoted errors.

The calculations discussed above are based on the approximation of replacing $T^{(0,0)}(\eta)$ by $T^{(0,0)}(\eta = 0)$ [see Sec. 4.3]. Further refinement of the stabilization point and nearby points in the η trajectories is possible within the CAP-FSMRCC method by incorporating the CAP in the generation of $T^{(0,0)}(\eta)$. Table 4.2 displays the energies obtained including the correct η dependence in the cluster amplitude, along with the approximated cluster amplitudes. The trajectories are shown graphically in Fig. 4.4. If we regard the above-mentioned "experimental" resonance parameters as

our benchmark, we find that using $T^{(0,0)}(\eta)$ in place of $T^{(0,0)}(\eta = 0)$ improves the calculated decay width [for the largest number of cluster amplitudes considered], while increasing the resonance energy even more.

Table 4.2 The dependence of energy and width of the $^2\Pi_g$ resonance on the number of cluster amplitudes ($T^{(1,0)}(\eta)$) in the (1,0) sector of Fock space. The results obtained for CAP-FSMRCC calculations that take into consideration the η dependence of $T^{(0,0)}(\eta)$ from CAP-CCSD are indicated by the suffix -*t*.

Number of cluster amplitudes	$\eta_{opt} \times 10^4$	$\lvert v_i(\eta_{opt})\rvert \times 10^4$	Energy(eV)	Width (eV)
152720	50	1.57	2.467	0.368
224400	50	1.17	2.475	0.372
224400-*t*	50	1.10	2.490	0.372
350600	50	1.13	2.483	0.376
350600-*t*	52	1.14	2.520	0.390

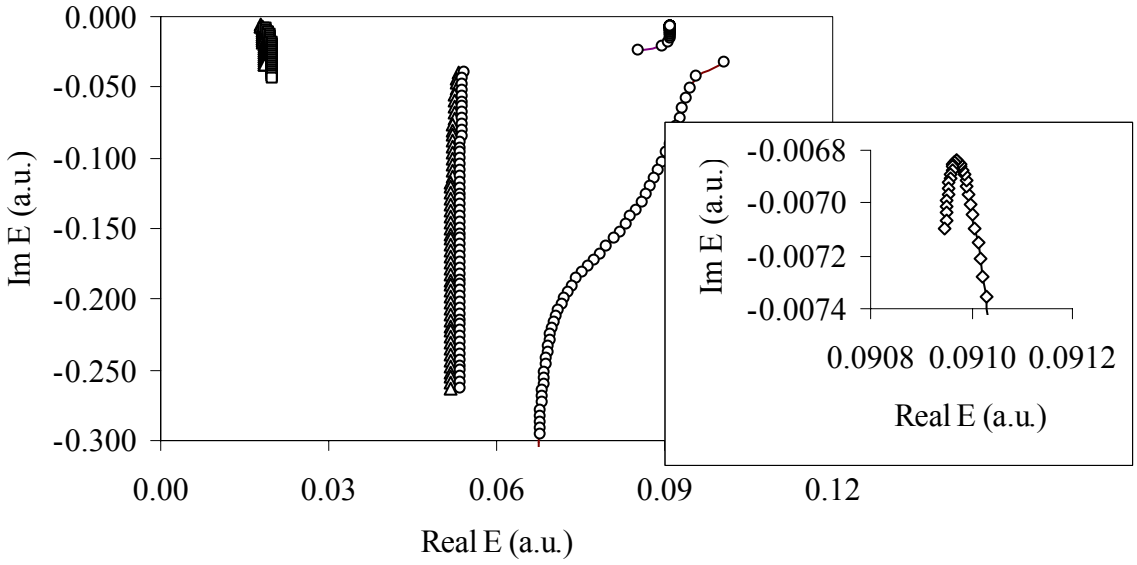

Figure 4.1 The η trajectories of the complex eigenvalues from CAP-FSMRCC calculations. The η values vary from 0.0010 to 0.0065. η is incremented linearly in steps of 0.0001. The region of stabilization of the trajectory corresponding to the resonance (second from the right) is magnified in the lower panel

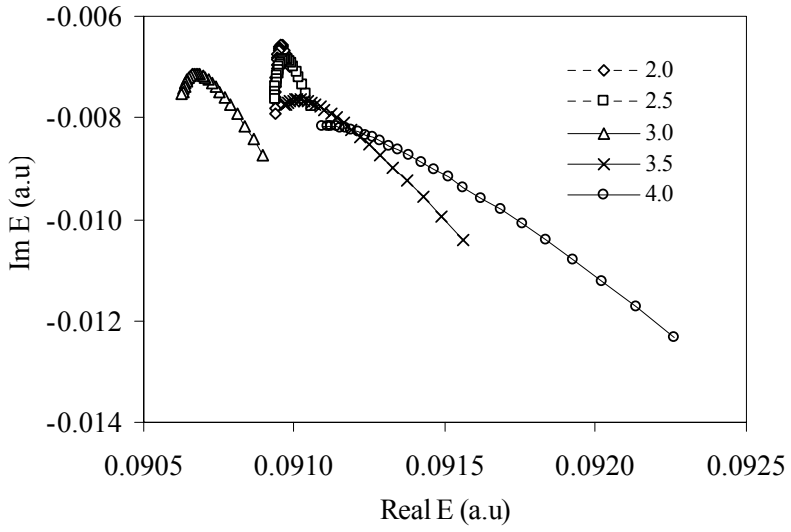

Figure 4.2 The η trajectories associated with the $^2\Pi_g$ resonance in elastic e-N_2 collisions for different CAP-box sizes. The δc values are given in the box.

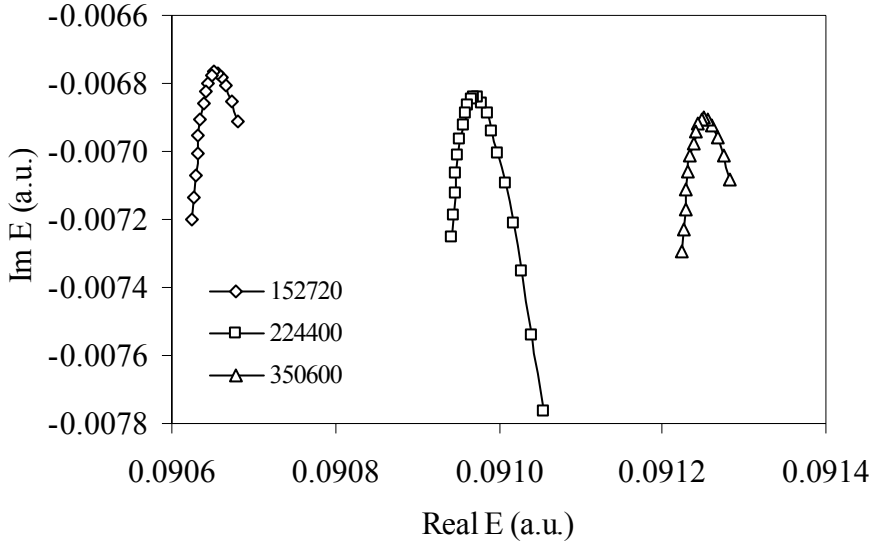

Figure 4.3 The resonance trajectories for a different number of cluster excitation amplitudes. The total numbers of cluster amplitudes are given in the box.

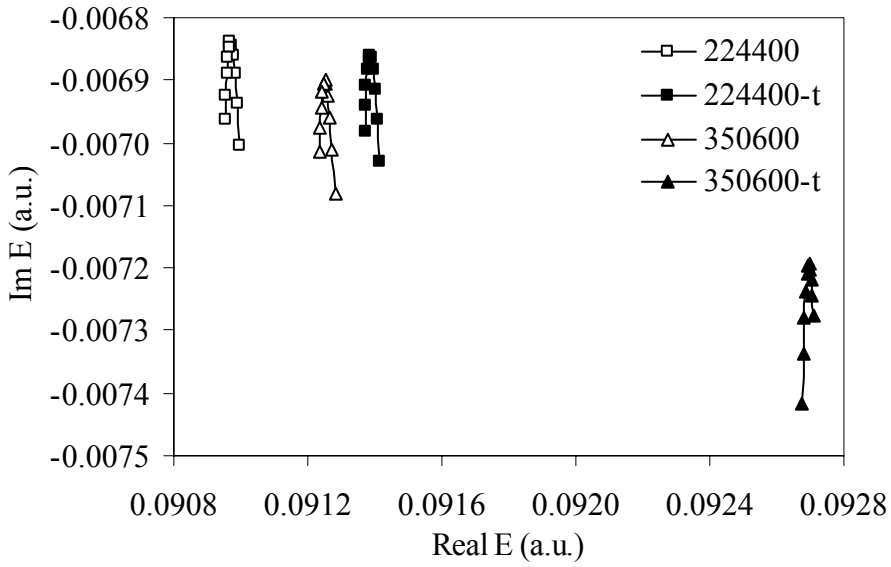

Figure 4.4 The η trajectories from actual cluster excitation amplitudes ($T^{(0,0)}(\eta)$) and approximated cluster excitation amplitudes ($T^{(0,0)}(\eta = 0)$). The total numbers of excitation amplitudes are given in the box. The calculations performed using $T^{(0,0)}(\eta)$ are indicated using the suffix *–t*.

4.3.2. Conversion of Resonance State to Bound State in e-N_2 Collision.

Over the past twenty years an extensive literature dealing with the change of resonance parameters with respect to internuclear distance has appeared.[24-29] While accurate data of this type are still scant, it is desirable to analyze such results using electron correlation calculations. The complex self-consistent-field method has been used to compute the complex potential energy curve of the $^2\Pi_g$ shape resonance state in e-N_2 scattering.[26] This complex SCF description of shape resonance encounters an interesting theoretical problem with regard to the conversion of electronic bound state to resonance with changing internuclear distance. The SCF energies of the anion and the neutral molecule in this calculation cross at an internuclear distance of 2.6 a.u., which differs significantly from the internuclear distance at which the SCF energy of the anion becomes complex [2.4 a.u.]. The reason for the behavior is evidently that the SCF approximation for the N+1 electron anion and the SCF approximation for the N electron neutral molecule are not consistent with each other. Other calculations that are largely based on the SCF concept find that the potential energy curves of N_2 and N_2^- cross at 2.4 a.u.[24-29]

The potential energy curve obtained by the SCF method even for N_2 molecule is not better than semiquantitative. The artificial steepness of this potential energy obtained by the SCF method causes a serious error in predicting the internuclear distance at which it crosses the $^2\Pi_g$ state of N_2^-. In order to demonstrate that the single-determinant SCF approach gives wrong results even for the ground state of N_2, we have performed such a calculation together with an SRCC and an MRCI calculation. For the MRCI calculation we used the Gaussian basis set 6-311++G(3df, 3pd), which does not contain any diffuse functions. At each R, we first ran a closed-shell RHF calculation for the target. The 1s core orbitals were frozen after this. The next step was a CASSCF calculation for N_2. The 2s-type orbitals were optimized, but no excitations out of these orbitals were allowed. The active space consisted of the three remaining occupied valence orbitals plus the energetically lowest nine virtual orbitals. After improved orbitals had been obtained using the CASSCF technique, the MRCI calculations followed, one for the target and one for the anion. We used the internally contracted MRCI code implemented in *Molpro*.[30] The reference space was

constructed from the active space used in the CASSCF calculation, but the virtual orbitals were allowed to be at most singly occupied in the references. The 2s-type orbitals were doubly occupied in the references, but were allowed to be excited in the construction of the MRCI space. For N_2, this strategy gave rise to 128 configurations [194 CSFs] in the reference space. The MRCI space consisted of 422978 contracted configurations [2534608 uncontracted configurations]. There were 126 configurations [303 CSFs] in the reference space for the anion, and the total number of contracted configurations in the N_2^- calculation was 850077 [5756459 uncontracted configurations]. The anionic MRCI potential energy curve is discussed below together with the CAP-FSMRCC results.

The SCF potential energy curve of N_2, the MRCI curve for the 6-311++G(3df, 3pd) basis set, and the SRCC curve for the TZ(7p2d) basis set mentioned earlier are shown in Fig. 4.5. Clearly, as expected, the shape of the SCF curve is not even close to the MRCI and SRCC curves: It is much too steep for distances larger than the equilibrium distance, and the SCF equilibrium distance is too small. The dissociation energy [D_0] of N_2 we obtain from the MRCI calculation is 9.51 eV, which agrees with experiment to within 3%.[31] By contrast, the SCF curve implies a dissociation energy of more than 35 eV. Single-reference coupled cluster theory is unsuitable to describe complete triple-bond breaking. But in the vicinity of the equilibrium geometry, the agreement between the SRCC and MRCI curves is evidently satisfactory.

We now turn our attention to the complex potential energy curve of the $^2\Pi_g$ state in e-N_2 scattering calculated using the CAP-FSMRCC method. Unlike most single-reference methods, FSMRCC methods are suited to "final state" studies of potential energy surfaces particularly in quasi-degenerate cases, especially with the ability to look at several surfaces in the same calculation.[32] The basic result of the FSMRCC calculation is an energy difference [Eq. (3.3.14)]. When added to the absolute energy of the (0,0) sector reference [Eq. (3.2.16)], it provides the absolute energy of the state of interest. In the (1,0) sector case, the state of interest has one electron added relative to the reference (0,0) state. We have performed CAP-FSMRCC calculations as described in Sec. 4.2 at internuclear distances between 1.8

a.u. and 3.2 a.u. We employed 350600 cluster amplitudes, applying the CAP only to the (1,0) sector of Fock space. Starting from the equilibrium geometry, the complex electron affinity calculation for N_2 requires smaller CAP strength as R is increased. The real part of the complex electron affinity also decreases with respect to internuclear distance. The real part of the electron affinity changes its sign at an internuclear distance of 2.80 a.u. The imaginary part also becomes negligibly small in magnitude at R=2.80 a.u. This clearly shows, in a perfectly consistent way, that as the internuclear distance increases, the decaying electronic resonance state becomes a bound state. Since the resonance state becomes a bound state at 2.80 a.u., we performed CAP-unperturbed FSMRCC calculations for the N_2^- bound state for larger internuclear distances. Figure 4.6 shows the real part of the potential energy curve of the $^2\Pi_g$ anionic state and the potential energy curve of the target. [The potential energy curve of N_2 is obtained by solving the CAP-unperturbed (0,0) sector of Fock space.]. The $^2\Pi_g$ resonance width calculated within the (1,0) sector of Fock space is displayed in Fig. 4.7. The non-smooth and jittery character of the CAP-FSMRCC anionic curve and the width curve are result of two fundamental facts (a) due to the finite basis set used and (b) due to the incomplete active space chosen for the calculation of effective Hamiltonian. For a finite basis set, the magnitude of the logarithmic velocity $\nu_i(\eta_{opt})$ at the stabilization point of the trajectory is practically never zero. At the optimization point, the real and imaginary part of $\nu_i(\eta_{opt})$ provides an accuracy of the resonance energy and width respectively. However, in the present calculations the error bars calculated are negligibly small. The CAP perturbation makes magnitude of the off diagonal elements of the effective Hamiltonian matrix a significant one for the electron absorption. The eigen roots of the effective Hamiltonian, which is not diagonally dominant, depends highly on the total number of active valence orbitals chosen for the effective Hamiltonian matrix calculation. Considerable accuracy may be achieved when the effective Hamiltonian is diagonalized over the complete virtual orbital space. It should be noted that, in figures 4.5 and 4.6 the SRCC and the MRCI curves have been calculated using different basis sets. For the same basis set, when the sufficiently accurate potentials are generated, the absolute energy of the potential energy curves calculated using the multireference treatment should be lower in energy than that of the corresponding single reference calculation.[33] This is true in our calculations also. The curves shown in Fig. 4.5 are

vertically shifted to make their minima coincide with the point of zero energy. Since the SRCC curve is much wider than the MRCI curve, the vertically shifted SRCC curve lies below the MRCI curve.

The graphs illustrate the conversion of the resonance to a bound state at R=2.80 a.u. Unlike the complex SCF calculation, the crossing of the FSMRCC energy for N_2 and the real part of the energy of N_2^- occurs at the same internuclear distance at which the resonance state becomes a bound state [where the imaginary part of the N_2^- energy vanishes]. Also included in Fig. 4.6 are the potential energy curves obtained from the CAP-unperturbed MRCI calculations for the neutral and the anionic system. The MRCI calculation of the anion is, strictly speaking, only valid where the $^2\Pi_g$ state is bound. Since the electron in the resonance state is quasibound, the real part of the resonance energy can be estimated by focusing on the bound part of the resonance wave function. The underlying assumption is that the energy shift induced by coupling to the continuum can be neglected. Such an approximation is not necessary within CAP-FSMRCC.

Another problem with configuration interaction-type methods is that it is difficult to achieve a balanced treatment of systems with differing particle numbers. In our MRCI calculations, we find that at the equilibrium geometry of N_2, N_2^- is higher in energy than N_2 by 3.4 eV. For large internuclear distances, the energy difference is 1.0 eV. Experimentally, however, it is known that the energetically lowest resonance state of N^- is 0.07 eV higher than the ground state of atomic nitrogen.[34] [N^- does not have any bound states.] The MRCI curve of N_2^- in Fig. 4.6 has been shifted vertically to reflect the correct asymptotic behavior. The MRCI energy of the anion is now 2.5 eV above the energy of the neutral molecule at equilibrium geometry, in agreement with the CAP-FSMRCC result. CAP-FSMRCC automatically provides an excellent balanced treatment of N_2 and N_2^-.

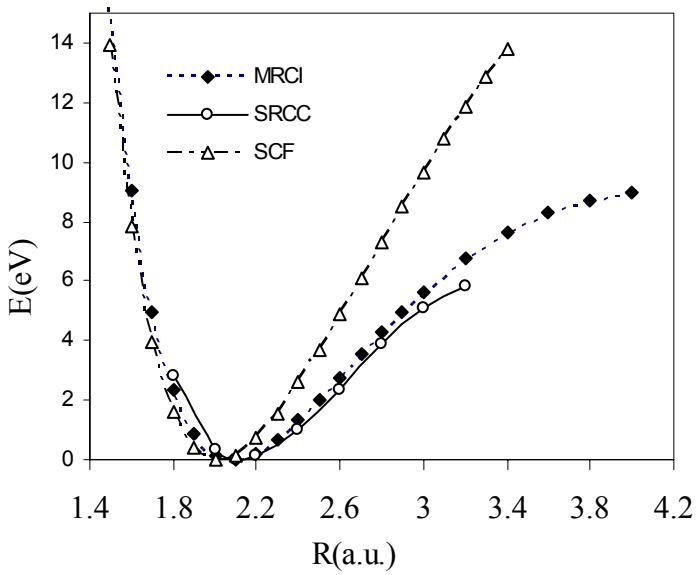

Figure 4.5 The potential energy curve of the electronic ground state of N_2 using three different *ab initio* methods (see the text). All the three curve curves have been vertically shifted so that their minima coincide with the point of zero energy.

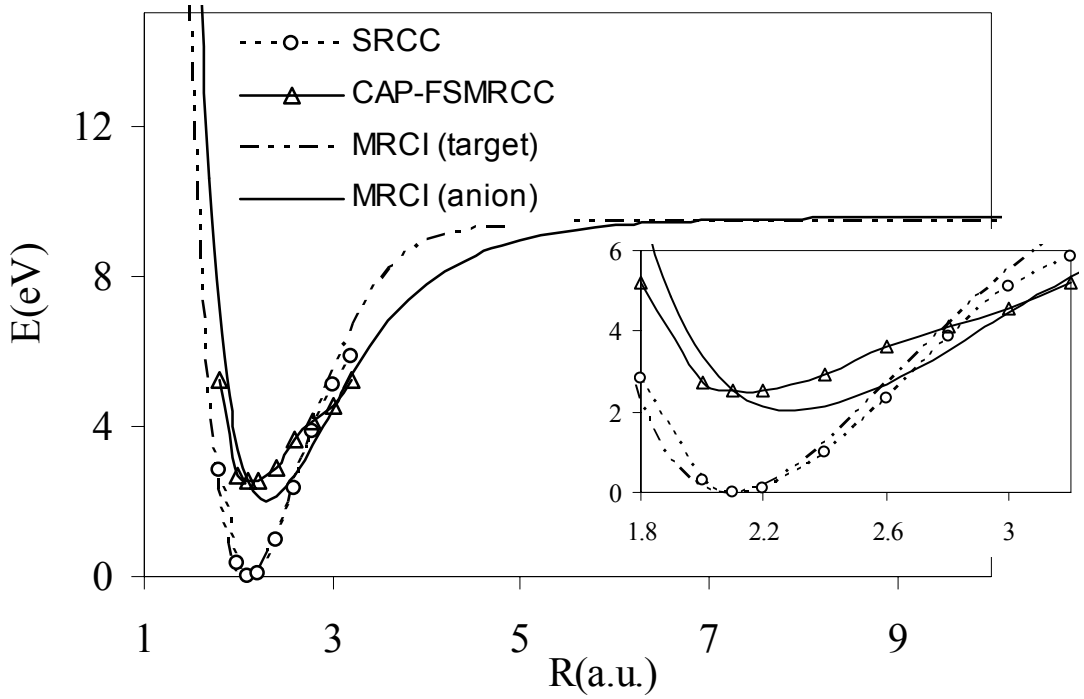

Figure 4.6 The potential energy curve of the ground state of N_2 (dashed lines) and the real part of the complex potential energy curve of the $^2\Pi_g$ state of N_2^- (full lines). Both coupled cluster and MRCI results are shown.

In the MRCI calculation, we find the crossing point a little above R=2.6 a.u. [R=2.80 a.u. according to the CAP-FSMRCC calculation]. For comparison, Nestmann and Peyerimhoff, employing the MRD-CI method, reported that curve crossing occurs at R=2.7 a.u.[22] Recent MRCI studies by Gianturco and Schneider suggest that the N_2 and N_2^- potential energy curves cross at an internuclear distance of about 2.8 a.u.[35] In spite of the apparent variation of predictions, we would like to stress the fact that all electron-correlation calculations agree that the crossing point cannot be below R=2.6 a.u. Most likely it lies close to R=2.8 a.u.

We have two reasons for believing this. First, the potential energy curves calculated by Birtwistle and Herzenberg [36] by fitting the experimental vibrational-excitation cross section data within the boomerang model cross at an interatomic distance that is about 0.7 a.u. above the equilibrium distance of the neutral target, i.e. around R = 2.8 a.u. This is inconsistent with the SCF calculations, but consistent with our CAP-FSMRCC many-body calculation. Second, the most serious attempt within the framework of the boomerang model to calculate vibrational-excitation cross sections near the $^2\Pi_g$ resonance in e-N_2 scattering is the work of Dube and Herzenberg.[37] The parameterized potential energy curve of N_2^- calculated in their work is in perfect agreement with our CAP-FSMRCC curve, at least for internuclear distances smaller than 2.5 a.u. [Dube and Herzenberg emphasize that their anionic potential energy curve is only valid near the potential energy minimum of N_2^-.] Moreover, the R-dependence of the decay width, $\Gamma(R)$, is in fact very similar to the one we calculated (Fig. 4.7). As demonstrated by Dube and Herzenberg, very good agreement with experiment can be achieved using data that are very similar to our *ab initio* data.

From the potential energy calculations employed here, we find that it is important to include electron correlation effects in determining the behavior of resonance states in the crossing region. In contrast to the complex SCF model, the CAP-FSMRCC method, with its systematic inclusion of correlation effects, provides a balanced treatment of N and N+1 electron systems. Also note that the crossing point determined here is substantially larger than the two values obtained with the complex SCF method. This makes sense, as potential energy curves based on SCF calculations

are known to rise too steeply with increasing internuclear distance, thereby artificially shifting the crossing point to shorter bond lengths. Therefore, the present chapter has established that the combination of the CAP-FSMRCC potential energy curve corresponding to the $^2\Pi_g$ state with the SRCC potential energy curve corresponding to the ground state of N_2 is more than just a new description of known results.

Figure 4.6 reveals another interesting feature: There is a second crossing point—at R=7.3 a.u. Between the two crossing points, the anionic molecule is electronically bound; outside this range, the $^2\Pi_g$ state is metastable. This is a very peculiar situation, which does not seem to have received any attention so far. Such a second crossing point can also be seen in Fig. 4.1 in the paper by Gianturco and Schneider, but they do not mention it anywhere in the text.[35] It is clear that a second crossing point must exist, since N^- is metastable. We are convinced that the *ab initio* studies presented in this chapter supply the currently most complete picture of the $^2\Pi_g$ potential energy curve of N_2^-.

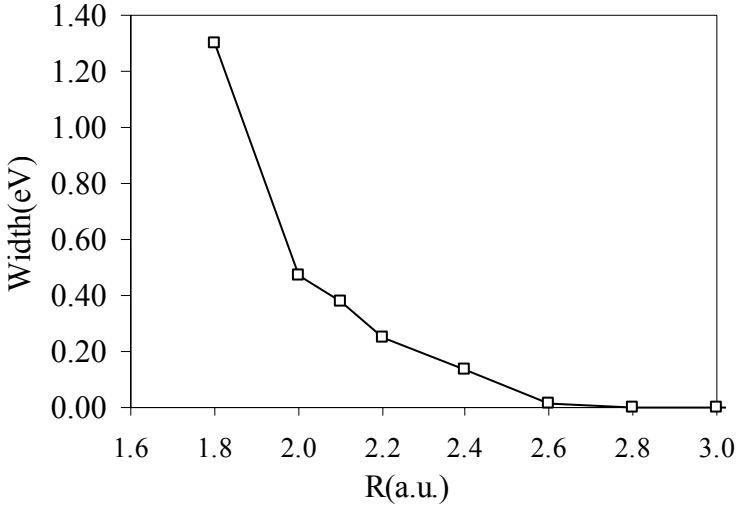

Figure 4.7 Dependence of the calculated width of the $^2\Pi_g$ shape resonance state of N_2^- on internuclear distance.

4.3. Conclusion

In this chapter, we have shown how the highly correlated method of Fock space multireference coupled cluster, which is already known to be suitable for accurate calculation of properties of electronically excited, bound states, can be extended to the treatment of resonance states in electron-molecule collisions. To that end, we introduced a complex absorbing potential, which enables the direct calculation of resonance parameters using bound-state methods. Our focus here was on practical aspects of CAP-FSMRCC. We have identified computational strategies that ensure that a CAP-FSMRCC calculation, in spite of its dependence on the CAP strength parameter η, is hardly more expensive than an FSMRCC calculation of a bound excited state. In order to demonstrate the accuracy achievable with CAP-FSMRCC, we presented calculations of the $^2\Pi_g$ resonance that is excited in electronically elastic collisions of electrons with nitrogen molecules. The results obtained from experiment and various theoretical methods, including the findings of this work, are collected in Table 4.3. Our results for energy and width are in good agreement with experiment and other theoretical methods. Of all *ab initio* calculations based on a CAP, the CAP-FSMRCC result is closest to the resonance parameters extracted from experiment. The present results clearly demonstrate the utility of the CAP-FSMRCC approach for the study of metastable electronic states. Our calculations support the view that the temporary anion formation in the electron-molecule collision process can be well described by multireference methods. Finally we note that both the dynamical and nondynamical correlation effects are extremely important in determining the resonance states near the internuclear distance at which the resonance becomes a bound state. The inclusion of correlation in this case drastically alters the internuclear distance at which the resonance anionic curve crosses with the neutral target curve. CAP-FSMRCC is a state-of-the-art method that opens the possibility of routine *ab initio* studies of resonances exploiting the extraordinary power of coupled-cluster techniques.

Table 4.3 Energy and width of the $^2\Pi_g$ shape resonance in e-N_2 scattering at the equilibrium geometry of N_2.

Method	Energy(eV)	Width(eV)
Estimate based on experimental data[28]	2.32	0.41
Linear algebraic method[30]	2.13	0.31
Schwinger multichannel method[31]	2.26	0.39
R-Matrix with/without inclusion of polarized states[32]	2.27/1.90	0.35/0.26
MRDCI extrapolation method[33]	2.62	0.45
CAP/static-exchange plus polarization[20]	1.76	0.20
CAP/CI[20]	2.97	0.65
Schwinger variational principle combined with $\Sigma^{(2)}$/ $\Sigma^{(3)}$ [34]	2.609/2.534	0.583/0.536
CAP/ $\Sigma^{(2)}$ [23]	2.58	0.55
CAP-FSMRCC (this work)	2.520	0.390

References

1. D. E. Golden, *Adv. At. Mol. Phys*. **14**, 1 (1978); G. J. Schulz, *Rev. Mod. Phys*. **45**, 423 (1973); P. G. Burke, *Adv. At. Mol. Phys*. **4**, 173 (1968).
2. V. I. Kukulin, V. M. Krasnopol'sky, and J. Horácek, *Theory of Resonances* (Kluwer, Dordrecht, 1989).
3. W. P. Reinhardt, Ann. Rev. Phys. Chem. **33**, 223 (1982); N. Moiseyev, *Phys. Rep.* **302**, 211 (1998).
4. E. Balslev and J. M. Combes, Commun. *Math. Phys*. **22,** 280 (1971); J. Aguilar and J. M. Combes, *ibid.* **22,** 269 (1971); B. Simon, *ibid.* **27**, 1(1972); B. Simon, *Ann. Math*. **97,** 247 (1973).
5. U. V. Riss and H.-D. Meyer, *J. Phys. B* **26**, 4503 (1993).
6. G. Jolicard and E. J. Austin, *Chem. Phys. Lett*. **121**, 106 (1985).
7. C. W. McCurdy, in *Autoionization: Recent Developments and Applications,* edited by A.Temkin (Plenum, New York, 1985) pp 153-70.
8. M. K. Mishra, Y. Öhrn, and P. Froelich, *Phys. Lett*. A **84**, 4 (1981).
9. N. Rom, N. Lipkin, and N. Moiseyev, *Chem. Phys*. **151**, 199 (1991).
10. N. Moiseyev, *J. Phys. B* **31**, 1431 (1998).
11. U.V. Riss and H.-D. Meyer, *J. Phys. B* **31**, 2279 (1998).
12. R. Santra and L. S. Cederbaum, *J. Chem. Phys*. **115**, 6853 (2001).
13. T. Sommerfeld, U. V. Riss, H.-D. Meyer, L. S. Cederbaum, B. Engels, and H. U. Suter, *J. Phys. B*. **31**, 4107 (1998).
14. R. Santra, L. S. Cederbaum, and H.-D. Meyer, *Chem. Phys. Lett*. **303**, 413 (1999).
15. S. Feuerbacher, T. Sommerfeld, R. Santra, and L. S. Cederbaum*, J. Chem. Phys.* **118**, 6188 (2003).
16. N. Medikeri and M. Mishra, *Int. J. Quantum Chem*. **S28**, 29 (1994).
17. M. Berman, H. Estrada, L. S. Cederbaum, and W. Domcke, *Phys. Rev. A* **28**, 1363 (1983).
18. M. Berman, O. Walter, and L. S. Cederbaum, *Phys. Rev. Lett*. **50**, 1979 (1983).
19. B. I. Schneider and L. A. Collins, *Phys Rev. A*. **30**, 95 (1984).
20. W. M. Huo, T. L. Gibson, M. A. P. Lima, and V. McKoy, *Phys. Rev. A* **36**, 1632 (1987).
21. C. J. Gillan, C. J. Noble, and P. G. Burke, *J. Phys. B* **21**, L53 (1988).
22. (a) B. M. Nestmann and S. D. Peyerimhoff, *J. Phys. B*. **18**, 615 (1985); (b) **18**, 4309 (1985).

23. H.-D. Meyer, *Phys. Rev. A* **40**, 5605 (1989).
24. A.U. Hazi, T. N. Rescigno and M. Kurilla, *Phys. Rev. A* **23**, 1089 (1981).
25. C. W. McCurdy and R.C. Mowrey, *Phys. Rev. A* **25,** 2529 (1982).
26. J. G. Lauderdale, C. W. McCurdy and A.U. Hazi, *J. Chem. Phys* **79**, 2200 (1983).
27. T. Sommerfeld and L. S. Cederbaum, *Phys. Rev. Lett*. **80**, 3723 (1998); J. Zobeley, R. Santra and L.S. Cederbaum, *J. Chem. Phys*. **115**, 5076 (2001).
28. N. Chandra and A. Temkin, *Phys. Rev. A* **13**, 188 (1976).
29. B. I. Schneider, M. Le Dourneuf, and Vo Ky Lan, *Phys. Rev. Lett.* **43**, 1926 (1979).
30. H.-J. Werner and P. J. Knowles, *J. Chem. Phys*. **89**, 5803 (1988).
31. K. P. Huber and G. Herzberg, *Constants of diatomic molecules* (Van Nostrand Reinhold, New York, 1979).
32. D. E. Bernholdt and R. J. Bartlett, *Adv. Quantum Chem*. **34**, 271 (1999).
33. X. Li and J. Paldus, *J. Chem. Phys*. **113**, 9966 (2000); **115**, 5774 (2001)
34. J. Mazeau, F. Gresteau, R. I. Hall, and A. Huetz, *J. Phys. B* **11**, L557 (1978); D. Spence and P. D. Burrow, *J. Phys. B* **12**, L179 (1979).
35. F. A. Gianturco and F. Schneider, *J. Phys. B* **29**, 1175 (1996).
36. D. T. Birtwistle and A. Herzenberg, *J. Phys. B.* **4,** 53 (1971).
37. L. Dube and A. Herzenberg, *Phys. Rev. A* **20**, 194 (1979).
38. T. Sommerfeld and R. Santra, *Int. J. Quantum Chem*. **82**, 218 (2001).

Chapter 5

Correlated Complex Independent Particle Potential for Calculating Electronic Resonances

Abstract**:** We have formulated and applied an analytic continuation method for the recently formulated correlated independent particle potential [A. Beste and R. J. Bartlett, J. Chem. Phys. **120**, 8395 (2004)] derived from Fock space multireference coupled cluster theory. The technique developed is an advanced *ab initio* tool for calculating the properties of resonances in the low-energy electron-molecule collision problem. The method proposed quantitatively describes elastic electron-molecule scattering below the first electronically inelastic threshold. A complex absorbing potential is utilized to define the analytic continuation for the potential. A separate treatment of electron correlation and relaxation effects for the projectile-target system and the analytic continuation using the complex absorbing potential is possible, when an approximated form of the correlated complex independent particle potential is used. The method, which is referred to as CAP-CIP, is tested by application to the well-known $^2\Pi_g$ shape resonance of e-N_2 and the $^2B_{2g}$ shape resonance of e-C_2H_4 [ethylene] with highly satisfactory results.

5.1. Introduction

From the computational view point, there are many methods by which a resonance can be calculated. Instead of extracting the resonance parameters from the cross section, the metastable state can be described by an eigenfunction associated with a complex eigenenergy.[1-5] The success of this approach, which is a direct calculation of resonance eigenvalues of the Hamiltonian, has stimulated a considerable activity aimed at the formulation and implementation of new classes of theoretical and computational methods for the calculation of resonance parameters.[1-4] The method of analytic continuation of the Hamiltonian in the complex plane eliminates many of the theoretical difficulties.[3,4,6-10] The advantage of this method to investigate resonances is that the resonance parameters can be obtained by using L^2 wave functions. This method in which the asymptotic wave functions are not included offers a great computational advantage. The idea underlying analytic continuation of the Hamiltonian using complex absorbing potentials to calculate the resonance parameters is to introduce an absorbing boundary condition in the exterior region of the molecular scattering target.[7-10] In this way the wave function of the scattered electron becomes square integrable. The CAP procedure is minimally invasive in the sense that neither the internal structure of the physical Hamiltonian is affected nor is there any need to use other basis sets than usual real Gaussians.[11] Thus, this method appears to offer great promise for the determination of accurate energies in a computationally viable form by the modification of the existing electronic structure codes for the bound states.

In the CAP treatment of electronic resonance states, electron absorption is accomplished by replacing the molecular Hamiltonian H by

$$H(\eta) = H - i\eta W , \qquad 5.1.1$$

where η is a real, non-negative number referred to as CAP strength parameter. W is a local, positive-semidefinite one-particle operator. In the limit $\eta \to 0^+$, $H(\eta)$ defines an analytic continuation of H.[8] Significant strides have been made in the theoretical development and practical implementation of the complex absorbing potential method, which permits direct and simultaneous determination of both the resonance

position and width from the eigenvalue of an analytically continued Hamiltonian. This approach has been successfully applied to molecular shape resonances within frameworks which, respectively, neglected or included the electron correlation effects.[12-19]

In this Chapter we formulate an analytic continuation method for the correlated potential derived within the recently formulated correlated independent particle [CIP] theory.[20] In this correlated independent particle model, the effective Hamiltonian is composed of Fock operator and a correlation potential. Within this model the kinetic energy and the exchange energy can be expressed exactly leaving the correlation energy functional as the remaining unknown. The idea behind the development of this correlated independent particle theory is to reproduce the exact ionization potentials and electron affinities as orbital energies. The Fock space coupled cluster approach employs an effective Hamiltonian which is energy independent and universal for all orbitals. A correlation potential is extracted which yields the exact ionization potentials and electron affinities and a set of molecular orbitals. The energy independent effective one electron operator formulated can be viewed as a realization of the extended Koopmans' theorem,[21] where the ground state wave function is represented by the coupled cluster wave function.

Here we report the derivation of a correlated complex effective potential using the Fock space multireference coupled cluster [FSMRCC] theory and the analytic continuation scheme based on a complex absorbing potential [CAP] developed by Cederbaum and coworkers for electronic structure calculations.[8,10-17]. The correlated complex potential defines the analytical continuation scheme for the correlated independent particle theory which now has the general form, $(\boldsymbol{f} + V_c(\eta))\phi_P(\eta) = \varepsilon(\eta)\phi_P(\eta)$, where $\boldsymbol{f}$ is the Fock operator and $V_c(\eta)$ is the correlated complex potential to be determined. We choose to impose the condition of exactness of the ionization potentials [IPs] and electron affinities [EAs] as the negative of the complex orbital energies. Justification for this choice is offered by the extended Koopmans' theorem where the eigenvalues of the two distinct effective one-particle operators represent the IPs and EAs, respectively, of an analytically continued Hamiltonian. The method developed is particularly important for

quantitatively describing shape resonances in collisions of low-energy electrons with molecules. It is applicable to resonances of states below the first inelastic threshold, depending on the number of model space states chosen. Electronically inelastic collisions cannot be described. These states, however, will be dominated by only one-particle determinants. The position and width of such a resonance are obtained from the corresponding complex EA. The development of a correlated complex effective potential permits the calculation of the correlated resonance energy from an independent particle model theory. We refer to this method as complex absorbing potential based correlated independent particle [CAP-CIP] method. The proposed method is theoretically equivalent to the analytically continued FSMRCC method [CAP-FSMRCC].[18,19] But the present method offers significant computational advantages.

This chapter is organized as follows. In Section. 5.2 we examine the correlated effective potential formalism using the FSMRCC approach in order to review the basic concepts. In Section 5.3 we generalize the correlated effective potential to a correlated complex effective potential using a CAP. Finally in Section. 5.4 we derive computationally viable approximated forms of correlated effective potentials. In that section we present and analyze the numerical test and computational advantages of an approximated correlated complex potential by calculating the complex effective Hamiltonians for the (1,0) sector of FSMRCC theory for the N_2 and C_2H_4 [ethylene] molecule. Diagonalization of these complex effective Hamiltonians gives the resonance parameters for the $^2\Pi_g$ shape resonance in e-N_2 collision and the $^2B_{2g}$ shape resonance in e-C_2H_4 collision.

5.2. Theoretical Background

Before proceeding a few additional comments are in order. The theoretical background of the correlated independent particle formalism and an extensive discussion about the formulation of a correlated potential and the corresponding diagrammatic approach can be found in the literature.[20] In the present chapter we discuss the analytic continuation of a specific correlated effective potential and the

relevant theoretical background. We first briefly describe the correlated independent particle model derived from the FSMRCC method.

In the correlated independent particle approach, the restricted Hartree-Fock determinant $|\phi_0\rangle$ corresponding to the unperturbed N-electron target is chosen as the vacuum. With respect to this vacuum, holes and particles are defined. Depending on the energies of interest, these are further divided into active and inactive sets such that each determinant $|\phi_i\rangle$ of the model space has m active particles and n active holes. For example, when studying an (N+1)/(N-1)-electron state, the model space consists of determinants representing one active particle/hole. These are called one-particle or one-hole model spaces. The active particles or holes can be so defined as to make the model space complete. [22] For each sector (m,n) of Fock space, our zeroth-order wave function consists of a linear combination of model-space determinants $|\phi_i^{(m,n)}\rangle$,

$$|\Psi_\mu^{0(m,n)}\rangle = \sum_i C_{i\mu} |\phi_i^{(m,n)}\rangle . \qquad 5.2.1$$

$C_{i\mu}$ are the model space coefficients and (m,n) denotes the particle-hole rank of the Fock space sector. The exact (m,n) sector eigenfunctions of H can be written in the Fock space method using Lindgren's normal-ordered ansatz [23] as

$$|\Psi_\mu^{(m,n)}\rangle = \Omega |\Psi_\mu^{0(m,n)}\rangle , \qquad 5.2.2$$

$$\Omega = \{e^{\tilde{T}^{(m,n)}}\} , \qquad 5.2.3$$

where Ω is the wave operator, and the curly brackets indicate normal ordering of the operator within them. The wave operator in FSMRCC theory is known to be valence-universal [22] and this ensures connectivity and size-extensivity of the Fock space equations. In general, the wave operator for the Fock space of m active particles and n active holes correlates all lower active particle-active hole Fock space sectors. The cluster operator $\tilde{T}^{(m,n)}$ corresponding to the wave operator for the (m,n) sector is defined to consist of cluster operators for the lower Fock space sectors:[22,24]

$$\tilde{T}^{(m,n)} = \sum_{a=0}^{m}\sum_{b=0}^{n} T^{(a,b)} \qquad 5.2.4$$

Hence, the operator used is capable of describing the problem of lower valence sectors. In particular,

$$\tilde{T}^{(1,0)} = T^{(0,0)} + T^{(1,0)} \; ; \; \tilde{T}^{(0,1)} = T^{(0,0)} + T^{(0,1)} \; , \qquad 5.2.5$$

where $T^{(0,0)}$ is the cluster operator for the single reference coupled cluster case, containing only hole-particle excitation operators.

The normal ordering of the wave operator prevents the different T operators to contract among themselves and leads to a decoupling of the Bloch equations for different sectors. Equations for cluster amplitudes for different sectors can be solved using the subsystem-embedding-condition [SEC],[24] i.e., first the equations for the lowest sectors are solved. With the T operators of the lower sectors as constants, equations for higher Fock space sectors are solved progressively upwards. The Bloch equations[25] for general (m,n) sector can be written as

$$P^{(k,l)} H\Omega P^{(k,l)} = P^{(k,l)} \Omega H_{eff} P^{(k,l)}$$
$$k = 0,1,...m \qquad 5.2.6$$
$$l = 0,1,...n$$

$$Q^{(k,l)} H\Omega P^{(k,l)} = Q^{(k,l)} \Omega H_{eff} P^{(k,l)}$$
$$k = 0,1,...m \qquad 5.2.7$$
$$l = 0,1,...n$$

where

$$H_{eff} = P^{(m,n)} \Omega^{-1} H \Omega P^{(m,n)} \qquad 5.2.8$$

is an effective Hamiltonian[26] whose eigenvalues determine the roots of the Fock space sector (m,n):

$$\mathbf{H}_{eff}\mathbf{C} = \mathbf{C}\mathbf{E} \, . \qquad 5.2.9$$

The symbols $P^{(k,l)}$ and $Q^{(k,l)}$ used in the above equations denote the projection operator for the (k,l) sector of model space and its complementary space, respectively.

The vacuum expectation value of the effective Hamiltonian is the energy of the closed-shell N-electron state [E^{SRCC}] or zero-valence problem. Using the fact that the zero-valence sector cluster operator commutes with the cluster amplitudes of other sectors, we can decouple the zero valence sector from the rest of the FSMRCC calculation.[22,27] The eigenvalues of the resultant decoupled effective Hamiltonian become equivalent to the eigenvalues of the Fock space effective Hamiltonian generated from the normal ordered electronic Hamiltonian, H_N , i.e.

$$\bar{H}_{N,eff} = H_{eff} - E^{SRCC}, \qquad 5.2.10$$

where $\bar{H}_N = (H_N e^{T^{(0,0)}})_{connected,open}$.

Diagonalizing the effective Hamiltonian in the above equation we directly obtain the energy difference between our state defined by (m, n) model space and the coupled cluster state defined by (0, 0) model space function. For (1,0) and (0,1) model spaces diagonalization of the effective Hamiltonian yields the correlated electron EAs and IPs, respectively:

$$\bar{\mathbf{H}}^{(1,0)}_{N,eff} = (\mathbf{C}^{(1,0)}_{PP})\boldsymbol{\varepsilon}^{EA}_{p}(\mathbf{C}^{(1,0)}_{PP})^{-1}; \quad \bar{\mathbf{H}}^{(0,1)}_{N,eff} = (\mathbf{C}^{(0,1)}_{PP})\boldsymbol{\varepsilon}^{IP}_{p}(\mathbf{C}^{(0,1)}_{PP})^{-1}, \qquad 5.2.11$$

where the matrix $\mathbf{C}^{(0,1)}_{PP}$ contains the eigenvectors of the effective Hamiltonian $\bar{\mathbf{H}}^{(0,1)}_{N,eff}$ obtained when diagonalizing the effective Hamiltonian over the model space **P**. A rather safe way to avoid the energy dependence or intruder state problems consists in diagonalizing the effective Hamiltonian in the entire **P** and **Q** space. If the effective Hamiltonian is expressed in canonical Hartree-Fock orbitals, the correlation potential for the (1,0) and (0,1) sectors can be found by subtracting the unoccupied and occupied orbital energies from the diagonal elements of the corresponding effective Hamiltonian,

$$(\boldsymbol{\varepsilon}^{EA}_{HF} + \mathbf{V}^{(1,0)}_{C})\mathbf{C}^{(1,0)}_{PP} = \mathbf{C}^{(1,0)}_{PP}\boldsymbol{\varepsilon}^{EA}_{p}; \; (\boldsymbol{\varepsilon}^{IP}_{HF} + \mathbf{V}^{(0,1)}_{C})\mathbf{C}^{(0,1)}_{PP} = \mathbf{C}^{(0,1)}_{PP}\boldsymbol{\varepsilon}^{IP}_{p} \quad .5.2.12$$

Ignoring inevitable coupling between the (1,0) and (0,1) sector correlation potentials, we can formally add the two contributions together to give an energy independent correlation potential for the CIP model for all the orbitals in the (0,1) and (1,0) sectors:

$$\tilde{\mathbf{V}}_C = \mathbf{P}^{(1,0)}\mathbf{V}_C^{(1,0)}\mathbf{P}^{(1,0)} + \mathbf{P}^{(0,1)}\mathbf{V}_C^{(0,1)}\mathbf{P}^{(0,1)} \quad . \qquad 5.2.13$$

With this $\tilde{\mathbf{V}}_C$ the combined eigenvalue problem is given by

$$(\boldsymbol{\varepsilon}_{HF} + \tilde{\mathbf{V}}_C)\mathbf{C} = \mathbf{C}\boldsymbol{\varepsilon} \quad . \qquad 5.2.14$$

Since $\bar{\mathbf{H}}_{N,eff} = \boldsymbol{\varepsilon}_{HF} + \tilde{\mathbf{V}}_C$ can equivalently be regarded as an effective one-particle operator in an orbital space, we can obtain new orbitals as solutions of the biorthogonal eigenvalue equation

$$\bar{H}_{N,eff}\left|\phi_m\right\rangle = (f + \tilde{V}_C)\left|\phi_m\right\rangle = \varepsilon_m\left|\phi_m\right\rangle \qquad 5.2.15$$

where f is the Fock operator. The $\boldsymbol{\varepsilon}$ matrix in Eq. 5.2.14 contains the negative of the exact principal IPs an EAs as orbital energies,

$$\varepsilon_m = \left\langle\varphi_m\right|\bar{H}_{N,eff}\left|\phi_m\right\rangle, \qquad 5.2.16$$

where $\delta_{nm} = \left\langle\varphi_n \mid \phi_m\right\rangle$.

The FSMRCC diagrams to obtain the explicit V_c equations for the (1,0) sector are given in Fig. 5.1, and the diagrams for the (0,1) sector can be derived from those diagrams by hole-particle reversal. The relevent diagrams have been taken from Refs. 20 and 27. The single arrows indicate both active and inactive holes and particles, and double arrows represent only active holes or particles.

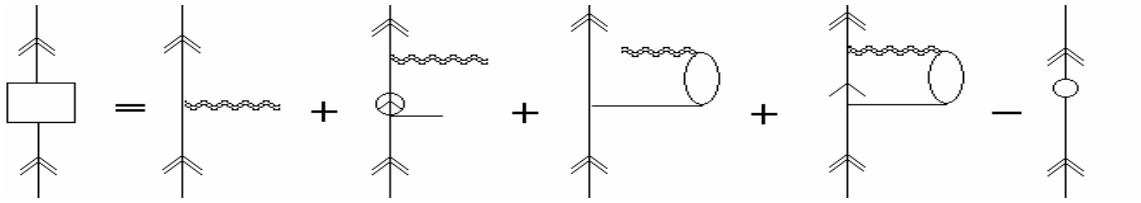

(a)

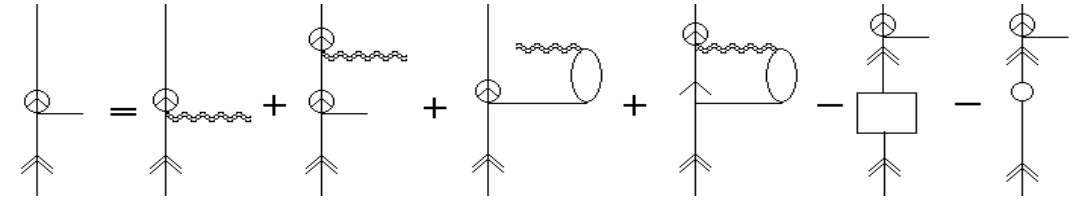

(b)

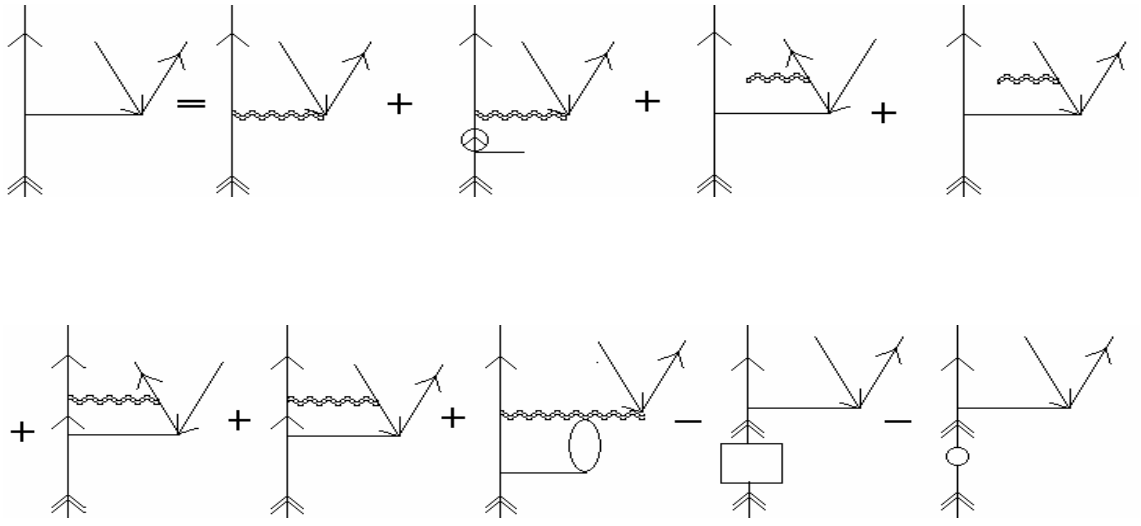

(c)

Figure 5.1 The CAP-unperturbed FSMRCC diagrams. (a) $V_c^{(1,0)}$, (b) $T_1^{(1,0)}$ and (c) $T_2^{(1,0)}$ diagrams. Active particles are depicted by double arrows, inactive particles by encircled arrows. Plain arrows indicate that all particles and holes are to be included. H-bar interaction lines are denoted by wavy lines, and straight lines are used for the cluster excitations.

5.3. The Correlated Complex Potential

The correlated complex potential $\tilde{V}_C(\eta)$ can be derived by incorporating a complex absorbing potential in the correlated potential $\tilde{V}_C$. Our objective is to solve Eq.5.2.14 using this correlated potential. A particular focus here is to utilize this approach in order to compute both energy and width of shape resonances in electron-molecule collisions. Since the complex absorbing potential serves to render the wave function of the projectile square-integrable, while it must leave the target unaffected, the CAP must be introduced, in principle, only into the description of the (N+1)/(N-1)-electron state. The N-electron ground state may be described by the Hamiltonian without CAP. In order for the CIP method to have a CAP unperturbed target state, we eliminate the effect of the CAP on the Hartree-Fock ground state by the replacement

$$\hat{W} \rightarrow \hat{P}\hat{W}\hat{P} \ , \qquad 5.3.1$$

where

$$\hat{P} = \sum_i |\phi_i\rangle\langle\phi_i| \qquad 5.3.2$$

projects onto the subspace of unoccupied orbitals. The redefinition is easily accomplished by setting

$$\langle\phi_p|\hat{W}|\phi_q\rangle = 0 \qquad 5.3.3$$

if either p or q is an occupied orbital. We also impose the condition that the cluster amplitudes in the (0,0) sector be invariables with respect to the CAP:

$$T^{(0,0)}(\eta) = T^{(0,0)}(\eta = 0) \ . \qquad 5.3.4$$

In this section we develop a correlated complex potential for the (1,0) sector of the Fock space. As our objective is to introduce the CAP potential—a one-body potential— into the FSMRCC theory, we would need to introduce it in both the (0,0) and (1,0) sectors to completely define the valence universal wave operator for the CAP perturbed Hamiltonian,

$$H(\eta) = H - i\eta W. \qquad 5.3.5$$

Because of the subsystem embedding condition [Sec. 5.2] enforced for solving the cluster amplitudes, the first step would be to introduce the CAP one-body term in the (0,0) sector of the Fock-Space. However, the physical and mathematical concepts [Eqs. (18-21)] discussed at the beginning of this section, make it possible to apply the CAP perturbation directly to the next hierarchical sector of Fock space [(1,0) sector in the present case] defined by the subsystem embedding condition. Within FSMRCC, the only one-body interaction terms entering the (1,0) sector of Fock space are the one-body interaction terms of $\bar{H}_N$ [see Eq. 5.2.10]. Similarly to the $\bar{H}_N$ interaction, in order to include the CAP perturbation in the (1,0) sector of Fock space, the CAP perturbation term can be transformed into a $\bar{W}_N$ interaction term:

$$\bar{W}_N(\eta) = [-i\eta W_N e^{T^{(0,0)}}]_{connected,open} \ . \qquad 5.3.6$$

With the CAP interaction term satisfying Eq. 5.3.3 and the $\bar{W}_N$ defined by Eq. 5.3.6, the procedure to accomplish the analytic continuation for the effective Hamiltonian is to replace all the one-body particle-particle interactions (interactions defined strictly for the virtual orbital space) of $\bar{H}_N$ diagrams entering $V_C^{(1,0)}$ and the $T^{(1,0)}$ amplitudes with a new particle-particle interaction of the form

$$\left(\bar{H}_N(\eta)\right)_{one\ \ body} = \left(\bar{H}_N\right)_{one\ \ body} + \bar{W}_N(\eta) \ . \qquad 5.3.7$$

As in the conventional FSMRCC method, the new set of nonlinear $T^{(1,0)}(\eta)$ amplitudes equations can be solved iteratively. The solutions of the new effective Hamiltonian,

$$\bar{\mathbf{H}}_{eff}^{(1,0)}(\eta)\mathbf{C}_{PP}^{(1,0)}(\eta) = (\boldsymbol{\varepsilon}_{HF}^{EA} + \mathbf{V}_C^{(1,0)}(\eta))\mathbf{C}_{PP}^{(1,0)}(\eta) = \mathbf{C}_{PP}^{(1,0)}(\eta)\boldsymbol{\varepsilon}_p^{(1,0)}(\eta), \qquad 5.3.8$$

are theoretically equivalent to the solutions of the Bloch equation

$$H(\eta)_N \Omega(\eta) P^{(1,0)} = \Omega(\eta) H(\eta)_{N,eff} P^{(1,0)} \ , \qquad 5.3.9$$

where $H(\eta)_N$ is the normal ordered form of the Hamiltonian $H(\eta)$ given in Eq. 5.3.5. Thus, the solutions of Eq. 5.3.8, $\varepsilon_p^{(1,0)}(\eta)$, are the correlated complex EAs of the Hamiltonian $H(\eta)$. In a similar way the correlated complex potential for the (0,1) sector, $V_c^{(0,1)}(\eta)$ can be calculated by replacing the particle-particle one-body part of the $\bar{H}_N$ interactions in $V_c^{(0,1)}$ and $T^{(0,1)}$ with the particle-particle $\bar{H}_N(\eta)$ given in Eq. 5.3.7.

As in the correlated independent particle model, an energy independent correlated complex potential can be constructed,

$$\tilde{\mathbf{V}}_C(\eta) = \mathbf{P}^{(0,1)}\mathbf{V}_C^{(0,1)}(\eta)\mathbf{P}^{(0,1)} + \mathbf{P}^{(1,0)}\mathbf{V}_C^{(1,0)}(\eta)\mathbf{P}^{(1,0)} \ . \qquad 5.3.10$$

With this $\tilde{\mathbf{V}}_C(\eta)$, the combined eigenvalue problem can be written as

$$\left(\boldsymbol{\varepsilon}_{HF} + \tilde{\mathbf{V}}_C(\eta)\right)\mathbf{C}(\eta) = \mathbf{C}(\eta)\boldsymbol{\varepsilon}(\eta) \ . \qquad 5.3.11$$

This equation can equivalently be regarded as an effective one-particle operator in an orbital space and we can obtain new orbitals as solutions of the biorthogonal eigenvalue equation similar to Eq. 5.2.16. Since the effective Hamiltonian is complex non-Hermitian, diagonalization yields the right eigenvectors $|\phi_m(\eta)\rangle$ as well as the left eigen vectors $\langle\varphi_m(\eta)|$:[28]

$$\bar{H}_{N,eff}(\eta)|\phi_m(\eta)\rangle = \left(f + \tilde{V}_C(\eta)\right)|\phi_m(\eta)\rangle = \varepsilon_m(\eta)|\phi_m(\eta)\rangle \ ,$$

$$\bar{H}^{\dagger}_{N,eff}(\eta)|\varphi_m(\eta)\rangle = \left(f + \tilde{V}_C(\eta)\right)^{\dagger}|\varphi_m(\eta)\rangle = \varepsilon^*{}_m(\eta)|\varphi_m(\eta)\rangle \ . \qquad 5.3.12$$

The $\boldsymbol{\varepsilon}(\eta)$ matrix in Eq. 5.3.11 contains the negative of the exact principal complex IPs and EAs as diagonal elements,

$$\varepsilon_m(\eta) = \langle\varphi_m(\eta)|\bar{H}_{N,eff}(\eta)|\phi_m(\eta)\rangle, \qquad 5.3.13$$

where $\delta_{nm} = \langle\varphi_n \mid \phi_m\rangle$.

5.3.1. Approximated Forms of $\tilde{V}_c(\eta)$

The analytic continuation methods, which are optimal for isolating and characterizing resonances, have computational advantages over theoretical methods that treat the full scattering problem including nonresonant contributions to the scattering cross section.[1-3,11] However, some practical difficulties arise in the computation of resonance parameters using analytic continuation methods. Much of the difficulty follows from two fundamental facts.

First, as the calculations are performed using a finite basis set, an important problem is to find out which complex eigenvalue in the discrete spectrum may correspond to a resonant state. Given a complete basis set, for every resonance state there exists an eigenvalue $E(\eta)$ of $H(\eta)$ with the property $\lim_{\eta \to 0^+} E(\eta) = E_r - i\Gamma/2$, whereas in the approximate numerical treatments using a finite basis set, the resonance energy shows certain stability properties; in practice they are often determined from "stabilization graphs" based on the fact that the complex velocity,

$$v_i(\eta) = \eta dE_i / d\eta \ , \qquad 5.3.14$$

of one of the trajectories is minimum in magnitude near the resonance energy.[8,12] The graphical solution to optimize the analytic continuation parameters is time consuming and computationally expensive as the underlying electronic structure calculations must be performed several times using a large basis set.

Second, since the electron correlation and relaxation effects are important in finding the position and width of resonances, the *ab initio* methods, in which the analytic continuation scheme has been framed, must also describe correlation energy accurately. The calculation of accurate resonance parameters requires addressing the heavy computational expenses due to the stabilization graphs and subtleties of electron correlation. The difficulties of the stabilization method have been further increased by the optimization of the geometric parameters which minimizes the CAP perturbation and maximizes the overlap with the wave function of the scattered electron. One approach by which these difficulties can be reduced to a manageable

level is detailed in this section. This particular approach is numerically checked by applying it to the well-known $^2\Pi_g$ shape resonance in e-N_2 and the $^2B_{2g}$ shape resonance in e-C_2H_4.

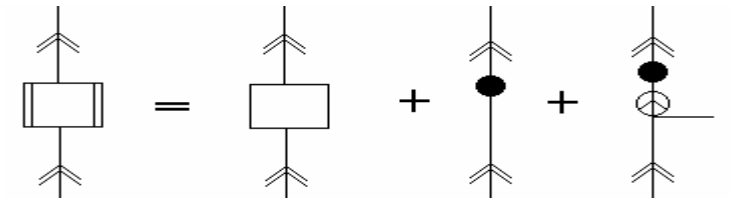

(a)

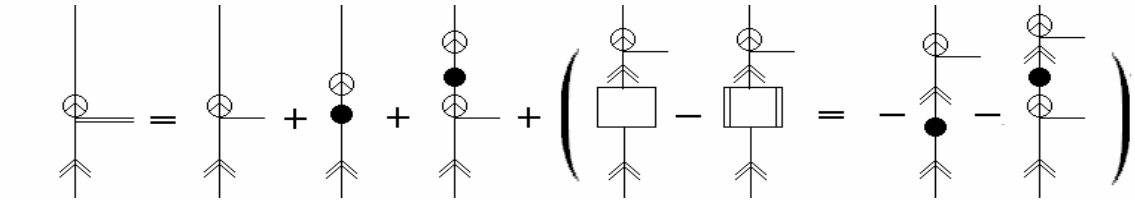

(b)

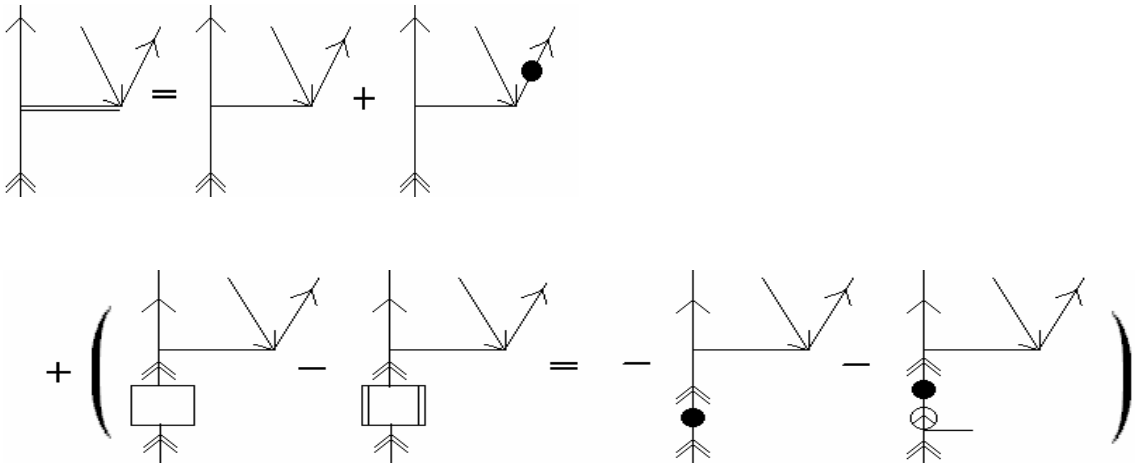

(c)

Figure 5.2 The CAP-perturbed FSMRCC diagrams. (a) $V_c^{(1,0)}(\eta^1)$, (b) $T_1^{(1,0)}(\eta^1)$ and (c) $T_2^{(1,0)}(\eta^1)$ diagrams. In addition to the diagrammatic elements explained in Fig. 5.1, CAP-related symbols are introduced. The W-bar perturbation is denoted by filled circle, vertical double lines indicate CAP-perturbed excitations, and the CAP-perturbed correlated potential is symbolized by the box with vertical double lines.

In order to get the correlated independent particle potential, first we have to solve the nonlinear FSMRCC equations. To begin, an expression for the first iterative solution of the $V_c^{(1,0)}(\eta)$ problem can be obtained from the CAP unperturbed $V_c^{(1,0)}$ by replacing the one-body part of the $\bar{H}_N$ interactions with the CAP augmented one-body part of the Hamiltonian interactions $\bar{H}_N(\eta)$ given in Eq. 5.3.7. The diagrammatic representation of the resulting $V_c^{(1,0)}(\eta)$, which we termed as $V_c^{(1,0)}(\eta^1)$ (where the superscript '1' stands for the iteration number), is given in Fig. 5. 2. Using this $V_c^{(1,0)}(\eta^1)$ together with the $\bar{H}_N(\eta)$ interactions from Eq. 5.3.7, the new $T^{(1,0)}(\eta^1)$ diagrams can be generated. Note that, in these $T^{(1,0)}(\eta^1)$ diagrams, we have taken out the CAP unperturbed $V_c^{(1,0)}$ contribution from $T^{(1,0)}(\eta^1)$ and substituted it with the $V_c^{(1,0)}(\eta^1)$ diagrams. This CAP contribution can be written in terms of $\bar{H}_N(\eta)$ [Eq. 5.3.7] and the CAP unperturbed amplitudes as shown in the parentheses of the amplitude diagrams in Fig. 5.2. Following the procedure, using the new $T^{(1,0)}(\eta^1)$ amplitudes the $V_c^{(1,0)}(\eta^2)$ can be generated. This iterative procedure can be continuted until the eigenvalues of $\bar{H}_{N,eff}(\eta)$ converges. The computation of the quantitites $V_c^{(1,0)}(\eta^1)$, $V_c^{(1,0)}(\eta^2)$ and $T^{(1,0)}(\eta^1)$ is simple and direct, which results from the fact that all these terms may be written in terms of the corresponding unperturbed terms and $\bar{H}_N(\eta)$ interactions. Solving $T^{(1,0)}(\eta^2)$ and $V_c^{(1,0)}(\eta^3)$ requires, of course, a computational effort equivalent to that of a CAP-FSMRCC iterative step because these terms utilize the perturbed amplitudes and $\bar{H}_N(\eta)$. Qualitatively speaking, the convergence of this procedure will be fast, since it always uses $T_1^{(1,0)}$ and $T_2^{(1,0)}$, which are converged amplitudes in the (1,0) sector of the CAP-unperturbed Hamiltonian, as the initial guess for the $T_1^{(1,0)}(\eta)$ and $T_2^{(1,0)}(\eta)$ amplitudes. Although CAP-FSMRCC and the present method are theoretically equivalent in defining the analytic continuation of the Hamiltonian $\boldsymbol{H}$, there is a practical difference between the implementations of the two methods. For the former the analytic continuation scheme starts from the definition of the many-body Hamiltonian and the diagonalization of the complex effective Hamiltonian yields the resonance energy relative to the target state, while for the latter the analytic

continuation scheme starts from the real FSMRCC effective Hamiltonian and the diagonalization of the iteratively solved new complex effective Hamiltonian yields an equivalent energy difference.

Considerable simplifications may be achieved for the resonance trajectory generation when the iterations are terminated after the $V_c^{(1,0)}(\eta^2)$ calculation. Such a termination of the iterative procedure is justified by the fact that the effective Hamiltonian and the $T^{(1,0)}$ amplitudes are converged quantities for the CAP unperturbed effective Hamiltonian and the eigenvalues of this effective Hamiltonian correspond to the correlated electronic states of the (N+1)-electron system. The dynamic and nondynamic correlation for (N+1)-electron states are retained in this procedure. In principle, a suitably chosen CAP should define an exact analaytic continuation for the Fock space (1,0) sector with a minimum change in the correlation energy. The main advantage of terminating the iterative procedure at the second step of the complex correlated potential calculation over the CAP-FSMRCC procedure is that a) it does not need any modification of the FSMRCC calculation for bound states, just a few trivial changes in the final $T^{(1,0)}$ amplitude and the $\bar{H}_{N,eff}$ matrix; b) the most expensive part of the calculation [constructing the $T^{(1,0)}$ matrix; this matrix can be stored once it is generated and can be used for $T^{(1,0)}(\eta)$] does not need to be repeated and $T^{(1,0)}(\eta^1)$ can be constructed very easily from $T^{(1,0)}$ by adding a few diagrams. On the other hand, in the case of CAP-FSMRCC for each η value a computationally expensive procedure must be performed for the calculation of $T^{(1,0)}(\eta)$.

The simplest quantum mechanical description of the eigenvalues obtained from the first and second order analytically continued correlated effective potential

$$\bar{H}_{N,eff}(\eta^1)\left|\phi_m^1\right\rangle = \left(f + \tilde{V}_c(\eta^1)\right)\left|\phi_m^1\right\rangle = \varepsilon_m(\eta^1)\left|\phi_m^1\right\rangle$$
$$\bar{H}_{N,eff}(\eta^2)\left|\phi_m^2\right\rangle = \left(f + \tilde{V}_c(\eta^2)\right)\left|\phi_m^2\right\rangle = \varepsilon_m(\eta^2)\left|\phi_m^2\right\rangle \qquad 5.3.15$$

is that they are conceptually similar to the eigenenergies of the analytically continued Hamiltonian at the independent particle level of theories, but has an additional

advantage of retaining the lion's share of the dynamic and nondynamic electron correlation of the analytically continued Hamiltonian in terms of the correlation of the CAP-unperturbed Hamiltonian. The final description of the energy levels thus stands out for its simplicity.

5.4. Results and Discussion

5.4.1. $^2\Pi_g$ Shape Resonance in N_2^-

In the following, we present the numerical calculation of the $^2\Pi_g$ shape resonance in N_2^- using the $V_c^{(1,0)}(\eta^1)$ and $V_c^{(1,0)}(\eta^2)$ potentials. This resonance has been studied extensively by other theoretical methods.[12,14,17,19,29-34]

In our calculations we chose a box-shaped CAP[13] of the form [given] in equations 4.2.3 and 4.2.4, which can be easily represented in a Gaussian basis set. It has been applied in the peripheral region of the target to absorb the scattered electron while keeping the target unperturbed. The CAP box parameters c_i (i=1, 2, 3) can be optimized accordingly in the calculations. The N_2 molecule is placed along the z axis symmetrical to the origin with a bond length of 2.07 a.u. The CAP box is set up by $c_x = c_y = \delta c$, $c_z = 1.035 + \delta c$, where c_x, c_y, c_z are the distances from the center of the coordinate system along the x, y, and z axis, respectively, and δc is a nonnegative variable. A TZ(7p2d) basis[12] has been employed on each N atom.

In practice we would not solve a correlated independent equation of the form given in Eq. 5.3.12, but instead we calculate the effective Hamiltonian for the (1,0) Fock space sector using $V_c^{(1,0)}(\eta^1)$ and $V_c^{(1,0)}(\eta^2)$ and solve the eigenvalue problem in Eq. 5.3.8. We selected the thirty energetically lowest virtual orbitals to span our active particle space. Consequently, the effective Hamiltonian is represented by a 30×30 matrix, and we will obtain thirty electron affinities. The four high lying virtual orbitals have been frozen for the calculation. We first calculate the effective Hamiltonian for the (1,0) effective Hamiltonian—and thus $V_c^{(1,0)}$—for the CAP

unperturbed system and then use the corresponding $T^{(1,0)}$ and $V_c^{(1,0)}$ in the subsequent $V_c^{(1,0)}(\eta^1)$ and $V_c^{(1,0)}(\eta^2)$ calculations.

In this procedure, for the calculation of $V_c^{(1,0)}(\eta^1)$ and $V_c^{(1,0)}(\eta^2)$, we used the amplitudes defining $T^{(1,0)}$ scaled by a complex factor,

$$t_i^{a(1,0)} = t_i^{a(1,0)} \times \frac{\bar{F}_{ii} - \bar{F}_{aa}}{(\bar{F}_{ii} + \bar{W}_{ii}) - (\bar{F}_{aa} + \bar{W}_{aa})} \,, \qquad 5.4.1$$

$$t_{ij}^{ab(1,0)} = t_{ij}^{ab(1,0)} \times \frac{(\bar{F}_{ii} + \bar{F}_{jj}) - (\bar{F}_{aa} + \bar{F}_{bb})}{(\bar{F}_{ii} + \bar{F}_{jj} + \bar{W}_{ii} + \bar{W}_{jj}) - (\bar{F}_{aa} + \bar{F}_{bb} + \bar{W}_{aa} + \bar{W}_{bb})} \,, \qquad 5.4.2$$

where $\bar{F}$ is the one-body part of the $\bar{H}$ interaction given in Eq. 5.3.7. This scaling makes the amplitudes equivalent to the amplitudes from the first iterative step of CAP-FSMRCC theory.

The $^2\Pi_g$ shape resonance is identified by plotting the complex electron affinity spectra [from Eq. 5.3.8] using these $V_c^{(1,0)}(\eta^1)$ and $V_c^{(1,0)}(\eta^2)$ for various box sizes and CAP strengths. On a single processor machine, the CAP-unperturbed FSMRCC calculation ($V_c^{(1,0)}$) took 20 days to converge the cluster amplitudes. The calculation of $V_c^{(1,0)}(\eta^1)$ and $V_c^{(1,0)}(\eta^2)$ for 500 different η values ranging from zero to $1\text{x}10^{-2}$ at a step size of $2\text{x}10^{-5}$ took only less than an hour to complete. A similar CAP-FSMRCC calculation for the complete trajectory would have taken a minimum of 500x20 days.

The Siegert energy for elastic e-N_2 scattering has been studied in two sets of CAP-CIP calculations. First, to calculate the optimum box size for which the absorbing potential is best adapted to the basis set and the size of the target system, CAP-CIP calculations were performed for various CAP-box sizes. The velocity of the trajectory at the stabilization point is smallest for a box size of δc=3.0 compared to other box sizes. Therefore, all further investigations of the complex resonance eigenvalues were performed using this box size. The first 250 points of the η trajectories of the resonance eigenvalues calculated using the potentials $V_c^{(1,0)}(\eta^1)$

and $V_c^{(1,0)}(\eta^2)$, which we call first and second order trajectories, respectively, are displayed graphically in Fig. 5.3. To examine the role of CAP effects on the electron correlation, we have also performed a zeroth order calculation using the potential

$$V_c^{(1,0)}(\eta^0) = V_c^{(1,0)} - i\eta\bar{W} . \qquad 5.4.3$$

The zeroth order trajectory generated using this potential is also given in Fig. 5.3. This zeroth order trajectory helps us to estimate the extent of correlation and relaxation primarily due to the CAP effects. A suitable measure is

$$\Delta E_{CORR}^{CAP} = \left| E(\eta_{opt}) - E(\eta_{opt}^0) \right| , \qquad 5.4.4$$

where $E(\eta_{opt}^0)$ is the Siegert energy point in the zeroth order trajectory, $E(\eta_{opt})$ the Siegert energy from the first or second order trajectory, and η_{opt} is the corresponding optimum η value. ΔE_{CORR}^{CAP}, which is the absolute value of the energy difference between the Siegert energy from the first/second order trajectory and the Siegert energy from the zeroth order trajectory, is analogous to the correlation energy used in bound-state electronic structure calculations. The ΔE_{CORR}^{CAP} calculated for the first and second order trajectories are 6.94×10^{-4} a.u. and 6.29×10^{-4} a.u., respectively. It is interesting to note that the electron correlation effects due to the CAP apparently influence the trajectory only marginally. It also highlights the importance of using a highly correlated wave function for the CAP-unperturbed Hamiltonian. Although the calculated ΔE_{CORR}^{CAP} quantities are small, it is obvious from Fig. 5.3 that the electronic correlation contribution due to the CAP is an important quantity in calculating the accurate stabilization point in the trajectory. Quite clearly the second order trajectory shows more stabilization compared to the first order trajectory, as $V_c^{(1,0)}(\eta^2)$ uses the CAP-perturbed $T^{(1,0)}$ amplitudes while $V_c^{(1,0)}(\eta^1)$ does not use the CAP perturbation terms [other than the scaling given in Eqs. 5.4.1 and 5.4.2]. The absolute value of the energy difference between the Siegert energy from the first and second order trajectories is 6.47×10^{-5} a.u., which means that the complete iterative procedure is finished after the second step if an energy convergence criterion of 0.1 mH is applied.

The trajectories given in Fig. 5.3 are slightly different from the stabilization curves generated using the CAP-FSMRCC calculation.[19] The optimum point of η in the present calculation is 0.00286 while in the CAP-FSMRCC calculation it was 0.00500. The optimum resonance parameters are also different. The primary reason for the difference between the two calculations is the dimension of the calculations. The CAP-FSMRCC calculation was performed using 20 active particles, and the number of cluster amplitudes was not higher than 350600, while the present calculation is performed using 30 active particles and 1448280 cluster amplitudes. [A CAP-CIP calculation using 20 active orbitals and 350600 cluster amplitudes reproduced the corresponding entry in Table 4.2] Such a large-size calculation is particularly important. It may be shown that for a particular Fock space sector in the FSMRCC method, the values of the roots obtained by diagonalizing the effective Hamiltonian are independent of the dimension of the active space used for the calculation. However, the approximate FSMRCCSD method does not satisfy this invariance.[35] Morevover, the CAP perturbation makes the magnitude of the off-diagonal elements of the effective Hamiltonian matrix a significant one. Hence, the eigenvalues of the effective Hamiltonian, which is not diagonally dominant, depend highly on the total number of active valence orbitals chosen for the effective Hamiltonian matrix calculation. Considerable accuracy may be achieved when the effective Hamiltonian is diagonalized over the complete virtual orbital space. The outstanding efficiency of the CAP-CIP method has already enabled us to improve on our previous CAP-FSMRCC calculation. The values for the energy and width obtained using the Table 5.1. The CAP-CIP data show good agreement with these results.

Table 5.1 Energy and width of the $^2\Pi_g$ shape resonance in e-N_2 scattering at the equilibrium geometry of N_2. See also Table 4.3 for a comparison with other methods

The present method using	Energy(eV)	Width(eV)
$V_c^{(1,0)}(\eta^0)$	2.280	0.482
$V_c^{(1,0)}(\eta^1)$	2.298	0.507
$V_c^{(1,0)}(\eta^2)$	2.297	0.492

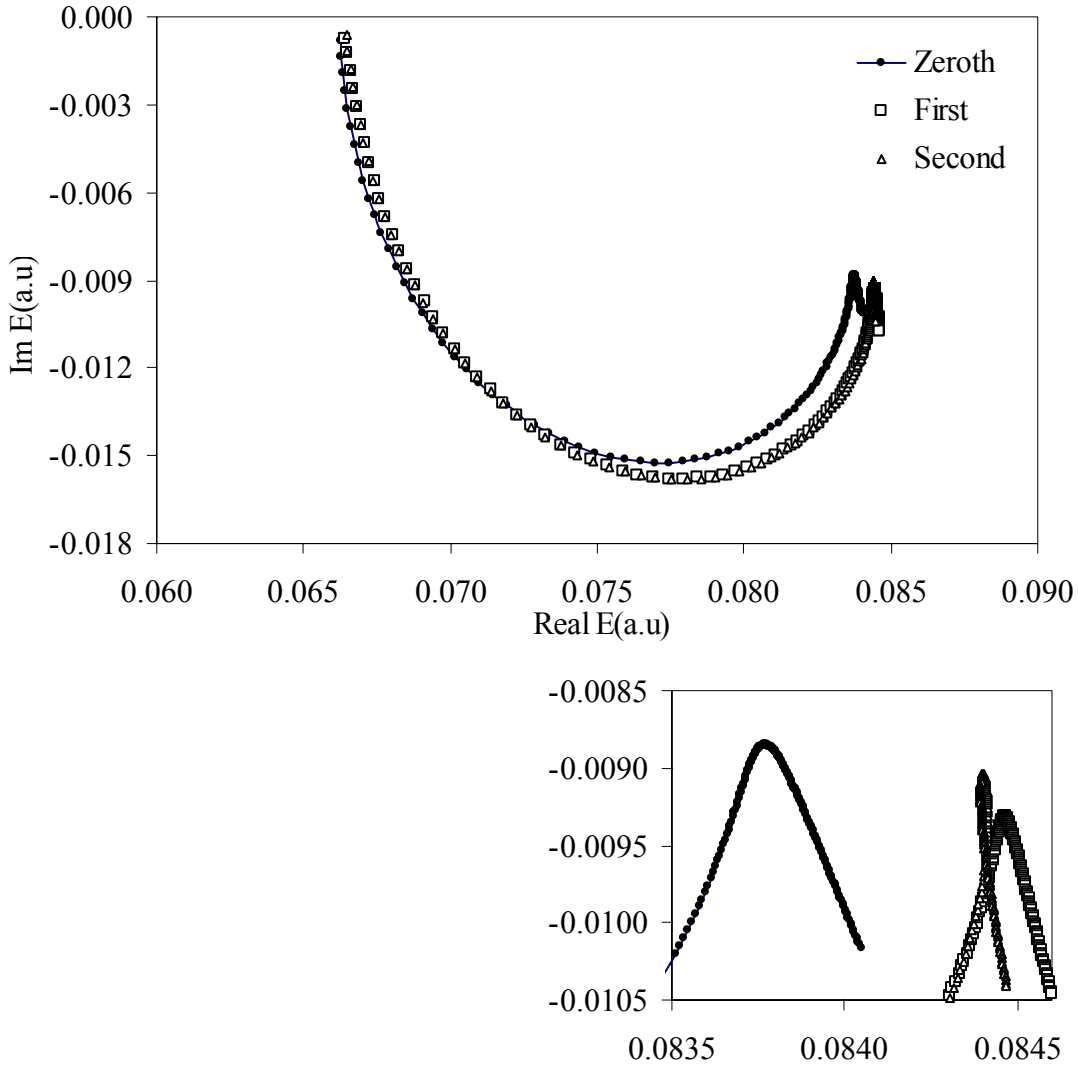

Figure 5.3 The η trajectories for the $^2\Pi_g$ shape resonance in e-N_2 scattering. The complex eigenvalues used in the trajectories are obtained from $V_c^{(1,0)}(\eta^0)$, $V_c^{(1,0)}(\eta^1)$ and $V_c^{(1,0)}(\eta^2)$ calculations. The η values vary from 0.00002 to 0.00500. η is incremented linearly in steps of 0.00002. The region of stabilization of the trajectories [corresponding to the resonance position] is magnified in the lower panel.

5.4.2. $^2B_{2g}$ Shape Resonance in $C_2H_4^-$

It is known that isolated C_2H_4 (ethylene) anion is not electronically stable.[36] There are several experimental and theoretical reports available in the literature that describe the position and lifetime of the low-energy $(\pi)^2(\pi^*)^1\left(^2B_{2g}\right)$ shape resonance of ethylene anion.[36-43] In particular, the observation of the $^2B_{2g}$ state of

ethylene anion by electron transmission spectroscopy shows that the resonance is centered near 1.78 eV with a width of approximately 0.7 eV.[37] The vibrational excitation studies of Walker *et al.*[38] and the absolute elastic scattering and vibrational excitation cross sections experiments done by Panajotovic *et al.*[39] confirm these findings. Although significant vibrational excitation occurs, the vibronic width in each channel is approximately constant. The electron transmission spectrum of ethylene[38] shows exceedingly weak vibrational substructure. Thus a single calculation of a resonance width has meaning within the usual fixed nucleus approximation used in this study.

We have used a basis set consisting of 72 Cartesian Gaussians, two s-type Gaussians centered on each hydrogen atom and (5s,9p)[40] basis on each carbon atom, giving nine orbitals of π^* symmetry to accommodate the resonance electron. Thirty low lying virtual orbitals have been taken as the active valence orbitals for the (1,0) sector. The geometry of the molecule has been optimized at the level of second order Møller-Plesset (MP2) perturbation theory. The ground state D_{2h} geometry thus obtained has been used for the resonance calculations. The molecule is placed in such a way that the molecular plane coincides with the XZ plane, with the principal axis of rotation being the Z axis.

The procedure applied for the calculation of the $^2B_{2g}$ resonance state in ethylene is the same as the procedure explained in the above subsection. The stabilization of the resonance trajectory is maximum when the CAP box parameters c_x, c_y, and c_z equal 6, 5, and 7 a.u., respectively. In Fig. 5.4 we plot the η trajectory of the $^2B_{2g}$ shape resonance state obtained from CAP-CIP calculations using the three approximated potentials, $V_c^{(1,0)}(\eta^0)$, $V_c^{(1,0)}(\eta^1)$ and $V_c^{(1,0)}(\eta^2)$. The optimum η values for the zeroth, first and second order trajectories are 0.00650, 0.00648, and 0.00672 a.u., respectively. The ΔE_{CORR}^{CAP} calculated for the first and second order trajectories are 5.93 x10^{-4} a.u. and 3.72 x10^{-4} a.u. The absolute value of the energy difference between the Siegert energy points from the first order and second order trajectory, which is a measure of the degree of convergence of the Siegert energy, is 2.20x10^{-4} a.u.

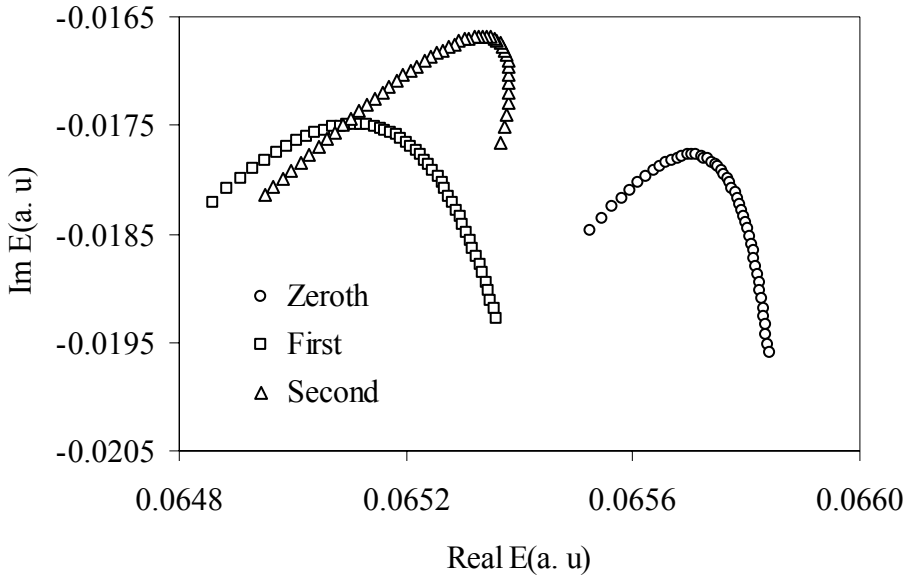

Figure 5.4 The η trajectories for the $^2B_{2g}$ shape resonance in electron-ethylene scattering. The trajectories are generated using the complex spectra obtained in $V_c^{(1,0)}(\eta^0)$, $V_c^{(1,0)}(\eta^1)$ and $V_c^{(1,0)}(\eta^2)$ calculations. The η values vary from 0.0050 to 0.0100. η is incremented linearly in steps of 0.0001.

Table 5.2 compares our theoretical results with the experimental observations and the results from other theoretical methods available in the literature. The results of our theoretical calculations are in good agreement with the experimental measurements.[37-39] Our calculated width seems to be a little too large, while other theoretical calculations find too narrow a width. (Fixed-nuclei calculations are, of course, not expected to achieve perfect agreement with experiment.) For instance, Donnelly[40] employed the second order treatment of the coordinate-rotated electron propagator, revealing a $^2B_{2g}$ shape resonance with small width. The momentum density distribution for the Dyson amplitude calculations done by this author highlights the need for a multireference treatment of this particular shape resonance. The independent potential derived from our calculation is truly electron-correlated and multideterminant in character. The results from our CAP-CIP calculation show that the metastable anion formation, like in any other anion formation, requires the inclusion of dynamic and nondynamic electron correlation.

Table 5.2 Energy and width of the $^2B_{2g}$ shape resonance in e-C_2H_4 scattering.

Method	Energy(eV)	Width(eV)
Experiment (see text) (Refs. 37-39)	1.78	0.7
Complex Kohn variational calculation (Ref. 42)	1.83	0.460
Schwinger iterative variational method (Ref. 41)	2.5	---
Second order electron propagator theory based on complex scaling method (Ref. 40)		
(5s,8p) basis	2.49	0.234
(5s,9p) basis	1.88	0.442
Bivariational SCF based on complex scaling method (Ref. 41)		
(5s,7p) basis	1.93	0.2
The present method using		
$V_c^{(1,0)}(\eta^0)$	1.788	0.9675
$V_c^{(1,0)}(\eta^1)$	1.772	0.9520
$V_c^{(1,0)}(\eta^2)$	1.778	0.9076

5.5. Conclusion

The attitude reflected in this work is that a resonance is a discrete eigenstate [outside of Hilbert space], which is separable from the nonresonant scattering continuum. Using analytic continuation concepts, it is possible to focus on resonances and treat them utilizing techniques developed for bound states. In this chapter, we have derived a combination of a complex absorbing potential with an effective one-electron potential that describes the interaction of an electron with a many-electron target. A remarkable feature of this effective potential is that it does not depend on the kinetic energy of the scattering electron. Traditional optical potentials[44-50] that describes the elastic scattering of a particle by a many-body target for, in principle, arbitrary projectile energy, are energy-dependent. This makes sense, since the response of the target depends on the projectile energy. For instance, when

a new inelastic scattering channel opens up, i.e. if the target molecule can emerge from the collision in an excited state, this must manifest itself in a loss of flux in the elastic channel. This consideration indicates that the energy-independent one-particle potential derived within the framework of FSMRCC is not such a universal optical potential. Rather, it describes elastic electron-molecule collisions below the first inelastic threshold. This energy range is of great practical interest (see, for example, Refs. [51-54]). The extraordinary power of the Fock space formulation of the coupled cluster approach to the many-body problem allows one to describe these low-energy scattering processes in terms of an energy-independent one-particle potential.

The CAP-CIP method which we have proposed here is similar to our earlier work on CAP-FSMRCC. There is, however, a major difference. In the CAP-FSMRCC method, the CAP is incorporated with the uncorrelated system and the analytic continuation procedure is achieved within the correlation energy calculation, whereas in the CAP-CIP method analytic continuation is defined for an already correlated system. Both methods are theoretically equivalent, and the exact results from both need a similar computational effort. However, an approximated form of the correlated potential in the CAP-CIP method considerably reduces the computational expenses. The way of looking at the analytic continuation procedure for the FSMRCC method through an independent particle theory helps us to derive the correlated complex potential. More generally, we would like to mention that the calculation of the correlated complex potential from the correlated potential and the cluster amplitudes explicitly separates the calculation of the electron correlation effects and the correlation effects due to the CAP. This formalism thus allows for the study of the convergence properties of the FSMRCC procedure and the analytic continuation procedure separately.

The absolute error in the eigenvalues of $\bar{H}_{N,eff}(\eta)$ due to the truncation implemented in the calculation of $\tilde{V}_c(\eta)$ is small. The advantages of using $\tilde{V}_c(\eta^1)$ and $\tilde{V}_c(\eta^2)$ for resonance calculations can be summarized as follows:

1. The quantitative characterization of electronic resonances is possible using a bound state calculation.
2. Dynamic and nondynamic electronic correlation is included.
3. The repetitive FSMRCC calculations are avoided.
4. The analytic continuation for the effective Hamiltonian from FSMRCC calculation is direct and simple. The required modifications in the code for the entire procedure are additions to $\bar{H}_{N,eff}$ and $\tilde{T}$, so they do not affect the inner part of the FSMRCC programmes.
5. Since the complete FSMRCC calculation is performed only for the CAP unperturbed Hamiltonian, a large-scale effective Hamiltonian calculation is possible by defining a large number of valence particle as active.
6. The eigenvalues $\bar{H}_{N,eff}(\eta)$ calculated using $\bar{H}_{N,eff}(\eta^0)$ and $\tilde{V}_c(\eta^0)$ give a preliminary idea about the stabilization parameter (CAP strength) and the position and width of the resonance.
7. The accurate stabilization point can be obtained by performing a converged $\tilde{V}_c(\eta)$ calculation for the η values near optimized values obtained from the above approximation.

In summary we would like to say that the CAP-CIP method, based on the correlated complex potentials $\tilde{V}_c(\eta^1)$ and $\tilde{V}_c(\eta^2)$, is a very promising and computationaly viable formalism for calculating the resonances in low-energy electron-molecule collision problems. The first numerical application of CAP-CIP, which demonstrates the accuracy of the method, is encouraging.

References

1. A.I. Baz', Ya.B. Zel'dovich, and A.M. Perelomov, *Scattering, Reactions, and Decays in Nonrelativistic Quantum Mechanics* (Nauka, Moscow, 1971)
2. B. D. Buckley, P. G. Burke, and C. J. Noble, in *Electon molecule collisions*, edited by I. Shimamura and K. Takayanagi.(Plenum Press New York,1984) pp.495-556.
3. W. P. Reinhardt, Ann. Rev. Phys. Chem. **33**, 223 (1982); Y.K. Ho, *Phys. Rep*. **99,** 2 (1983).
4. N. Moiseyev, *Phys. Rep*. **302**, 211 (1998).
5. V. I. Kukulin, V. M. Krasnopol'sky, and J. Horácek, *Theory of Resonances* (Kluwer, Dordrecht, 1989).
6. E. Balslev and J. M. Combes, *Commun. Math. Phys*. **22,** 280 (1971); J. Aguilar and J. M. Combes, *ibid.* **22,** 269 (1971); B. Simon, *ibid.* **27**, 1(1972); B. Simon, *Ann. Math*. **97,** 247 (1973).
7. N. Moiseyev, *J. Phys. B*. **31**,1431 (1998)
8. U. V. Riss and H.-D. Meyer, *J. Phys. B* **26**, 4503 (1993).
9. G. Jolicard and E. J. Austin, *Chem. Phys. Lett*. **121**, 106 (1985); G. Jolicard, J. Humbert, *Chem. Phys*. **118,** 397 (1987)
10. R. Santra and L. S. Cederbaum, Phys. Rep. **362**, 1 (2002).
11. R. Santra and L. S. Cederbaum*, J. Chem. Phys*. **115**, 6853 (2001).
12. T. Sommerfeld, U. V. Riss, H.-D. Meyer, L. S. Cederbaum, B. Engels, and H. U. Suter, *J. Phys. B* **31**, 4107 (1998).
13. R. Santra, L. S. Cederbaum, and H.-D. Meyer, *Chem. Phys. Lett*. **303**, 413 (1999).
14. T. Sommerfeld and R. Santra, *Int. J. Quantum Chem*. **82**, 218 (2001).
15. T. Sommerfeld, U. V. Riss, H.-D. Meyer, and L. S. Cederbaum, *Phys. Rev. Lett*. **79**, 1237 (1997).
16. R. Santra and L. S. Cederbaum, *J. Chem. Phys*. **117**, 5511 (2002).
17. S. Feuerbacher, T. Sommerfeld, R. Santra, and L. S. Cederbaum, *J. Chem. Phys*. **118**, 6188 (2003).
18. Y. Sajeev and S. Pal, *Mol. Phys*. **103**, 2267,(2005).
19. Y. Sajeev, R. Santra, and S. Pal, *J. Chem. Phys*. **122**, 234320 (2005).
20. A. Beste and R. J. Bartlett, *J. Chem. Phys*. **120**, 8395 (2004).

21. J. M. O. Matos and O. W. Day, *Int. J. Quantum Chem*. **31**, 871 (1987); O. W. Day, D. W. Smith and C. Garrod, *Int. J. Quantum Chem*. **90**, 294 (2002).
22. D. Mukherjee and S. Pal, *Adv. Quantum. Chem*. **20**, 291 (1989); U. Kaldor and M. A. Haque, *Chem. Phys. Lett*. **128**, 45 (1986); U. Kaldor and M. A. Haque*, J. Comp. Chem*. **8**, 448 (1987); D. Mukherjee, Pramana **12**, 1 (1979); M. A. Haque and D. Mukherjee, J. *Chem. Phys*. **80**, 5058 (1984).
23. I. Lindgren*,* Int. J. Quantum Chem. **S12**, 33 (1978); I. Lindgren, *J. Phys. B* **24**, 1143 (1991); I. Lindgren, *Phys. Script*. **32**, 291 (1985); W. Kutzelnigg, *J. Chem. Phys*. **77**, 3081 (1982): W. Kutzelnigg and S. Koch, *J. Chem. Phys*. **79**, 4315 (1983).
24. I. Lindgren and D. Mukherjee*, Phys. Rep*. **151**, 93 (1987).
25. C. Bloch, *Nucl. Phys*. **6**, 329 (1958).
26. P. Durand and J. P. Malrieu, *Adv. Chem. Phys*. **67**, 321 (1987); J. P. Malrieu, P. L. Durand, and J. P. Daudey*, J. Phys. A* **18**, 809 (1985).
27. C. M. L. Rittby and R. J. Bartlett, *Theo. Chem. Acta.* **80**, 469 (1991).
28. P. O. Löwdin, *Adv. Quantum Chem*. **20**, 87 (1989).
29. M. Berman, H. Estrada, L. S. Cederbaum, and W. Domcke, *Phys. Rev. A* **28**, 1363 (1983).
30. B. I. Schneider and L. A. Collins, *Phys Rev. A*. **30**, 95 (1984).
31. W. M. Huo, T. L. Gibson, M. A. P. Lima, and V. McKoy, *Phys. Rev. A* **36**, 1632 (1987).
32. C. J. Gillan, C. J. Noble, and P. G. Burke, J. Phys. B **21**, L53 (1988).
33. B. M. Nestmann and S. D. Peyerimhoff, *J. Phys. B*. **18**, 615 (1985); **18**, 4309 (1985).
34. H.-D. Meyer, *Phys. Rev. A* **40**, 5605 (1989).
35. D. E. Bernholdt and R. J. Bartlett, *Adv. Quantum. Chem*. **34**, 271 (1999).
36. J. Simons and K. D. Jordan, *Chem. Rev*. **87**, 535 (1987).
37. P. D. Burrow and K.D. Jordan, *Chem. Phys. Lett*. **36**, 594 (1975).
38. I. C. Walker, A Stamatovic, and S. F. Wong, *J. Chem. Phys*. **69**, 5532 (1978).
39. R. Panajotovic, M. Kitajima, H. Tanaka, M. Jelisavcic, J. Lower, L. Campbell, M. J. Brunger, and S. J. Buckman*, J. Phys. B*. **36**, 1615 (2003).
40. R. A. Donnelly, *J. Chem. Phys*. **84**, 6200 (1986).
41. M. N. Medikeri and M. K. Mishra, *Chem. Phys. Lett*. **246**, 26 (1995).

42. B. I. Schneider, T. N. Rescigno, B. H. Lengsfield III, and C. W. McCurdy, *Phys. Rev. Lett*. **66,** 2728 (1991).
43. L. M. Brescansin, L. E. Machado, and M.-T. Lee, *Phys. Rev. A* **57**, 3504 (1998).
44. H. Feshbach, *Theoretical Nuclear Physics: Nuclear Reactions* (Wiley, New York, 1992).
45. H. Feshbach, *Ann. Phys*. (N.Y.) **5**, 357 (1958).
46. H. Feshbach, *Ann. Phys*. (N.Y.) **19**, 287 (1962).
47. J. S. Bell and E. J. Squires, *Phys. Rev. Lett*. **3**, 96 (1959).
48. F. Capuzzi and C. Mahaux, *Ann. Phys*. (N.Y.) **239**, 57 (1995).
49. T. N. Rescigno, C. W. McCurdy, and B. I. Schneider, *Phys. Rev. Lett*. **63**, 248 (1989).
50. H.-D. Meyer, *J. Phys. B* **25**, 2657 (1992).
51. B. Boudaiffa, P. Cloutier, D. Hunting, M. A. Huels, and L. Sanche, *Science* **287**, 1658 (2000).
52. A. M. Scheer, K. Aflatooni, G. A. Gallup, and P. D. Burrow, *Phys. Rev. Lett*. **92**, 068102 (2004).
53. F. Martin, P. D. Burrow, Z. Cai, P. Cloutier, D. Hunting, and L. Sanche*, Phys. Rev. Lett.* **93**, 068101 (2004).
54. H. Abdoul-Carime, S. Gohlke, and E. Illenberger, *Phys. Rev. Lett*. **92**,168103 (2004).

List of Publications

1. *Fock space multi-reference coupled cluster calculations based on an underlying bivariational self consistent field on Auger and shape resonance*
   Y. Sajeev, M. K. Mishra, N. Vaval and S. Pal, *J. Chem. Phys*., **120**, 67 (2004)
2. *A general formalism of the Fock space multireference coupled cluster method for investigating molecular electronic resonances*

   Y. Sajeev and Sourav Pal, *Mol. Phys*. **103**, 2267-2275 (2005)
3. *Analytically continued Fock space multireference coupled-cluster theory: Application to the* $^2\Pi_g$ *shape resonance in e-*N_2 *scattering.*

   Y. Sajeev, Robin Santra and Sourav Pal, *J. Chem. Phys*, **122**, 234320 (2005)
4. *Correlated complex independent particle potential for calculating electronic resonances.*
   Y. Sajeev, Robin Santra and Sourav Pal, *J. Chem. Phys.* **123**, 204110 (2005)
5. *Optimization of Nonlinear Optical Properties by Substituent Position, Geometry and Symmetry of the Molecule: An ab Initio Study*

   D. Davis, K. Sreekumar, Y. Sajeev and S. Pal, *J. Phys. Chem. B* **109**, 14093 (2005)